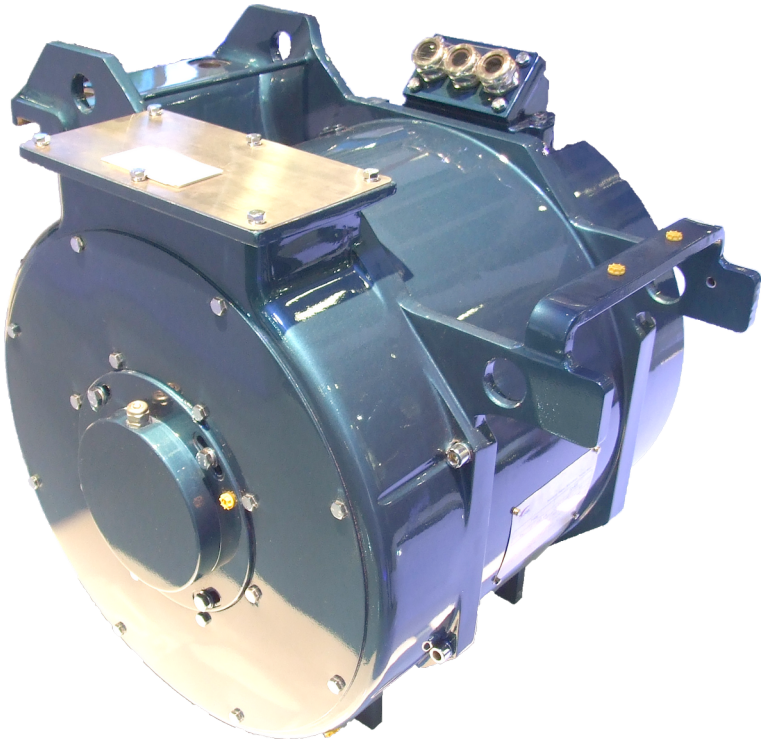


DESIGN OF ELECTRIC MACHINES 1

EVROPSKÁ UNIE
Evropské strukturální a investiční fondy
Operační program Výzkum, vývoj a vzdělávání

MINISTERSTVO ŠKOLSTVÍ, MLÁDEŽE A TĚLOVÝCHOVY

FAKULTA ELEKTROTECHNICKÁ ZÁPADOČESKÉ UNIVERZITY V PLZNI

ESF II project of the University of West Bohemia project no. CZ.02.2.69/0.0/0.0/18_056/0013239

Symbols and Abbreviations

BLDC	brushless direct current machine
CGS	centimetre-gram-second system of units
ČSN	Czech technical standard
p.u.	per unit
MTPA	maximum torque per ampere
PMSM	permanent magnet synchronous motor
PMSG	permanent magnet synchronous generator
PWM	pulse-width modulation
SI	international system of units Le Système International d'Unités
TEFC	totally enclosed fan cooled motor
THD	total harmonic distortion

$2p$	number of poles	[-]
$2u$	number of coil sides in a slot	[-]
a	penetration depth	[m]
a_ν	penetration depth of ν^{th} harmonic component	[m]
$a_=$	number of parallel branches of a DC winding	[-]
$a_\sim$	number of parallel branches of an AC winding	[-]
A	linear current density	[$A.m^{-1}$]
A_i	linear current density of inner diameter of an axial machine	[$A.m^{-1}$]
b	linear machine width	[m]
b_b	winding bar width	[m]
b_o	slot opening width	[m]
b_p	pole width	[m]
b_{PM}	permanent magnet width	[m]
b_{ps}	pole shoe width	[m]
b_s	slot width	[m]
b_t	tooth width	[m]
B	magnetic flux density	[T]
B_1	fundamental harmonic component of the air gap magnetic flux density	[T]
B_{av}	magnetic flux density average value	[T]
B_c	magnetic flux density for compensation of commutation effect	[T]
B_{max}	maximal flux density of air-gap pulsations	[T]
B_p	pole magnetic flux density	[T]
B_{p1}	magnitude of magnetic flux density pulsations in stator teeth	[T]
B_{p2}	magnitude of magnetic flux density pulsations in rotor teeth	[T]
B_{PM}	magnetic flux density in a permanent magnet	[T]
B_r	remanent magnetic flux density of a permanent magnet	[T]
B_{ref}	reference value of magnetic flux density for determination of iron-core losses	[T]
B_{rms}	RMS value of the magnetic flux density	[T]
B_{r20}	remanent magnetic flux density of a permanent magnet at 20 °C	[T]

B_s	slot magnetic flux density	[T]
B_t	tooth magnetic flux density	[T]
B_t'	apparent value of tooth magnetic flux density	[T]
B_y	yoke magnetic flux density	[T]
B_δ	air gap magnetic flux density magnitude	[T]
B_v	vth harmonic component magnetic flux density	[T]
c	insulation distance between winding overhangs	[m]
c	denominator of the number of slots per pole and phase expressed as fraction	[-]
c	relative price (chapters 3.4, 3.5)	[$p.u.$]
C	Esson's factor	[$VAmin.m^{-3}$]
C	number of columns of a Tingley schema (chapter 4.4)	[-]
C_1	armature magnetic field shape factor for cylindrical rotor machine	[-]
C_{d1}	direct axis armature magnetic field shape factor for salient pole rotor machine	[-]
C_E	torque equation Esson's factor	[$Nm.m^{-3}$]
C_l	linear machine Esson's factor	[$N.m^{-2}$]
C_{q1}	quadrature axis armature magnetic field shape factor for salient pole machine	[-]
d_0	diameter of central circle of an involute	[m]
D_1	armature diameter	[m]
D_2	diameter of secondary side of a machine	[m]
D_c	commutator diameter	[m]
D_e	machine outer diameter	[m]
D_i	machine inner diameter (shaft diameter)	[m]
D_s	average diameter of shorting rings	[m]
D_y	yoke average diameter	[m]
f	frequency	[Hz]
f_p	magnetic field pulsations frequency	[Hz]
f_{ref}	reference value of frequency for determination of iron-core losses	[Hz]
F	cooling area of a machine	[m^2]
F_0	no-load magnetomotive force	[A]
F_a	armature magnetomotive force	[A]
F_{ac}	compensated armature magnetomotive force	[A]
F_{an}	non-compensated armature magnetomotive force	[A]
F_b	brushes friction force	[N]
F_c	compensation winding magnetomotive force	[A]
F_d	direct axis armature magnetomotive force component	[A]
F_{d1}	fundamental harmonic component of direct axis armature magnetomotive force	[A]
F_f	field winding magnetomotive force	[A]
F_{fr}	rated load field winding magnetomotive force	[A]
F_i	interpole magnetomotive force	[A]
F_m	magnetomotive force of an m-phase winding	[A]
F_{m1}	magnetomotive force of a single phase	[A]
F_{m100}	armature magnetomotive force at rated magnetic flux density	[A]
F_{PM}	permanent magnet magnetomotive force	[A]
F_q	quadrature axis armature magnetomotive force component	[A]

F_{q1}	fundamental harmonic component of quadrature axis armature MMF	[A]
F_t	magnitude of magnetomotive force of a single coil turn	[A]
F_1	fundamental harmonic component of a magnetomotive force	[A]
F_δ	air gap magnetomotive force	[A]
h_1	height of a slot part with a coil	[m]
h_o	height of a slot opening	[m]
h_p	pole height	[m]
h_{ps}	height of a pole-shoe	[m]
h_{PM}	permanent magnet height	[m]
h_s	total slot height	[m]
h_t	tooth height	[m]
h_w	wire height	[m]
h_y	yoke height	[m]
H	magnetic field strength	[$A.m^{-1}$]
H_c	permanent magnet coercive magnetic field strength	[$A.m^{-1}$]
H_{c20}	permanent magnet coercive magnetic field strength at 20 °C	[$A.m^{-1}$]
H_{ci}	intrinsic permanent magnet coercive magnetic field strength	[$A.m^{-1}$]
$H_{c\vartheta}$	permanent magnet coercive magnetic field strength at rated temperature	[$A.m^{-1}$]
H_{PM}	permanent magnet magnetic field strength	[$A.m^{-1}$]
H_t	tooth magnetic field strength	[$A.m^{-1}$]
H_{ta}	average tooth magnetic field strength	[$A.m^{-1}$]
H_δ	air gap magnetic field strength	[$A.m^{-1}$]
i	electric current time dependency (chapter 12.2)	[A]
i	electric current	[$p.u.$]
i	insulation distance between brushes	[-]
i_d	direct axis component of electric current	[$p.u.$]
i_q	quadrature axis component of electric current	[$p.u.$]
I	electric current RMS value	[A]
I_{0a}	active component of no-load current	[A]
I_{0r}	reactive component of no-load current	[A]
I_a	armature current	[A]
I_a	current through winding parallel branch	[A]
I_b	current through brush set	[A]
I_c	RMS value of current through one conductor	[A]
I_f	field winding current	[A]
I_{Fe}	iron-core losses equivalent current	[A]
I_s	total electric current through one slot (RMS value)	[A]
I_t	total machine current	[A]
J	moment of inertia (chapters 3.4 and 3.5)	[$kg.m^2$]
J	current density	[$A.m^{-2}$]
J_b	brushes current density	[$A.m^{-2}$]
J_f	field winding current density	[$A.m^{-2}$]
k_B	magnetic field shape factor	[-]
k_C	Carter’s factor	[-]

k_{Cv}	Carter's factor for cooling channels	[-]
k_d	stator sheet desaturation factor	[-]
k_{d1}	fundamental harmonic component winding distribution factor	[-]
k_D	ratio between outer and inner diameter of the armature	[-]
k_e	eddy currents losses factor	$[W.kg^{-1}.Hz^{-2}T^{-2}]$
k_{exc}	iron core excess loss coefficient	$[W.kg^{-1}.Hz^{-1,5}T^{-2}]$
k_E	electromotive force coefficient	[-]
k_{Fe}	stacking factor	[-]
k_h	iron core hysteresis loss coefficient	$[W.kg^{-1}.Hz^{-1}T^{-2}]$
k_I	current transformation ratio	[-]
k_m	mechanical losses factor	[-]
k_s	surface losses coefficient	[-]
k_{sat}	magnetic circuit saturation factor	[-]
k_{sk}	slot skewing factor (chap. 11.2)	[-]
k_t	friction factor	[-]
k_{tt}	technological factor of teeth iron core losses	[-]
k_{ty}	technological factor of yoke iron core losses	[-]
k_V	voltage transformation ratio	[-]
k_{w1}	fundamental harmonic component winding factor	[-]
k_{w1}	stator fundamental harmonic component winding factor (chap. 11.2, 11.3)	[-]
k_{w2}	rotor fundamental harmonic component winding factor (chap. 11.2, 11.3)	[-]
k_y	yoke magnetomotive force correction factor	[-]
k_{y1}	fundamental harmonic component winding pitch factor	[-]
k_Z	impedance transformation ratio	[-]
k_β, k_β'	leakage inductance correction factors	[-]
k_δ	coefficient for air gap length choice	[-]
k_σ	interpole leakage coefficient	[-]
$k_\sim$	AC current losses increase coefficient	[-]
K	number of commutator lamellae, number of winding coils	[-]
K_1	number of coils in one winding segment	[-]
K_f	number of winding coils per phase	[-]
K_p	number of commutator lamellae between consequent brushes of equal potential	[-]
l	length of the stator stack	[m]
l_1	length of a stator stack of a known machine	[m]
l_b	brush length	[m]
l_b	winding bar length	[m]
l_c	average coil turn length	[m]
l_{ef}	effective length of a stator stack including radial ventilation channels	[m]
l_f	average length of a field winding coil turn	[m]
l_{Fe}	stator stack iron length	[m]
l_{Fep}	pole iron stack length	[m]
l_i	electromagnetic length of the machine in the centre of the air gap	[m]
l_{is}	length of an iron section	[m]
l_o	length of a winding overhang	[m]

l_{of}	length of winding overhang offset	[m]
l_p	length of a leakage path between two adjacent poles	[m]
l_{ps}	length of a leakage path between two adjacent pole shoes	[m]
l_{PM}	permanent magnet length	[m]
l_s	slot length	[m]
l_{sr}	length of one segment of a shorting ring	[m]
l_v	ventilation channel length (chap. 5.3.4)	[m]
l_w	length of a winding wire	[m]
l_x	lenngth of a stator stack of a scaled machine	[m]
l_y	length of an average yoke flux line	[m]
l_{yred}	reduced length of an average yoke flux line	[m]
L	linear machine active length	[m]
$L_{1\sigma}$	stator leakage inductance	[H]
$L_{2\sigma}$	rotor leakage inductance	[H]
$L_{2\mu}$	squirrel cage magnetizing inductance	[H]
L_d	direct axis inductance	[H]
L_{dif}	differential leakage inductance	[H]
L_{max}	inductance maximal value	[H]
L_{min}	inductance minimal value	[H]
L_{ps}	length of a pole shoe	[m]
L_p	pole length	[m]
L_q	quadrature axis inductance	[H]
L_s	shorting ring leakage inductance	[H]
L_μ	magnetizing inductance	[H]
L_σ	winding leakage inductance	[H]
$L_{\sigma b}$	bar leakage inductance	[H]
$L_{\sigma c}$	coil leakage inductance	[H]
$L_{\sigma s}$	leakage inductance of a slot part of a coil	[H]
$L_{\sigma w}$	wire/conductor leakage inductance	[H]
m	number of armature winding phases	[-]
m	machine mass (chap. 3.4, 3.5)	[kg]
m'	mathematical number of armature winding phases	[-]
m_1	number of stator winding phases	[-]
m_2	number of rotor winding phases	[-]
m_g	mass of a machine group	[$p.u.$]
m_s	specific machine mass	[kg/VA]
m_t	machine teeth mass	[kg]
m_y	machine yoke mass	[kg]
m_{Fe}	machine iron mass	[kg]
M	machine torque	[Nm]
M_i	machine inner torque	[Nm]
n	number of machines in a group (chap. 3.5)	[-]
n	speed of a machine	[$ot.min^{-1}$]
n_p	number of parallel wires	[-]

n_{PM}	number of permanent magnets	[-]
N_b	number of rotor barriers	[-]
N_{bs}	number of bushes in a set	[-]
N_c	number of coil turns	[-]
N_{cs}	number of conductors in series	[-]
N_f	number of field winding coil turns	[-]
N_i	number of inter pole coil turns	[-]
N_r	number of rotor poles	[-]
N_s	number of winding turns in series	[-]
N_{s1}	number of stator winding turns in series	[-]
N_{s2}	number of rotor winding turns in series	[-]
o	circumference of an involute basic circle	$[m]$
p	number of machine pole-pairs	[-]
p_b	brush pressure	$[Pa]$
P	machine output power	$[W]$
P_2	number of phasors of a rotor winding	[-]
P_i	inner power of the machine	$[W]$
P_{in}	machine input power	$[W]$
P_r	rated power of the machine	$[W]$
q	number of slots per pole and phase	[-]
q_0	numerator of number of slots per pole and phase expressed as fraction	[-]
Q	number of armature slots	[-]
Q_1	number of stator slots	[-]
Q_2	number of rotor slots	[-]
Q_b	number of bars	[-]
r	radius	$[m]$
r_a	armature resistance	$[p.u.]$
R	number of rows in Tingley's schema (chap. 4.4)	[-]
R	electrical resistance	$[\Omega]$
R_1	stator electrical resistance	$[\Omega]$
R_2	rotor electrical resistance	$[\Omega]$
R_{1g}	Görges' circle radius	$[A]$
R_a	armature winding electrical resistance	$[\Omega]$
R_{a2}	electrical resistance of a squirrel cage parallel branch	$[\Omega]$
R_b	electrical resistance of a winding bar	$[\Omega]$
R_c	radius of a coil loop	$[m]$
R_f	field winding electrical resistance	$[\Omega]$
R_{Fe}	iron core equivalent resistance	$[\Omega]$
R_g	radius of Görges' polygon	$[A]$
R_p	length of a radius vector in Görges' polygon	$[\Omega]$
R_s	electrical resistance of one segment of a shorting ring	$[\Omega]$
$R_\sim$	electrical resistance while leading AC current	$[\Omega]$
S	machine apparent power	$[VA]$
S_b	brush cross-section	$[m^2]$

S_b	bar cross-section	$[m^2]$
S_c	number of coil segments of an AC winding	[-]
S_f	field winding wire cross-section	$[m^2]$
S_i	inner apparent power of a machine	$[VA]$
S_p	amount of coil segments per phase of an AC winding	[-]
S_{ps}	area of pole shoes	$[m^2]$
S_r	rated apparent power of the machine	$[VA]$
S_s	slot cross-section	$[m^2]$
S_{sr}	cross-section of a shorting ring	$[m^2]$
S_w	winding wire cross-section	$[m^2]$
S_δ	air gap are over one pole pitch	$[m^2]$
t	time	$[s]$
t_{Fe}	thickness of iron part of steel sheets	$[m]$
t_{is}	insulation thickness	$[m]$
t_l	lamella pitch	$[m]$
t_p	pole pitch	$[m]$
t_{p2}	machine secondary part pole pitch	$[m]$
t_{ps}	pole pitch in number of slots	[-]
t_s	slot pitch	$[m]$
t_{sh}	steel sheet thickness	$[m]$
t_{sk}	slot skew pitch	$[m]$
t_y	yoke pole pitch at the level of slot bottom	$[m]$
T_c	commutation time	$[s]$
u	voltage	$[p.u.]$
u	voltage time dependence (chap. 12.2)	$[V]$
u_i	back EMF time dependence	$[V]$
u_i	back electromotive force	$[p.u.]$
u_r	time dependence of a reactive voltage	$[V]$
U	voltage RMS value	$[V]$
U_b	brushes voltage drop	$[V]$
U_f	field winding voltage	$[V]$
U_i	back EMF RMS value	$[V]$
U_{i1}	stator back electromotive force	$[V]$
U_{i2}	rotor back electromotive force	$[V]$
U_{i20}	rotor back electromotive force in no-load state	$[V]$
U_{ic}	conductor back electromotive force	$[V]$
U_{im}	magnitude of back electromotive force	$[V]$
U_l	voltage between consequent lamellas	$[V]$
U_n	machine rated voltage (phase-to-phase)	$[V]$
U_{pn}	rated value of a phase-to-neutral voltage	$[V]$
U_r	reactive voltage while commutation	$[V]$
v	speed	$[m.s^{-1}]$
v_c	commutator peripheral speed	$[m.s^{-1}]$
V	number of machine conductors	[-]

V	machine volume (chap. 3.4, 3.5)	[m^3]
V_c	number of conductors in a slot	[-]
V_s	number of conductors in series	[-]
w_m	magnetic energy density	[J/m^3]
W_m	magnetic energy	[J]
W_{m1}	magnetic energy of a single phase	[J]
x	dimension of a machine	[$p.u.$]
x_d	machine direct axis reactance	[$p.u.$]
x_q	machine quadrature axis reactance	[$p.u.$]
x_σ	machine leakage reactance	[$p.u.$]
$X_{a\sigma}$	machine leakage reactance	[Ω]
y	coil distance in number of coil sides	[-]
y_1	coil pitch in number of coil sides	[-]
y_{1s}	coil pitch in number of slots	[-]
y_2	coil connection length in number of coil sides	[-]
y_c	commutator pitch in number of commutator lamellas	[-]
y_p	potential pitch on commutator in number of commutator lamellas	[-]
α	exponent part of frequency in general iron core losses expression (chap. 5.2)	[-]
α	angle between winding overhangs and axial plane	[rad]
α	resistance thermal coefficient	[K^{-1}]
α_2	angle between phasors in star of slots	[rad]
α_m	mechanical pole cover coefficient	[-]
α_{mech}	mechanical angle between following bars	[-]
α_o	angle between winding overhangs and front plane of the stator stack	[rad]
α_δ	electromagnetic pole coverage factor	[-]
α_ν	ν-th harmonic component electromagnetic pole coverage factor	[-]
β	coil pitch shortening factor	[-]
β	exponent part of flux density in general iron core losses expression (chap. 5.2)	[-]
γ	electrical conductivity	[S/m]
γ	magnetic flux coefficient for evaluation of Carter's factor	[-]
δ	mechanical air gap length	[m]
δ‘	electromagnetic air gap length	[m]
δ“	saturated electromagnetic air gap length	[m]
δ_i	interpole air gap length	[m]
δ_{max}	mechanical air gap length at the edges of the pole-shoes	[m]
δ_{min}	minimal mechanical air gap length	[m]
Δ	transformation factor between bars and shorting rings	[-]
Δp	relative machine losses	[W/kg]
Δp_e	eddy current iron core loss coefficient	[W/kg]
Δp_{Fe}	iron core loss coefficient	[W/kg]
Δp_h	hysteresis iron core loss coefficient	[W/kg]
Δp_{ref}	iron core loss coefficient for reference values of frequency and flux density	[W/kg]
Δp_t	teeth iron core loss coefficient	[W/kg]

Δp_y	yoke iron core loss coefficient	[W/kg]
ΔP	total machine losses	[W]
ΔP_{add}	additional losses	[W]
ΔP_b	brush winding I^2R (Joule) losses	[W]
ΔP_{bf}	brushes friction losses	[W]
ΔP_f	field winding I^2R (Joule) losses	[W]
ΔP_{Fe}	iron core losses	[W]
ΔP_j	I^2R (Joule) losses	[W]
ΔP_p	magnetic flux density pulsation losses	[W]
ΔP_{PWM}	pulse-width modulation feeding losses	[W]
ΔP_s	surface losses	[W]
ΔP_{sin}	sine wave feeding losses	[W]
ΔP_t	teeth iron core losses	[W]
ΔP_y	yoke iron core losses	[W]
$\Delta\vartheta$	temperature rise	[K]
ε	electrical slot skew angle	[rad]
ε	operator choosing winding type while calculation	[-]
ε	switching angle (chap. 12.2)	[rad]
ζ	proportional penetration depth	[-]
ζ_ν	ν-th harmonic proportional penetration depth	[-]
η	efficiency	[-]
ϑ	temperature	[$°C$]
Θ	magnetomotive force	[A]
Θ_i	interpole magnetomotive force	[A]
Θ_p	pole magnetomotive force drop	[A]
Θ_{ps}	pole shoes magnetomotive force drop	[A]
Θ_{PM}	permanent magnet magnetomotive force	[A]
Θ_t	tooth magnetomotive force drop	[A]
Θ_y	yoke magnetomotive force drop	[A]
Θ_δ	air gap magnetomotive force drop	[A]
κ_1	amount of galvanic independent winding sections of an AC winding	[-]
κ_2	amount of identical phasors in star of slots	[-]
κ_I	current transformation correction factor	[-]
λ	diameter ratio (chap. 12.3)	[-]
λ	slimness ratio (chap. 11.1)	[-]
λ	linear machine wave length (chap. 12.4)	[-]
λ_c	commutating coil reluctance factor	[-]
λ_o	winding overhangs reluctance factor	[-]
λ_{op}	slot opening reluctance factor	[-]
λ_s	slot reluctance factor	[-]
λ_{so}	slot including slot opening reluctance factor	[-]
Λ	reluctance	[H]
Λ_{op}	reluctance of leakage path between pole overhangs	[H]
Λ_p	reluctance of leakage path between poles	[H]

Λ_{os}	reluctance of leakage path between pole-shoes overhangs	[*H*]
Λ_{s}	reluctance of leakage path between pole-shoes	[*H*]
Λ_{σ}	reluctance of leakage paths	[*H*]
μ	order of spatial harmonic	[-]
μ_{PM}	relative permeability of a permanent magnet	[-]
μ_{r}	relative permeability	[-]
μ_{0}	permeability of vacuum	[$H.m^{-1}$]
ν	time harmonic component order	[-]
ξ	angular coordinate	[*rad*]
ξ	Hobart factor (chap. 9.3)	[$H.m^{-1}$]
π	Ludolphine number	[-]
ρ	proportional resistance	[$\Omega.m$]
φ_{0}	no-load phase shift between voltage and current	[*rad*]
φ_{k}	short-circuit phase shift between voltage and current	[*rad*]
Φ	magnetic flux	[*Wb*]
Φ_{p}	pole magnetic flux	[*Wb*]
Φ_{PM}	permanent magnet magnetic flux	[*Wb*]
Φ_{s}	slot magnetic flux	[*Wb*]
Φ_{sp}	slot pitch magnetic flux	[*Wb*]
Φ_{t}	tooth magnetic flux	[*Wb*]
Φ_{y}	yoke magnetic flux	[*Wb*]
Φ_{δ}	air gap magnetic flux	[*Wb*]
Φ_{σ}	leakage magnetic flux	[*Wb*]
ψ	phase shift between back EMF and current	[-]
ψ	magnetic flux linkage time dependency	[*Wb*]
τ_{dif}	differential leakage inductance factor	[-]
ω	mechanical angular speed	[$rad.s^{-1}$]
ω_{1}	power source angular frequency	[$rad.s^{-1}$]
ω_{ν}	mechanical angular speed of ν-th harmonic component	[$rad.s^{-1}$]

Table of Contents

Introduction....15
1 Design of Electric Machines and Related Standards....17
2 Power Equation for Rotary Electric Machines....19
3 The Law of Similarity and Growth....27
3.1 Properties of Machines with Identical Linear Current Density *A*....27
3.2 Properties of Machines with Equal Winding Current Density *J*....28
3.3 Properties of Machines with Linear Current Density Proportional to $\sqrt{x}$....29
3.4 Comparison of Approaches to Design of Similar Machines....29
3.5 Estimation of Weight of a Machine Group, Rise of Weight while Increasing Power....31
4 Winding of Electric Machines....33
4.1 Distributed Windings....34
4.2 Classification and Nomenclature of Winding Components....37
4.3 Classification and Nomenclature of DC Windings....40
4.4 Classification and Nomenclature of AC Windings....42
4.5 Winding Overhangs....45
5 Magnetic Circuits of Rotary Electric Machines....49
5.1 Magnetic Circuit Materials....49
5.2 The Mechanism of Generation of Iron Core Losses....50
5.3 Design of Magnetic Circuit....53
5.3.1 Magnetic Field in Teeth of an Electric Machine....53
5.3.2 Magnetic Field Distribution in the Armature Yoke....56
5.3.3 Magnetic Field of Excitation Poles and Yoke....59
5.3.4 Air Gap Magnetic Field....62
5.4 Saturation of the Magnetic Circuit and Related Characteristics....65
6 Equivalent Circuit Parameters....67
6.1 Winding Resistances....67
6.2 Machine Inductances....70
6.2.1 Magnetizing Inductance....70
6.2.2 Leakage Inductance....72
6.3 „Iron Resistance“....74
7 Losses in Electric Machines....75
7.1 I^2R (Joule) losses....75
7.2 Iron Core Losses....76
7.2.1 Losses Generated by Magnetizing Magnetic Flux....76
7.2.2 Pulsation Losses....77
7.2.3 Surface Losses....78
7.3 Permanent Magnet Losses....79
7.4 Mechanical Losses....80
7.4.1 Rotor Movement Caused Losses....80
7.4.2 Losses Caused by Brush Friction....81
7.5 Additional Losses....82

7.6 Pulse-Width Modulation Losses....82
7.7 Machine Efficiency....82
8 General Approach for Design of an Electric Machine....83
9 Specific Parts of DC Machine Design....85
9.1 Calculation of Fundamental Dimensions of the Machine....85
9.2 The design of DC Machine Excitation....89
9.3 The Design of Interpoles and Compensation Winding....93
9.4 Commutator Design....97
10 Specific Parts of Design of Synchronous Machines....99
10.1 Determination of Fundamental Machine Dimensions....100
10.2 The Design of Excitation of Synchronous Machines....104
10.3 Damper Design....110
11 Specific Parts of Design of Induction Machines....111
11.1 The Determination of Fundamental Dimensions of the Machine....112
11.2 The Design of Induction Machine Rotor....115
11.3 Equivalent Circuit Parameters and Important Points of Machine Characteristics....121
12 Notes to the Design of Special Types of Electric Machines....124
12.1 Synchronous Reluctance Machines....124
12.2 Switched Reluctance Machines....126
12.3 Axial Machines....128
12.4 Linear Machines....130
Appendix 1: Flowchart of the DC Machine Design....133
Appendix 2: Flowchart of the Synchronous Machine Design....134
Appendix 3: Flowchart of the Induction Machine Design....135

Introduction

Dear colleagues,
you have just obtained the lecture notes of Design of electric machines 1, a part of the series of subjects of this name, which is focused on electromagnetic design of rotary electrical machines. Considering a large number of boundaries to other parts of electrical engineering these notes cannot even try to clarify all the problems related to electric machines including their design, thus they are focused on the core of the design of electric machines themselves. These boundaries include knowledge of the principle of the function of electric machines as introduced in courses of Electrical Machines and Theory of electrical machines 1 and 2, the knowledge of fundaments of theory of electromagnetic field and the knowledge of electrical materials used fro electrical machines. The course of Design of electric machines 1 is the followed by identically named subject distinguished by number 2, which introduces specific constructional solutions supplemented by thermal and ventilation calculations.

Considering amount of relations to other courses, which introduce theoretical fundaments and derivations of phenomena practically used in Design of electric machines 1, these derivations are not included in these lecture notes while only results are presented. In case of included derivations these are included especially as a demonstration of approach to solved problem or as an extension of earlier obtained knowledge by parts, which do not appear in other subjects or which are hard to find in other literature.

From the references point of view the content of these lecture notes uses mainly earlier work of doc. Ing. Josef Červený, CSc., who summarized most of findings from other literature and his professional life in his two publications named *Přehled konstrukce elektrických strojů točivých* [1] (in Czech only) and *Stavba elektrických strojů* [2] (in Czech only), which formed first unofficial lecture notes to subjects to courses of Design of electrotechnical devices and Design of electric machines 1 and 2. These fundamental parts were supplemented by calculation methods mentioned in *Berechnung elektrischer Maschinen* [3] (in German only), *Stavba elektrických strojů* [4] (in Czech only) and *Vinutí elektrických strojů točivých* [5] (in Czech only). These, from today's point of view classical literature, was further supplemented partly by findings arising from the research performed at the faculty of Electrical Engineering and partly from current publications from conferences with focus on electrical machines. Since current literature often omits theoretical fundaments of certain parts of the calculation of electrical machines, it is also suitable to recommend publication from the 50's of 20th century as extending literature as it includes deeper analyses of some fundamental principles. The list of such publications would include e.g. *Teorie elektrických strojů* by prof. Bašta [6] (in Czech only) or five part series of books named *Elektrische Maschinen* by Rudolfa Richter, which forms the source of many later publications dealing with electric machines which appeared on the area of former Czechoslovakia..

The lecture notes of Design of electric machines 1 are divided into two main parts. The first part is formed by chapters 1 - 7 which include general design approaches universally valid for any type of electrical machine independently on its working principle and topology. In the second part of the lecture notes (chapters 8 - 12) these approaches are pplied to certain types of electric machines and

they are supplemented by specific parts which are not generally valid for other types of machines or their topologies. In other meaning, the first part of the lecture notes may be considered as a list of “ingredients” which knowledge is necessary for usage in a “recipe book” formed by second part.

As noted before, it is not practically possible to include the whole problem of the electric machines as electromechanical converters in a single publication. From those most known which could not be included it is possible to mention the claw pole synchronous machine, shaded-pole induction motor or more or less exotic types of machines like Schrage motor. Even though historic distribution of these topologies it is a matter of dear reader – electric machine student – to find related resources, in printed form in libraries or in electronic form in databases which can can be accessed through our university subscription service, as these overcome the possibilities of the course of Design of electric machines 1.

Even though mentioned limitations I do believe, that these lecture notes will remain your resource even after finishing your studies and that they provide you comprehensible explained compact approach to the design of electric machine. Use in peace.

In Přeštice, 23. 3. 2021 (Czech original)
??. ?. ???? (English translation)

Karel Hruska

1 Design of Electric Machines and Related Standards

As well as other industrial branches, even the design and manufacture of electric machines are bound by standards, which state the requirements on their properties, manufacture, usage and function. These standards have to be considered already during the machine design – whether standards related to used materials and their properties (wire cross-sections, properties of uses steel sheets etc.) or standards related to final duty of manufactured machines (regimes S#, cooling type, cooling medium etc.). All these standards by certain parts affect the final look and construction of the electric machine, which should be the output of the whole design process.

The technical standards are divided regarding their focus to certain groups which include most of information relating to solved problem. Historically the original series of standards in electrical engineering in the Czech Republic is denoted as ČSN 35 0000. This series is nowadays deprecated as certain parts are being replaced by newer international standards. However certain standards from this series are still valid. The standards of series ČSN 35 000 include general requirements on electric machines.

Currently the set of standards ČSN 35 0000 is almost completely replaced by series ČSN 60034, which numbering is identical with international standards and which includes the requirements and properties of industrial rotary electric machines. This set of standards in each part unifies tests of electric machines, testing conditions and method of evaluation of the results. Some of mentioned parts still refer the ending series ČSN 35 0000. Furthermore the series ČSN 60 034 includes requirements and method of declaring of protection class of electric machines (IP code), cooling of electric machines (IC code) and construction and mounting arrangement (IM code). With the design of the electric machine itself parts including evaluation of insulation system are bound. For the purpose of design of electric machines supplied from power converters the international standard ČSN CLC/TS 60034-25 forms an important part, which provides a comprehensive guidelines to design and includes notes about properties of machines designed specifically for feeding from power converters.

The set of standards ČSN 60034 is supplemented by a set ČSN 60349. This series of standards deals specifically with rotary electric machines designated for electric traction. This series extends the ČSN 60034 by specific requirements on tests and specifying e.g. definitions of thermal classes for traction environment.

The properties and tests of transformers are located in ČSN 60076.

The materials for electric machines are standardized in several sets of standards on base of the usage and composition of the material. For the purpose of the design of the magnetic circuit the crucial standard is ČSN 10106, which includes form and properties of steel sheets used in electrical engineering. This standard provides information about minimal B-H curves, which should be fulfilled by certain steel type and information about requirements on steel and insulation thickness (and thus lamination fill factor). The designation of steel sheets and losses is also included here.

The winding insulation system properties are then standardized in set ČSN 60085, which provides information about thermal evaluation and designation of the insulation system – so called thermal

class. Winding wires themselves are (including necessary insulation layers of the wires) unified in series ČSN 60317. This set of standards includes both round wires as well as wires of rectangular cross-section (including round edges). Depending on type, composition and insulation class the dimensions of the wires, insulation thicknesses, resistances and dielectric and mechanical properties are standardized here.

In relation to wide usage of permanent magnets the set ČSN 60404 becomes on importance, as it deals with magnetic materials. This standard in its part ČSN EN 60404-8-1 specifies magnetically hard materials (permanent magnets). It is necessary to note, that this standard uses exclusively the SI unit system, while the CGS designation of permanent magnets is relatively common all over the world.

Considering the fact that there can be a very specific requirements laid on the design of the electric machine, it is not possible to consider the above mentioned list of standard as comprehensive, rather as a necessary fundament for the design of the electric machine. As an example an additional requirement on resistance against mechanical shock can serve. This is specified in ČSN 62262 and it is denoted by an IK code, which may be shown on the name plate of the machine. Further boundaries may be formed by independent standards of the machine manufacturers.

2 Power Equation for Rotary Electric Machines

The core of the design of the electric machines is so-called power equation. Thus equation describes the relation between dimensions of an electric machine and its power or its torque. As shown later the relation for the design of a machine is identical whether a direct current machine or alternating current machine is being designed.

In terms of the design a lot of variables is being used while the crucial difference between the design of an AC or DC machine lies in consideration of RMS values of voltages and currents in case of the design of an AC machine. On the other hand in case of a DC machine the average values are used. In case of magnetic field variables (magnetic flux density B, magnetic flux Φ, magneto-motive force F, or Θ, magnetic field strength H) in both cases maximal values (amplitudes) of these variables are being used.

The design is then commonly performed for required power or torque, while both of them is given by so-called inner machine power P_i, which is proportional to the back EMF and machine current. Let us now compare both AC and DC current from the back EMF point of view.

Direct Current Machines	Alternating Current Machines
The voltage induced into a single winding turn is defined as $$U_{ic} = B_{av} l v \quad . \qquad (2.1)$$ To obtain average value of the voltage, it is also necessary to consider the average value of the air gap magnetic flux density, i.e. $$B_{av} = \frac{1}{t_p} \int_{t_p} B(\xi) d\xi \quad . \qquad (2.2)$$ The average value is then an integral of a flattened curve of the air gap magnetic flux density with magnitude of B_δ over one pole pitch t_p. This integral then corresponds with hatched area in Fig. 2.1 and it is proportional to the pole shoe width b_{ps}.	The voltage induced into a single winding turn is defined as $$u_i = -\frac{d\Phi}{dt} \quad . \qquad (2.3)$$ Let us now consider a purely sine-wave shaped magnetic flux time dependency $$\Phi(t) = \Phi \cos \omega_1 t \quad . \qquad (2.4)$$ The magnitude of the total magnetic flux in the air gap must be then derived from the average value of the air gap magnetic flux density. Considering harmonic layout of the B_δ, it is $$B_{av} = \frac{1}{t_p} \int_{t_p} B_\delta \sin \frac{\pi}{t_p} \xi \, d\xi = \frac{2}{\pi} B_\delta \quad . \qquad (2.5)$$

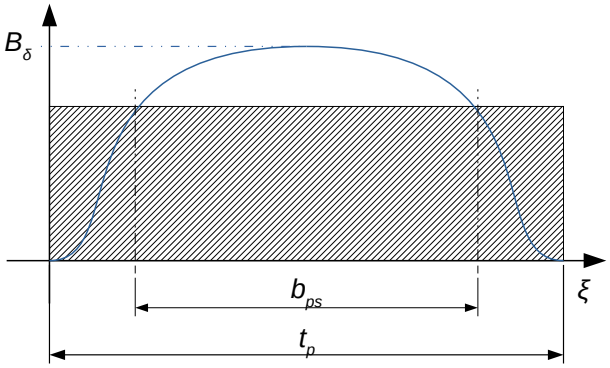


Fig. 2.1: DC Machine Air Gap Magnetic Flux Density

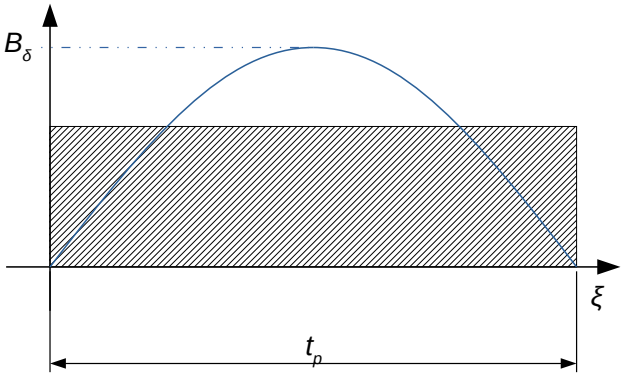


Fig. 2.2: AC Machine Air Gap Magnetic Flux Density

For the purpose of determination of the average value of the air gap magnetic flux density the pole coverage factor α_δ is defined as

$$\alpha_\delta = \frac{b_{ps}}{t_p} \quad , \tag{2.6}$$

which allows determination of the average value of the air gap magnetic flux density as

$$B_{av} = \alpha_\delta B_\delta \quad . \tag{2.7}$$

The speed of the movement of a conductor of a DC machine is then

$$v = \omega r = \frac{\omega_1}{p} r \quad , \tag{2.8}$$

where r is the armature radius given by its diameter D_1,
ω is mechanical angular speed,
ω_1 is the electrical angular frequency in winding conductors
and p is the number of machine pole pairs.

The relation (2.8) may be then modified to

$$v = \frac{2\pi f}{p} \cdot \frac{D_1}{2} = \frac{\pi D_1}{p} f \quad , \tag{2.9}$$

where the ratio of armature circumference and the amount of pole-pairs is equal to two pole pitches, thus we obtain

$$v = 2 t_p f \quad . \tag{2.10}$$

After insertion to (2.1) the result is

If we compare the result of the relation (2.5) with (2.7) for DC machines, it is obvious that even for AC machines an electromagnetic pole coverage factor may be introduced and it is equal to $\alpha_\delta = 2/\pi$.

The magnitude of air gap magnetic flux of an AC machine is then

$$\Phi = \int_{S_\delta} B_{av} dS = \\ = \int_{t_p} \int_{l} \alpha_\delta B_\delta dl\, d\xi = \alpha_\delta B_\delta t_p l \tag{2.13}$$

By derivation of (2.4) we obtain

$$u_i = -\frac{d}{dt}\left(\Phi \cos \omega_1 t\right) = \omega_1 \Phi \sin \omega_1 t \quad , \tag{2.14}$$

thus a harmonic voltage curve with a magnitude of

$$U_{im} = \omega_1 \Phi = 2\pi f \Phi \quad . \tag{2.15}$$

Its RMS value is then

$$U_i = \frac{2\pi}{\sqrt{2}} \Phi f \quad . \tag{2.16}$$

For a winding with N_s winding turns in series and winding factor k_{w1} we obtain the final relation

$$U_i = \frac{2\pi}{\sqrt{2}} N_s k_{w1} \Phi f \quad , \tag{2.17}$$

which is often simplified to a form

$$U_i = 4{,}44\, N_s k_{w1} \Phi f \quad . \tag{2.18}$$

$$U_{iv} = \alpha_\delta B_\delta l 2 t_p f = 2 \Phi f \quad . \tag{2.11}$$

But, the winding is composed of N_s winding turns in series which are affected by winding pitch factor k_{y1} and each coil turn is formed by two coil sides – wires – in series. In case of a DC machine the back EMF relation is

$$U_i = 4 N_s k_{y1} \Phi f \quad . \tag{2.12}$$

If we compare both results of back EMF calculation, we obtain (presuming identical amount of winding turns in series, winding factors, frequency and magnetic flux) following

$$\frac{U_{iAC}}{U_{iDC}} = \frac{\frac{2\pi}{\sqrt{2}} N_s k_{w1} \Phi f}{4 N_s k_{y1} \Phi f} = \frac{\pi}{2\sqrt{2}} = k_B \quad . \tag{2.19}$$

This result is often call magnetic field shape factor. Using this facto it is possible to write the back EMF relation generally as

$$U_i = 4 k_B N_s k_{w1} \Phi f \quad , \tag{2.20}$$

whereas depending on type of the machine the value of k_B = 1 corresponds with DC machines and k_B = 1.11 corresponds with AC machines.

The magnetic field shape factor is then defined as a ratio between RMS and average value of the air gap magnetic flux density i.e.

$$k_B = \frac{B_{rms}}{B_{av}} \quad . \tag{2.21}$$

The electromagnetic pole coverage factor α_δ gives the ratio between average value of the air gap magnetic flux density and its amplitude, thus it is defined as

$$\alpha_\delta = \frac{B_{av}}{B_\delta} \quad . \tag{2.22}$$

In case of direct current machines, permanent magnet machines and electrically excited synchronous machines an additional mechanical pole coverage factor α_m appears. There is a relation between both pole coverage factors (electromagnetic and mechanical), while their value is relatively close and in some literature they are not distinguished. The mechanical pole coverage factor is then defined as

$$\alpha_m = \frac{b_{ps}}{t_p} \tag{2.23}$$

and in value the α_δ is close to α_m whereas α_m is greater than α_δ. For an ideal sine wave shape of the air gap magnetic flux density it is valid that the values of both factors are

$$\alpha_\delta = \frac{2}{\pi} \wedge k_B = \frac{\pi}{2\sqrt{2}} \quad , \tag{2.24}$$

whereas for fundamental iteration of the design of the machine it is possible to use these values. In dependence on shape of the pole shoes or permanent magnets (DC machines, synchronous machines, permanent magnet machines) and saturation (induction machines) the values of these coefficients differ, whereas α_δ increases and k_B slightly drops.

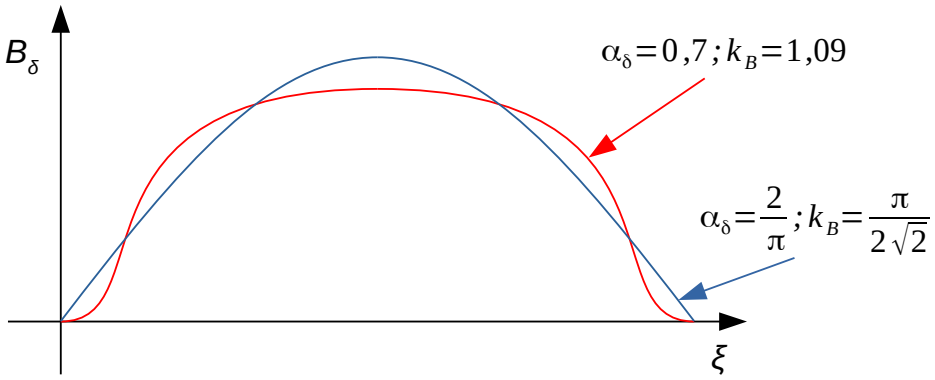


Fig. 2.3: The values of factors α_δ and k_B for different shapes of air gap magnetic flux density

The power of the machine may be then defined on base of its inner power P_i. In case of DC machines this power corresponds with real power whereas in case of AC machines it is physically inner apparent power S_i.

Direct Current Machines	Alternating Current Machines
Inner power of the machine is $$P_i = U_i I \quad , \qquad (2.25)$$ thus after substitution of back EMF $$P_i = 4 N_s k_{y1} \Phi f I \quad . \qquad (2.26)$$ Now let us introduce linear current density defined by $$A = \frac{\sum I}{\pi D_1} \quad , \qquad (2.27)$$ whereas the sum of machine currents is given by the amount of machine conductors V multiplied by current through these conductors I_c. From the amount of the winding turns in series and amount of winding parallel branches $a_=$ we get $$A = \frac{V I_c}{\pi D_1} = \frac{2 N_s a_= \frac{I}{a_=}}{\pi D_1} = \frac{2 N_s I}{\pi D_1} \quad . \qquad (2.28)$$ Thus the machine current is $$I = \frac{\pi D_1 A}{2 N_s} \quad . \qquad (2.29)$$ The inner power of the machine is after substitution	The inner apparent power of an m-phase machine is $$S_i = m U_i I \quad , \qquad (2.31)$$ which gives after substitution by back EMF $$S_i = m 4 k_B N_s k_{v1} \Phi f I \quad . \qquad (2.32)$$ Identically as in case of the direct current machines we can introduce the linear current density of an m-phase machine as $$A = \frac{2 m N_s a_\sim \frac{I}{a_\sim}}{\pi D_1} = \frac{2 m N_s I}{\pi D_1} \quad , \qquad (2.33)$$ and the current through the machine is then $$I = \frac{\pi D_1 A}{2 m N_s} \quad . \qquad (2.34)$$ The inner apparent power of an AC machine results $$S_i = m 4 k_B N_s k_{v1} \Phi f \frac{\pi D_1 A}{2 m N_s} \qquad (2.35)$$ which is after modification $$S_i = 2 \pi A k_{v1} k_B D_1 \Phi f \quad . \qquad (2.36)$$

$$P_i = 4 N_s k_{y1} \Phi f \frac{\pi D_1 A}{2 N_s} = 2 \pi A k_y D_1 \Phi f \tag{2.30}$$

In both cases we can replace the magnetic flux by

$$\Phi = \alpha_\delta B_\delta t_p l \quad , \tag{2.37}$$

frequency by

$$f = \frac{pn}{60} \tag{2.38}$$

and pole pitch by

$$t_p = \frac{\pi D_1}{2 p} \quad . \tag{2.39}$$

For a DC machine the inner power results

$$P_i = 2 \pi \alpha_\delta B_\delta A k_{y1} D_1 \frac{\pi D_1}{2 p} l \frac{pn}{60} \quad , \tag{2.40}$$

which is after modification

$$P_i = \frac{\pi^2}{60} \alpha_\delta B_\delta A k_{y1} D_1^2 l n \quad . \tag{2.41}$$

Now we can recognize the Esson's factor of DC machines

$$C = \frac{\pi^2}{60} \alpha_\delta B_\delta A k_{y1} \quad , \tag{2.42}$$

while obtaining the final form of the power equation

$$P_i = C D_1^2 l n \quad . \tag{2.43}$$

In case of AC machine the result is

$$S_i = 2 \pi \alpha_\delta B_\delta A k_{v1} k_B \frac{\pi D_1}{2 p} l D_1 \frac{pn}{60} \quad , \tag{2.44}$$

which gives

$$S_i = \frac{\pi^2}{60} \alpha_\delta B_\delta A k_{v1} k_B D_1^2 l n \quad . \tag{2.45}$$

The constants then give the Esson's factor for AC machines

$$C = \frac{\pi^2}{60} \alpha_\delta B_\delta A k_{v1} k_B \tag{2.46}$$

and we obtain identical form of the power equation as for the DC machines

$$S_i = C D_1^2 l n \quad . \tag{2.47}$$

If we compare Esson's factor as derived for DC and AC machines, then for identical values of air gap magnetic flux densities, linear current densities the only differences are formed only by coefficients α_δ, k_{y1} resp. k_{w1} a k_B. Based on differences in construction of each type of machine and further consequences it is possible to claim following:

- the electromagnetic pole coverage factor α_δ is commonly higher for DC machines than for AC machines
- the winding pitch factor k_{y1} is in any case (except AC windings with amount of slots per pole and phase equal to q = 1) greater than the winding factor k_{w1}, since the winding factor is defined as

$$k_{w1} = k_{y1} k_{d1} \quad , \tag{2.48}$$

where k_{d1} is the winding distribution factor, which is not defined for DC windings and for AC windings with nominator of the amount of slots per pole and phase greater than one it results always lower than one

- the magnetic field shape factor k_B is for DC machines approximately equal to one while for AC machines it is approximately 1.11, thus for DC machines it is always lower than for AC machines

In the end it is possible to state, that for DC and AC machines the following relation is valid

$$\left[\alpha_\delta k_{y1}\right]_{=} \simeq \left[\alpha_\delta k_{w1} k_B\right]_{\sim} \quad . \tag{2.49}$$

Thus, both types of machines have in case of identical values of magnetic fields and currents comparable electromagnetic usage.

The relation of the inner power from (2.43) or (2.47) to its output power is then given by the electromotive force factor k_E, which gives also the ratio between the back EMF and terminal voltage

$$k_E = \frac{U_i}{U} \quad . \tag{2.50}$$

The value of k_E is then lower than one for electric motors and larger than one for electric generators.

The values of k_E significantly differ according to machine type and it is necessary to determine the correct value from equivalent circuit parameters and voltage drops on them. In general, the values of k_E are close to one, but specific types of machines might have k_E significantly different (BLDC machines) or the k_E might be equal to one (electrically excited synchronous machines; in this case the difference in k_E may be compensated by correction of excitation of the machine) or it can be used as an undefined variable equal to one (synchronous reluctance machines).

Furthermore on base of the power equation it is possible to derive the torque equation

$$M_i = \frac{S_i}{\omega} = \frac{C D_1^2 l n}{\frac{\pi n}{30}} = \frac{30}{\pi} C D_1^2 l \quad , \tag{2.51}$$

where the Esson's factor for torque equation verges to

$$C_E = \frac{30}{\pi} C = \frac{30}{\pi} \cdot \frac{\pi^2}{60} \alpha_\delta B_\delta A k_{w1} k_B \quad , \tag{2.52}$$

which results in

$$C_E = \frac{\pi}{2} \alpha_\delta B_\delta A k_{v1} k_B \tag{2.53}$$

and the torque equation is then

$$M_i = C_E D_1^2 l \quad . \tag{2.54}$$

This means, that the volume of the machine is directly bound with the torque of the machine, not with its power. Furthermore from both equation it is obvious, that power nor torque of the machine

depend on the amount of machine phases. Thus, the increase of amount of machine phases does not bring any advantage from the power nor torque point of view.[1]

If an increase of power of the machine is required it may be achieved either by increase of its volume or by increase of its speed. But the increase of the speed is often limited by rotor outer diameter[2] which, together with bending of long and thin rotors, forms a certain physical border, over which traditional electric machines cannot be manufactured. This border is currently considered to be approximately 2 000 *MW*.

From electromagnetic usage point of view (Esson's factor) the limits are approximately following:

- the electromagnetic pole coverage factor is given by machine construction and it is always lower than 1
- the winding pitch factor k_{y1}/winding factor k_{w1} is always lower than 1
- the air gap magnetic flux density depends on type and size of the machine and it ranges from tenths of Teslas (small DC motors with ferrite magnets) up to values about 1.1 T[3] (large induction machines, synchronous generators, rare earth permanent magnet machines)
- the linear current density is extremely variable and it depends on size, type and cooling of the machine. E.g. for generators it is common to use

  A = 15 – 70 *kA/m* – for air cooled machines
  15 *kA/m* – small machines with shallow slots
  70 *kA/m* – large machines with deep slots

  A ~ 100 *kA/m* – hydrogen cooled machines
  A ~ 200 *kA/m* – machines cooled with combination water + hydrogen
  A ~ 300 *kA/m* – machines with superconducting winding

  The value of linear current density is often being chosen in combination with current density J (so-called AJ-criterion expressing thermal load of the machine), whereas the current density is commonly taken within period J = 3 – 15 *A/mm*^{2}, where lower values are used for poorly cooled machines of lower thermal class and higher values correspond with machines with better cooling and higher insulation thermal class.

The dimensions of the machines are often being chosen on base of combination (ratio) of D_1/l (so-called slimness ratio) to achieve optimal length of winding overhangs. The value of D_1 then must be chosen together with D_e to achieve standard shaft height. The power of the machine is then being tuned by its length, which leads to design of several power sets of machines with identical shaft height, where a single machine cross-section is being used for multiple machines of different power and thus lengths of the machine.

During the derivation above the D_1 was used for armature diameter, i.e. diameter of that part of the machine, which is equipped with slots with winding which is used for obtaining electrical power or

1 It is important to note, that this is true only for machines without special power feeding.
2 For $2p$ = 2 pole synchronous generators working at 50 or 60 *Hz* the limiting rotor diameter is approximately 1.2 *m*.
3 The usage of high magnetic flux densities lead to problems with excitation and saturation of teeth, which could be overcome by using slotless windings in combination with superconducting field winding.

which is being fed by power which is transformed from/to mechanical power. In case of synchronous machines the D_1 corresponds with inner diameter of the stator stack, in case of DC machines the D_1 dorresponds with rotor outer diameter. T means that the designation mach change depending on type of the machine and its topology. The most common layout of a machine with outer stator and inner rotor is shown in Fig. 2.4, whereas D_e is here the outer diameter of the stator stack, D_1 is inner diameter of the stator stack (=armature diameter), D_2 is outer rotor stack diameter and D_i is the inner diameter of the rotor stack. The length of the stator stack (i.e. without winding overhangs) is here for the purpose of simplicity denoted as l only, although in general it may include also several radial cooling ducts.

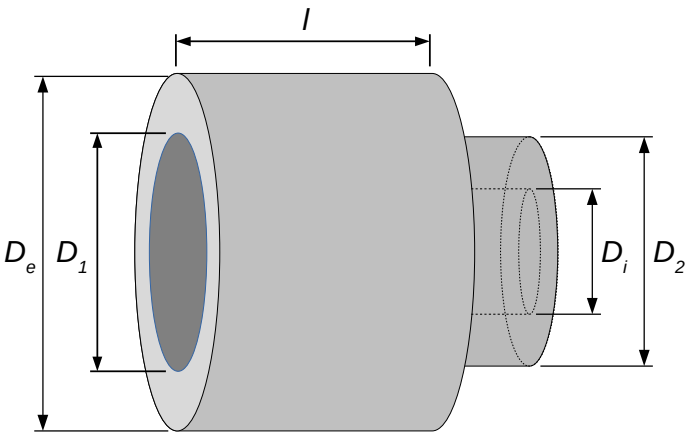


Fig. 2.4: Fundamental machine dimensions

3 The Law of Similarity and Growth

One of important conclusions of the power equation is that if there is a certain dimension limit, e.g. in diameter, it is possible to increase its power only by increase of the length of the machine while keeping constant speed. Reversely, in case of requirement of slight lowering of the machine power it is possible to use previously mage design and modify only the length of the machine to obtain a new machine. This approach brings more than economical advantages – except time savings for calculation of a new design, starting its manufacture from the scratch etc., it is possible on base of previous experience to predict the properties of a "new" machine.

This principle is generally designated as a law of similarity and growth and it is commonly used for a quick estimation of price of a new machine. Based on similarity of dimensions with other manufactured machines it is possible to estimate relatively accurately costs for manufacture of a new machine and to make an initial design with a good accuracy on base of experience with previously designed machines.

According to possibilities and properties of the original design it is possible to focus the design of a new machine into three directions, which will guarantee a similarity with previous machines. Since the design of electric machines includes many parameters, which may affect the properties of the designed machine, let us now consider fixing the values of the fundamental ones – machine speed n, number of poles $2p$, air gap magnetic flux density B_δ and magnetic pole coverage factor α_δ, magnetic field shape factor k_B, winding factor k_{w1} and electromotive force factor k_E. As variable parameters would remain the armature diameter D_1 and its length l. Let us presume replacement of both of these dimensions by a single dimension x, which would express the length of an unknown machine l_x in relation to length of a known machine l_1. Expressed in per units the x is:

$$x = \frac{l_x}{l_1}[p.u.] \tag{3.1}$$

From other parameters in the power equation only linear current density A and current density J remain variable. Now let us presume following options for design of a new electric machine:

1) constant linear current density A, variable winding current density J
2) constant winding current density J, variable linear current density A
3) as a compromise let us lie A proportional to square root of x (the reason will be explained)

3.1 Properties of Machines with Identical Linear Current Density *A*

Using constant linear current density causes fixing of the last variable from Esson's factor, which is now

$$C = \frac{\pi^2}{60}\alpha_\delta B_\delta A k_{w1} k_B = const. \tag{3.2}$$

According to power equation the power of the machine will rise with third power of x, since

$$S_i = C D_1^2 l n \simeq x^2 . x = x^3 \quad . \tag{3.3}$$

The current through one slot of the machine I_s is given by the slot pitch t_s and linear current density

$$I_s = A\,t_s \quad , \tag{3.4}$$

where the slot pitch is bound with the diameter of the machine, which is growing with x, hence

$$t_s = \frac{\pi D_1}{Q} \simeq x \quad , \tag{3.5}$$

thus the slot current is proportional to the multiplication of Ax.

From the current density point of view the slot current may be written as

$$I_s = S_s J \quad , \tag{3.6}$$

where the slot area is given by the multiplication of its width and depth, thus by the dimensions scaled (while having constant amount of slots) together with machine diameter. Its area is then proportional to

$$S_s = b_s h_s \simeq x\,.\,x = x^2 \tag{3.7}$$

and the current through a slot is proportionalto Jx^2. This leads to relation

$$Ax \simeq Jx^2 \quad , \tag{3.8}$$

from which, for constant A, results

$$J \simeq \frac{1}{x} \quad . \tag{3.9}$$

Thus with growing dimensions of the machine the current density in winding drops, which may result in low material usage and thus higher machine weight.

3.2 Properties of Machines with Equal Winding Current Density *J*

If the current density J is set as constant through a set of machines, it is possible on base of (3.9) write

$$A \simeq Jx \tag{3.10}$$

thus for constant J the linear current density is proportional to

$$A \simeq x \quad . \tag{3.11}$$

Identical proportionality will appear also in Esson's factor, thus for torque and power we obtain

$$M \simeq S_i = C\,D_1^2\,l\,n \simeq x\,.\,x^2\,.\,x \simeq x^4 \quad . \tag{3.12}$$

In this case the power of the machine will rice with fourth power of the dimensions, however due to increasing dimensions of the slot problems with cooling of the winding may appear.

3.3 Properties of Machines with Linear Current Density Proportional to $\sqrt{x}$

The dependence of the linear current density on square root of relative dimension of the machine x forms a compromise between both previously mentioned solutions. Using identical approach as in previous cases, it can be proven, that the Esson's factor is also proportional to the square root of x, thus for torque and power we obtain

$$M \simeq S_i = C\, D_1^2 l n \simeq \sqrt{x}.x^2.x \simeq x^{3,5} \quad . \tag{3.13}$$

The proposed machine derived from other ones using this approach will combine partially advantages and partially disadvantages of both previous approaches, whereas its suitability may be evaluated on base of comparison of other machine parameters.

3.4 Comparison of Approaches to Design of Similar Machines

To have an adequate comparison of designed machines it is necessary to move from purely electromagnetic parameters also to economical indicators like price of the machine, its specific mass and the mass to power ratio, which is currently very appreciated by the customers. The previous sections include fundamental considerations for linear current density A, winding current density J, power and torque of the machine M, P and Esson's factor C. The mass of the machine is then proportional to the volume of the machine, while having identical materials, the price will grow the same way. It is possible to write

$$m, c \simeq V \simeq x^3 \quad . \tag{3.14}$$

The next parameter to be compared is the specific mass of the machine, which is given as a ratio between the mass of the machine and its power

$$m_s = \frac{m}{S} \quad , \tag{3.15}$$

whereas the power differs for each of mentioned approaches.

From thermal point of view it is necessary to estimate the total winding losses. They may be simply estimated as

$$\Delta P_j \simeq R I^2 \simeq \frac{1}{\gamma} \cdot \frac{l_w}{S_s} \cdot \left(J S_s\right)^2 \simeq \frac{1}{\gamma} \cdot \frac{x}{x^2} \cdot J^2 x^4 \simeq J^2 x^3 \quad . \tag{3.16}$$

Also in this case the result will be different for each of mentioned approaches.

The next important component of losses are the iron core losses. They are, in general, proportional to the mass of the machine and for constant saturation they do not change. Thus it is possible to write

$$\Delta P_{Fe} \simeq \Delta p_{Fe} m_{Fe} \simeq x^3 \quad . \tag{3.17}$$

The total losses may be then simply estimated as an average between winding losses and iron core losses and they will be also specific for each of mentioned approaches.

The efficiency may be evaluated on base of proportional losses, which may be defined as

$$\Delta p = \frac{\Delta P}{S} \quad . \tag{3.18}$$

These losses are cooled via outer surface of the machine, which is proportional to the square of the linear dimension of the machine

$$F \simeq x^2 \quad . \tag{3.19}$$

The temperature rise of the machine may be then considered as a ratio between machine losses ad its cooling area

$$\Delta \vartheta = \frac{\Delta P}{F} \quad . \tag{3.20}$$

For machines with frequent starts the start-up time forms an important parameter, which may be derived from the torque of the machine

$$M = J \frac{d\omega}{dt} \tag{3.21}$$

and have it as a ratio

$$t = \frac{J}{S} \quad , \tag{3.22}$$

whereas the rotor moment of inertia can be calculated approximately as

$$J = \frac{1}{2} m r^2 \simeq x^{3.} x^2 \simeq x^5 \quad , \tag{3.23}$$

thus the start-up time results

$$t = \frac{x^5}{S} \quad . \tag{3.24}$$

The overview of included results is includes in Tab. 3.1. The more favourable results are denoted by bold letters, the less favourable are suppressed by grey text colour. The comparison shows, that the design of machines with constant linear current density leads to a set of machines with constant specific mass and constant temperature rise. This approach leads to production of robust machines with well predictable temperature rise and it is often used for traction machines.

On the other hand the design of machines with constant winding current density leads in case of design of larger machines to decrease of specific mass, but also to increase of temperature rise. This effect may be suppressed by better cooling, however the advantage in decrease of specific mass is the main point which leads to usage of this approach mainly in field of traction machines, where the mass of the machine is an observed parameter.

The last approach then forms a kind of conservative average between both previously mentioned. In none of parameters it can be marked as preferable, but similarly in none of parameters it is disadvantageous. Because of this result this approach is preferred while designing of sets of small industrial machines. The next advantage can be seen in graphical comparison of growth of the Esson's factor in dependence of dimension x (Fig. 3.1). As the figure shows, while considering growth of linear current density proportionally to $\sqrt{x}$, the Esson's factor grows significantly faster than when constant current density J is considered.

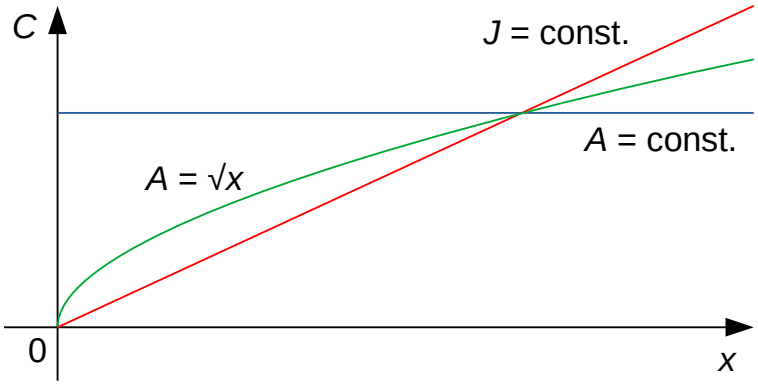


Fig. 3.1: The dependence of Esson's factor on linear dimension of the machine dimension x

Variable	Mark	Relation	Design Approach		
			A = const.	J = const.	$A = \sqrt{x}$
Linear current density	A	ad hoc	const.	x	$\sqrt{x}$
Winding current density	J	(3.8)	$1/x$	const.	$1/\sqrt{x}$
Power, torque	S, M	(3.3)	x^3	x^4	$x^{3,5}$
Esson's factor	C	(3.2)	const.	x	$\sqrt{x}$
Mass, price	m, c	(3.14)	x^3	x^3	x^3
Specific mass	m_s	(3.15)	const.	$\mathbf{1/x}$	$1/\sqrt{x}$
Winding losses	ΔP_j	(3.16)	x	x^3	x^2
Iron core losses	ΔP_{Fe}	(3.17)	x^3	x^3	x^3
Total losses	ΔP	---	$\mathbf{x^2}$	x^3	$x^{2,5}$
Specific losses	Δp	(3.18)	$1/x$	$1/x$	$1/x$
Cooling area	F	(3.19)	x^2	x^2	x^2
Temperature rise	$\Delta\vartheta$	(3.20)	**const.**	x	$\sqrt{x}$
Start-up time	t	(3.24)	x^2	$\mathbf{x}$	$x^{1,5}$

Tab. 3.1: Comparison of properties of machine sets designed by different approaches

3.5 Estimation of Weight of a Machine Group, Rise of Weight while Increasing Power

As show previous considerations in case of consideration of constant winding current density the power of the machine is proportional to the fourth power of its dimensions, thus its dimensions are proportional to the fourth root of the power of the machine

$$x = \sqrt[4]{S} \quad . \tag{3.25}$$

The mass of the machine is proportional to the third power of its dimensions, i.e.

$$m \simeq x^3 \simeq \left(\sqrt[4]{S}\right)^3 \simeq \sqrt[4]{S^3} \quad . \tag{3.26}$$

If we had a group of *n* machines of certain power, their mass would be proportional according to

$$m_g \simeq n\, m \simeq n \sqrt[4]{S^3} \quad . \tag{3.27}$$

But, if we design a single machine of *n*-times higher power, its size would be

$$x = \sqrt[4]{nS} \tag{3.28}$$

and its mass would increase to

$$m_1 \simeq x^3 \simeq \sqrt[4]{(nS)^3} \quad . \tag{3.29}$$

Comparing both values, the mass of a group of machines rises in comparison to a single machine in ratio

$$k = \frac{m_g}{m_1} = \frac{n \sqrt[4]{S^3}}{\sqrt[4]{(nS)^3}} = \frac{n}{n^{\frac{3}{4}}} = n^{\frac{1}{4}} = \sqrt[4]{n} \quad . \tag{3.30}$$

This means, that two machines with output power equivalent to a single machine would be 1.19-times heavier than a single machine. In case of three machines this ratio rises to 1.32 etc. It is obvious, that from the mass point of view it is advantageous to have a single machine of higher power rather than a group of lower powered machines.

Let us now evaluate the efficiency of machines as it depends on their power. Let us presume machines with ratio of powers

$$\frac{S_2}{S_1} = 2 \quad . \tag{3.31}$$

The ratio of their dimensions will be then

$$k = \frac{x_2}{x_1} = \frac{\sqrt[4]{S_2}}{\sqrt[4]{S_1}} = \sqrt[4]{\frac{S_2}{S_1}} = \sqrt[4]{2} = 1.19 \tag{3.32}$$

and the rise of the mass is proportional to the third power of their dimensions

$$m = k^3 = 1{,}19^3 = 1{,}68 \quad . \tag{3.33}$$

The losses in both machines are also proportional to the third power of their dimensions, thus while considering equation of real and apparent power ($P = S$) we can compare their efficiencies as

$$\frac{\eta_2}{\eta_1} = \frac{\dfrac{2S_1 - 1{,}68\Delta P}{2S_1}}{\dfrac{S_1 - \Delta P}{S_1}} = \frac{S_1 - 0{,}84\Delta P}{S_1 - \Delta P} \quad , \tag{3.34}$$

Thus, with the growth of the dimensions and power also the efficiency of the machine increases.

4 Winding of Electric Machines

The windings of electric machines belong, together with permanent magnets, to only active parts of electric machines, since these are the only parts, which actively generate the magnetic field and/or induced voltage. In general any ordered system of conductors serving for generation of magnetic field/induced voltage may be named a winding. Based on this definition not only windings of electric machines, but also coils of chokes, speakers and actuators may be called “windings.”

A fundamental division of winding types may be done to concentrated and distributed windings. The concentrated windings have all turns concentrated in a volume of a single coil. Such a windings have winding factors very close to one and they are designed only to achieve required amount of coil turns and wire cross-section. Typical examples of this type of windings are transformer windings and field windings of synchronous AC machines and DC machines.

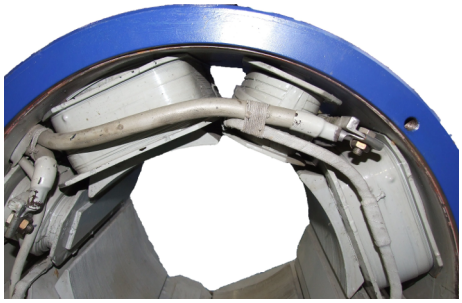


Fig. 4.1: Field Winding of a Direct Current Machine

For correct function of nowadays electric machines the distributed windings are most important. These windings are placed on the armature and they ensure their work as motors or generators. According to the direction of the magnetic flux through air gap, the distributed windings for traditional machines with radial magnetic flux direction are called drum windings, while windings of machines with axial direction of the magnetic flux are called disk windings. From design point of view both types of windings may be designed using identical methods while using identical or very similar relations, the main difference is then only the final construction of the winding itself.

In general it may be stated that the distributed windings have in dependence on purpose very variable topology, which may affect their design. In contrast to concentrated windings the properties of distributed windings may significantly affect the final behaviour of the machine – torque pulsations, noise, back EMF curve etc.

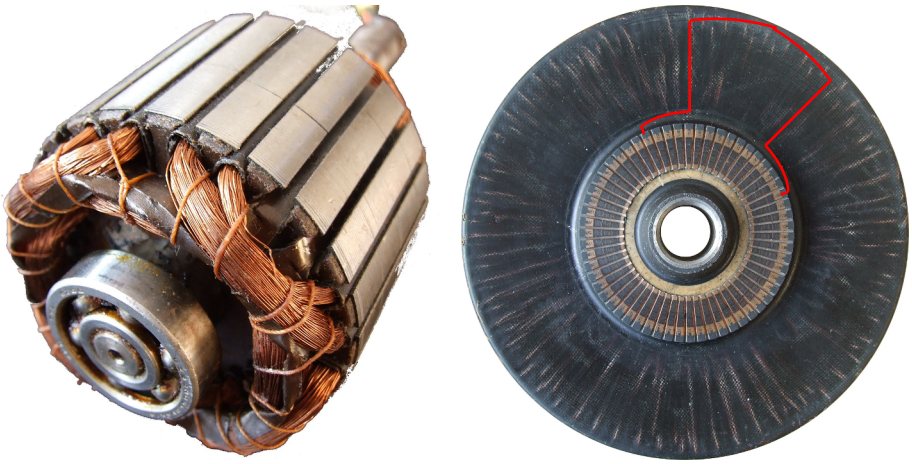


Fig. 4.2: Distributed drum winding (left) and a disk winding (right). The red line denotes the coil shape of the disk winding.

4.1 Distributed Windings

The fundamental element of distributed windings is a coil. Independently on its performance the fundamental topological parts of the coil can be recognized. These parts involve active parts – "coil sides" – and non-active parts – "winding overhangs," which connect coil sides. The coils may be then connected using coil wire or connection rings which are integrated in winding overhangs. From electromagnetic point of view the important parameters of a coil are the amount of the coil turns (recognized from total slot current) and the coil pitch. Although both parameters project into the electromagnetic design of the machine the coil pitch is used in the design of the winding topology, which precedes the machine design itself and which may be totally separated from the machine design (more machines may have identical basic winding topology). On the other hand the number of coil turns is specifically bound to a machine design and may not work with other machines.

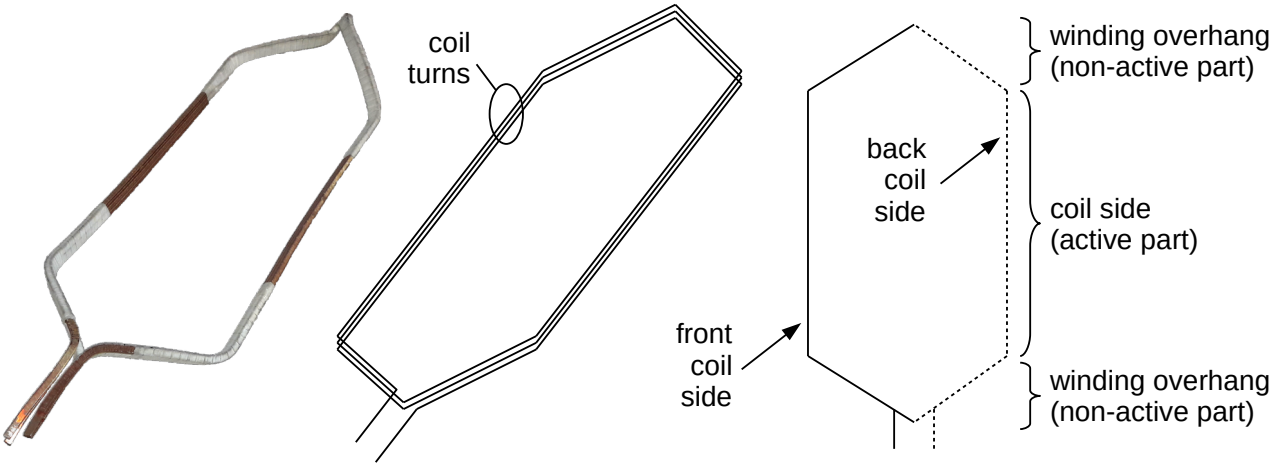


Fig. 4.3: Parts of a winding coil

In a manufactured machine, the coil sides are commonly laid in slots (with exception of slotless machines) while winding overhangs are placed outside of the magnetic circuit. In this case the winding overhangs create only leakage magnetic flux and they do not affect the magnetic field of the machine. The induced voltage in the winding overhangs is only minor part of the total back EMF. But, there is full current flowing through winding overhangs thus there are losses comparable with slot part arising in the winding overhangs. Because of this fact it is suitable to minimize the length of the winding overhangs, which may be achieved either by suitable choice of the winding type and its coil pitch or by suitable choice of the manufacture technology.

The windings may be further divided on base of several further parameters. According to the coil shape they may be divided to lap windings and wave windings and further derivatives of these fundamental types. As examples of these derivatives we can mention windings for slotless machines like Λ-windings and windings used by Maxon. Both these types are oriented to maximal reduction of winding overhangs which are in this case reduced to a bend wire on sides of stator stack. An independent type of winding is also a tooth winding, which is formed by a coil wound along a single tooth and its coil pitch is always equal to a single slot pitch. A comparison of these winding types is shown in Fig. 4.4, whereas mentioned types of coils may be also manufactured as asymmetrical or the may be combined (e.g. lap and wave winding in Latour winding for DC machines).

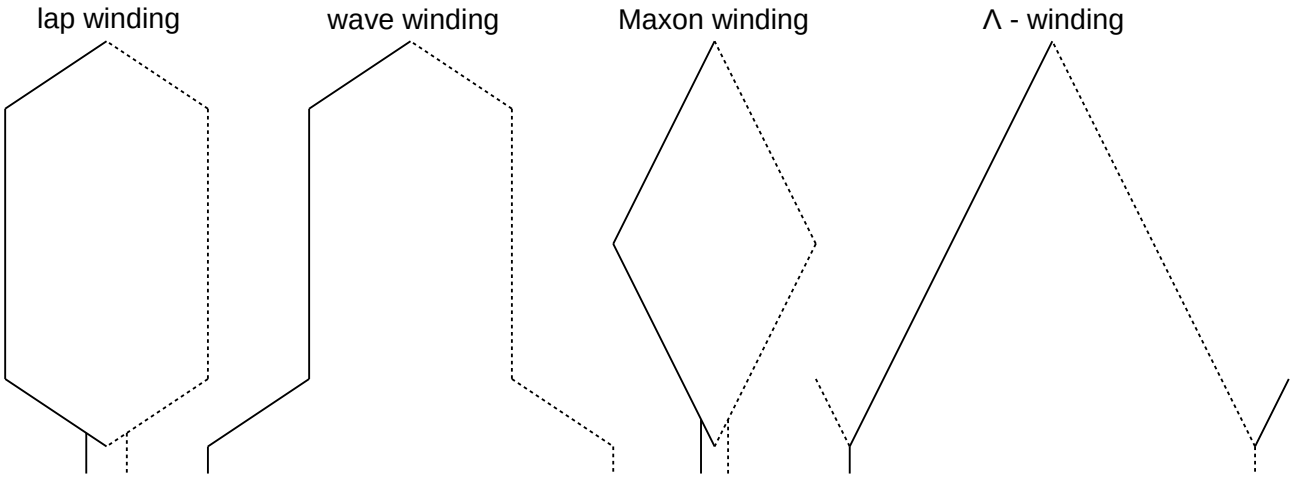


Fig. 4.4: Classification of windings according to coil shape

The coils are in case of AC windings connected to coil groups. According to used winding technology it is possible to wind these groups in concentric arrangement or in sequential connection of coils. Depending on winding direction of each pole it is possible to classify pole or pole-pair topology of the winding overhangs. The concentric coil layout is further used also for compensation winding of DC machines. Because of protection against bearing currents the pole layout of winding overhangs is the only used option in this case.

From constructional point of view it is also important to note, that in case of AC winding design only the locations of each coil side are calculated without considering of their connection. Thus, in case of AC windings the coils in a group may be connected either in sequential order or in concentric layout without significant impact on the work of the machine. Again, it is possible to apply identical design of the winding on a small machine with concentric winding as well as on a large machine with sequential winding.

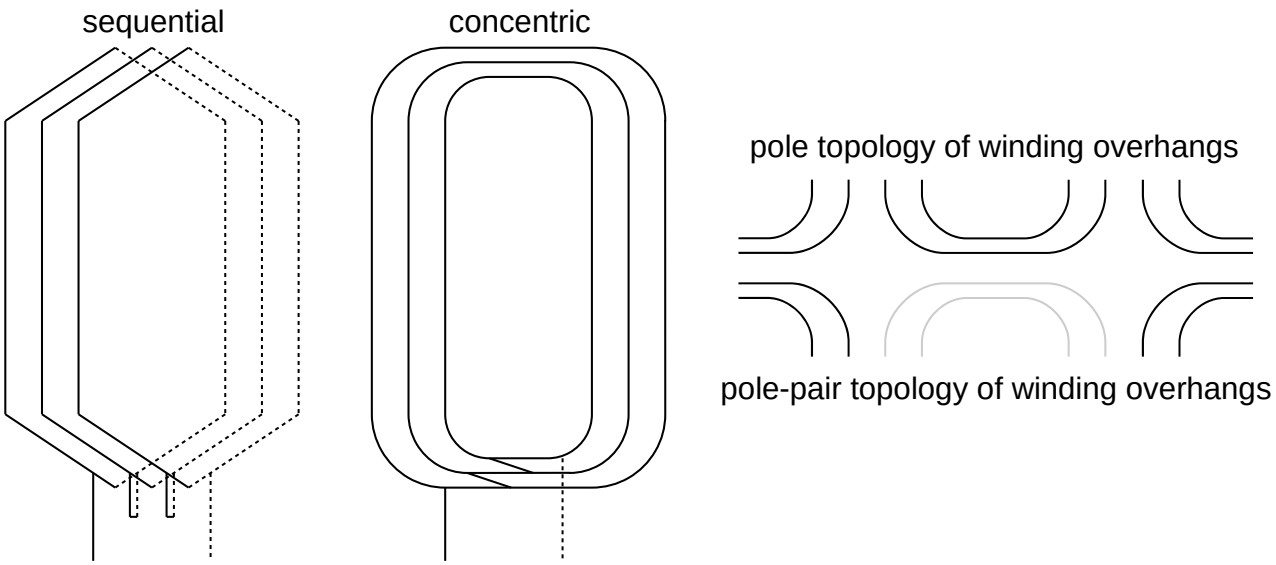


Fig. 4.5: Configuration of coils and winding overhangs

According to the manufacture technology it is possible to classify the windings to wound windings, inserted windings and drop-in windings, whose specific case are so-called hairpin windings. The wound windings are most commonly made of round cross-section wires, which are stepwise inserted into machine slots. This slot must be already equipped with slot insert (insulation layer) and in most cases the slot is semi-closed. The inserted windings are wound of pre-formed externally prepared coils which are inserted (whole or in parts) inserted into slots through slot opening. This means, that in this case the slots must be fully opened. In case of drop-in windings the wire (or coil) is inserted axially into the stator stack through the whole length of the slot. The slots of such a winding may be then partially or fully closed.

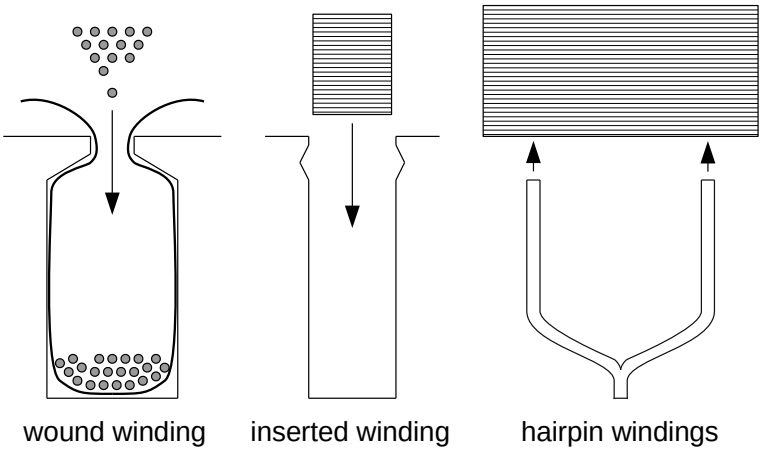


Fig. 4.6: Classification of winding according to manufacture technology

The slot may include a various amount of coil sides. In case of AC windings the most common numbers of coil sides in a slot are one or two. In case of DC windings three or more coil sides in a slot were historically used to achieve lower voltage between adjacent lamellae while machine commutation.

Regarding the connection of the coils to the commutator in relation to coil shape it is possible to divide the windings to windings with crossed and non-crossed connections. In case of lap windings the winding with crossed connections may be easily recognized by crossing of the coil wire near to the commutator. In case of wave windings similar crossing appears after a run around the whole armature and it can be heavily recognized.

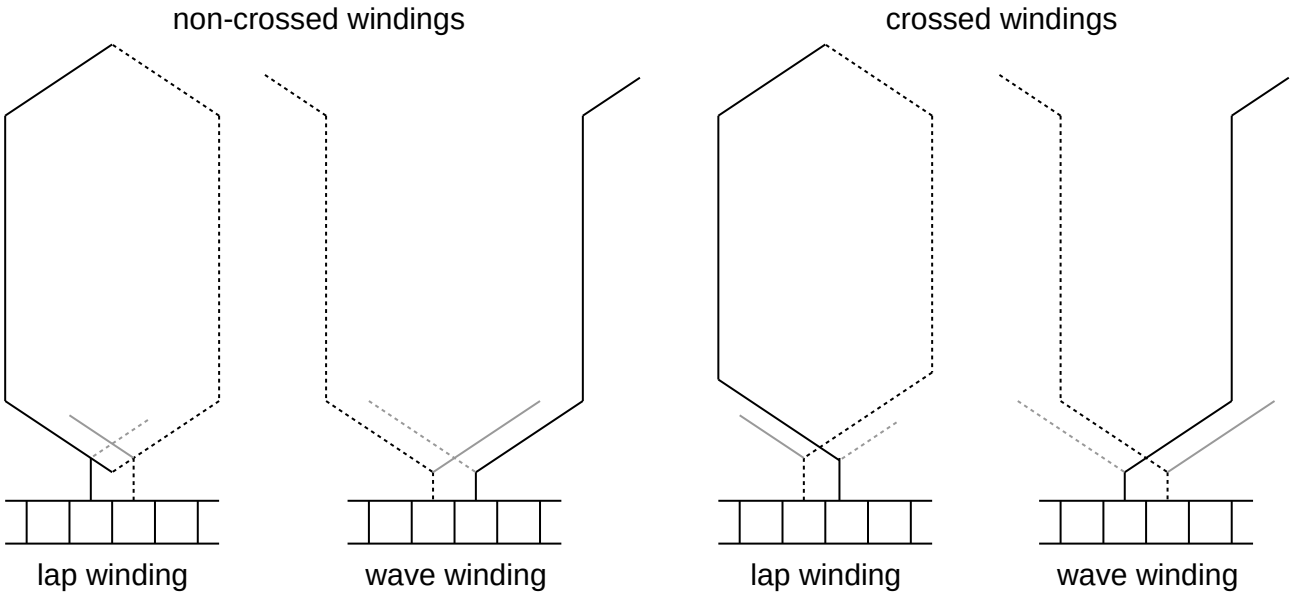


Fig. 4.7: Comparison of commutator connections for crossed and non-crossed windings

According to connection of coils and coil groups it is possible to recognize windings as windings with serial, combined parallel and multiple parallel connections. Mathematically this property may be expressed by a relation between the amount of parallel winding branches and the amount of machine poles. If the amount of parallel branches is equal to one, the winding is in serial connection, if it is more than one but less than the amount of poles, then it is a combined winding (the connection combines serial and parallel parts). In case the number of parallel branches is equal to the amount of machine poles, the winding is in parallel connection, in case of higher numbers it is a multiple parallel winding.

Based on the coil pitch the windings can be divided to tooth windings (the coil pitch is equal to one), shortened pitch windings (the coil pitch is smaller than the pole pitch), full pitch windings (the coil pitch is equal to the pole pitch) and extended pitch windings (the coil pitch is longer than pole pitch). In case of DC windings the tooth windings are not used while in case of AC machines the full pitch windings are not used.

4.2 Classification and Nomenclature of Winding Components

In the very beginning to the nomenclature and classification of winding components it is necessary to note, that the system of the winding nomenclature is generally extremely disunited and even in dependency to the geographical origin of different publications it differs. Among differences in nomenclature of each winding parts (e.g. the pole pitch t_p is commonly marked also as τ_p [5]) these differences include also the marking of coil sides (some publications use counting of coil sides, some count and mark slots only) or methods used for winding analyses (e.g. the commonly used Tingley's schema used in the Czech Republic is in Germany replaced by section map (der Zonenplan) which is basically an unrolled form of Tingley's schema). What is important is that the final winding designed by any approach must have in all cases identical parameters. In further chapters a nomenclature commonly used in some Czech literature and at the UWB using marking of all coil sides will be used. To have a comparison with other approaches see other publications dealing at least partly with winding and design of electric machines.

As mentioned before, the fundamental element of the winding is a coil. This is schematically drawn according to Fig. 4.8 whereas the front coil side is marked by its number and (if possible) it is drawn by solid line. The back coil sides remain unnumbered and they are drawn by a dashed line. The mentioned kind of coil drawing is used in case of all DC windings, in case of AC windings it is used only in case when it is possible to clearly distinguish winding phases by colour.

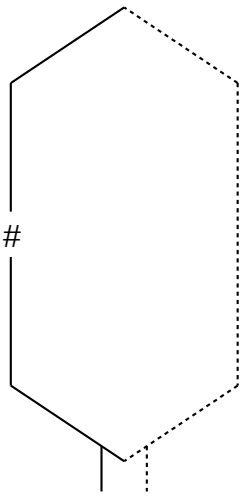


Fig. 4.8: A coil

The convention for coil side numbers says that front coil sides are numbered always with odd number whereas back coil sides are numbered by even numbers (e.g. in saw schema). In case of a single coil the difference between numbers of back and front coil side correspond with coil pitch in number of coil sides. The winding pitches calculated that way are not further indexed. If any pitch is counted in amount of slots, it is distinguished by letter "s" in its subscript. An overview of variables independent on winding type is shown in Tab. 4.1.

variable	label	units	calculation relation
number of slots	Q	slots	chosen
number of poles	$2p$	poles	chosen
number of pole-pairs	p	pole-pairs	chosen
number of coil sides in a slot	$2u$	coil sides	chosen
number of winding coils[4]	K	coils	$K = Qu$
pole pitch	t_{ps}	slots	$t_{ps} = \frac{Q}{2p}$
coil pitch ratio	β	-	chosen
coil pitch	y_{1s}	slots	$y_{1s} = \beta t_{ps}$
coil pitch	y_1	coil sides	$2u = 1 \Rightarrow y_1 = y_{1s}$ $2u > 1 \Rightarrow y_1 = 2u\, y_{1s} + 1$
coil length	y	coil sides	$y = 2 y_k$ [5]
coil return	y_2	coil sides	$y_2 = y - y_1$

Tab. 4.1: Nomenclature of variables independent on winding type

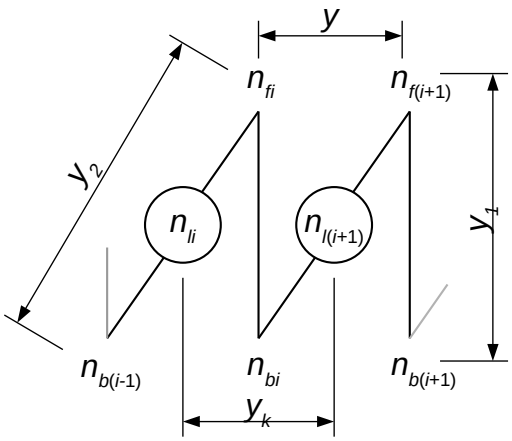


Fig. 4.9: Numbering of elements in saw schema

A step before drawing of the winding schema is drawing of so-called saw schema. The saw schema is a simplified form of winding schema, but it does not in any way reflect the coil shape. It only shows which coil sides belong to a coil and to which lamellae and coils is a certain coil connected. A coil is in the saw schema represented by one "saw tooth" (see Fig. 4.9) whereas in its top edge the front coil side is located and on its bottom the back coil side is located. In accordance to previous the front coil sides are again numbered using odd numbers and the back coil sides are numbered by even numbers whereas their distance corresponds with coil pitch y_1. The distance of front (and back) coil sides is then equal to coil length y and the distance between back coil side to following front coil side is equal to coil return y_2. In case the machine is equipped with commutator (DC machines) then also lamellae of the commutator are drawn whereas their numbering increases by commutator pitch y_k. At the start of numbering of the saw schema it is usual to mark the first lamella by number 1 and the adjacent front coil side also by number 1. This rule is violated only in case that the winding dissolves to more galvanic units.

The placement of the coil sides to slots or their numbering depends on winding type but it does not differ for AC and DC windings. The examples of numbering of slots and coil sides for one, two and four layer windings with appended system of numbering of two layer tooth windings are shown in Fig. 4.10.

4 In case of DC windings the number of commutator lamellae is equal to the number of coils. Nomenclature is same.
5 The commutator pitch y_k is a DC winding variable, but it is also used in case of AC windings as a helping variable to distinguish design of ap and wave windings.

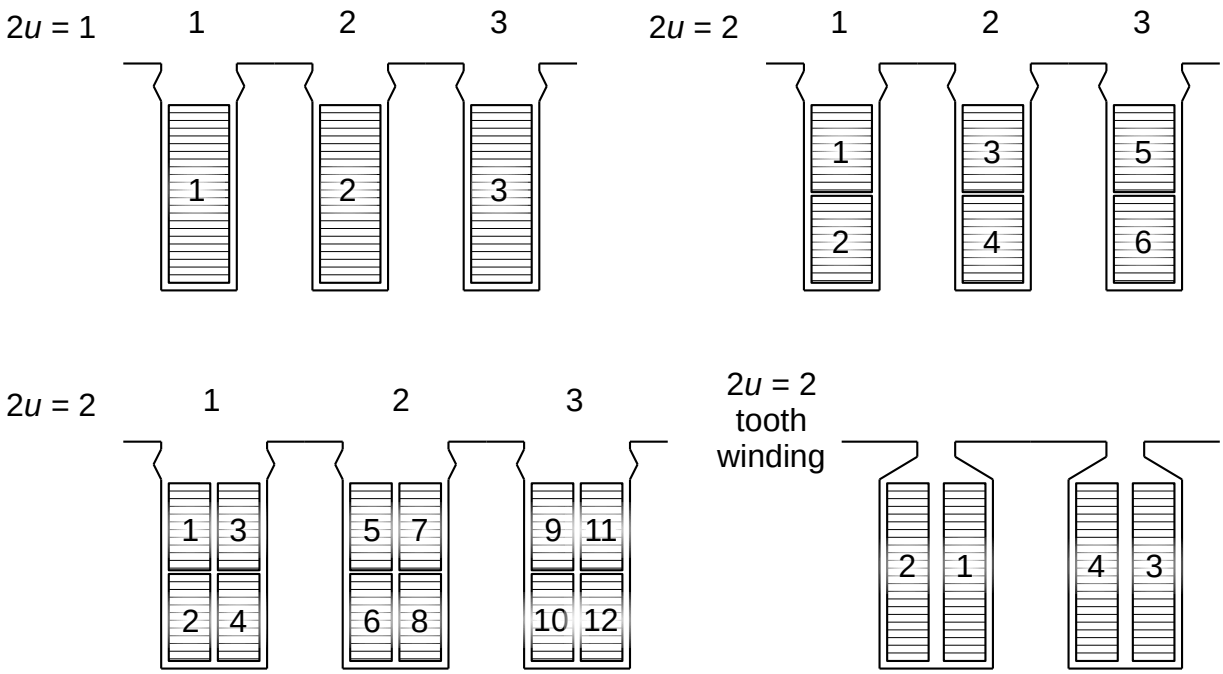


Fig. 4.10: Slot layout with coil sides

In case of a single layer winding it is obvious, that the numbers of coil sides correspond with numbers of slots. If we should keep the coil side numbering convention it is then necessary to use all odd slots for front coil sides and all even slots for back coil sides. As an after-effect of this winding type the total amount of coil sides is equal to the amount of armature slots and the total amount of slots is then one half of the amount of slots.

In case of two layer winding the front coil sides are laid in top position in the slot, the bottom position remains reserved for back coil sides. It is obvious, that the coil pitch counted in number of coil sides will be twice the coil pitch counted in number of slots increased by one to achieve bottom slot position, i.e.

$$y_1 = 2u\, y_{1s} + 1 \quad . \tag{4.1}$$

Since the number of coil sides is twice the amount of slots, the total amount of coils is then equal to the amount of slots.

The four layer winding only generalizes previous conclusions. Similarly to previous case it is necessary to use for transition from coil pitch in number of slots y_{1s} to coil pitch in number of coil sides y_1 use the relation (4.1). The total amount of coils then increases to double and the relation between amount of coils and amount of slots can be generally written as

$$K = Qu \quad . \tag{4.2}$$

The only exception from mentioned system are the tooth windings. In their case the coil sides are commonly oriented vertically which rotates the topology of the winding by 90 degrees clockwise. But, the derived relations are valid also for this type of winding.

The practical achievement of the winding may be then significantly more complicates than shown examples. It is possible for example to create to create physically multiple layered galvanic independent winding. In this case these windings are calculated as independent designs which will meet

in the final machine. Among others it is also possible to design a winding with multiple parallel branches which are further used independently as two galvanic individual windings.

4.3 Classification and Nomenclature of DC Windings

The fundamental property of DC windings is that they form a single galvanic unit and all coils are connected to commutator lamellae. On each lamella two coils of a single galvanic units contact therefore the number of commutator lamellae is equal to the number of coils of given galvanic unit *K*. The commutator forms a sliding contact which is equipped with brushes, whereas the distance between two brushes of equal polarity is equal to potential pitch

$$y_p = \frac{K}{p} \tag{4.3}$$

counted in amount of commutator lamellae. The distance between brushes of opposite potential is then one half of this distance. Since the commutator is a sliding contact, the potential pitch y_p is not required to be an integer.

The distance between contacts of front coil sides on the commutator is then given by commutator pitch y_k, again counted in the amount of lamellae. The commutator pitch should be close to the potential pitch but it must be an integer. In case that the winding should be divided into $a_=$ pairs if parallel branches, the difference of these pitches must be close to the number of parallel DC winding branches:

$$|y_p - y_k| \rightarrow a_= \quad . \tag{4.4}$$

The relation for calculation of commutator pitch may be then written as

$$y_k = \frac{\varepsilon K \pm a_=}{p} \quad , \tag{4.5}$$

where ε is an operator reflecting type of designed winding, on its base the number of parallel winding branches is derived to achieve y_k to be an integer.

For lap windings the value ε = 0, which simplifies (4.5) to

$$y_k = \pm \frac{a_=}{p} \quad , \tag{4.6}$$

where positive sign corresponds with windings with non-crossed connections and the negative sign with crossed connections. To design a wave winding the relation (4.5) with ε = 1 and positive sign for crossed winding connections and negative for non-crossed winding.

As seen in the saw schema a back coil side one coil and a front coil side of a next coil contact each other on a commutator lamella. The distance between front coil sides is therefore equal to double of the commutator pitch (since one lamella is connected to two coil sides), thus we have

$$y = 2\, y_k \quad . \tag{4.7}$$

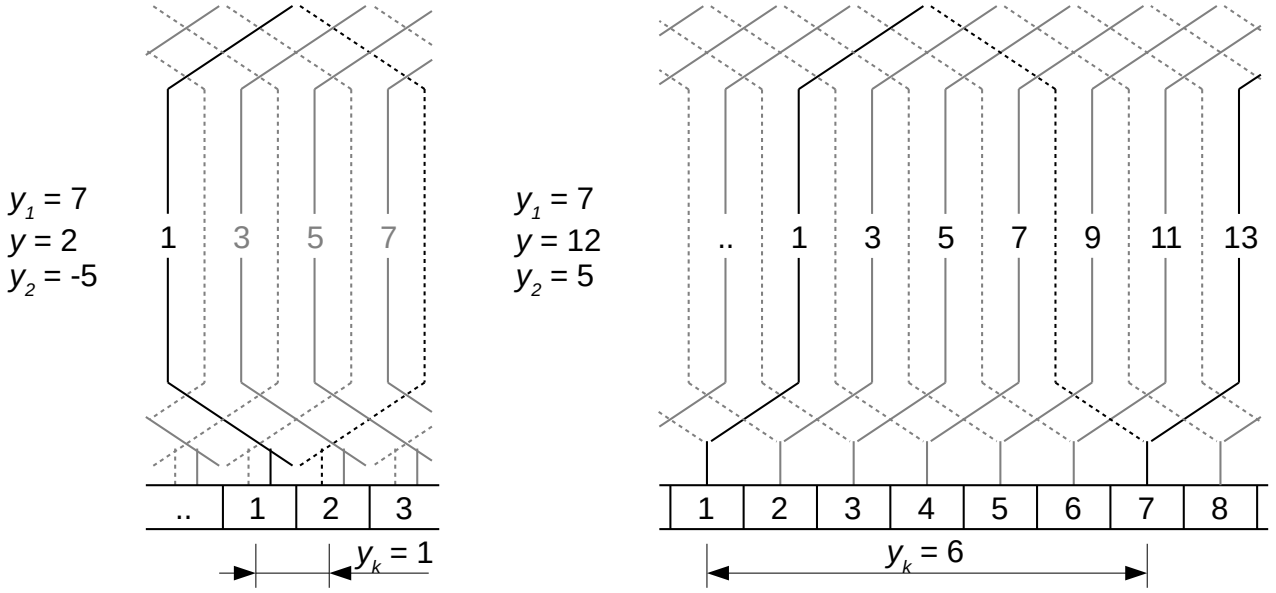


Fig. 4.11: Parts of schematics for a lap winding and a wave winding

The number of pairs of parallel DC winding branches $a_=$ must be derived from validity condition of (4.5), which says, that the result should be an integer. In case of a lap winding, which uses relation (4.6) there are only two possibilities: $a_= = p$, which leads to parallel winding where the number of parallel branches corresponds with the number of poles, or $a_= = kp$, where the result is a multiply (k-times) parallel winding.

In case of a wave winding, there are four possibilities:

1) $a_= = 1$, the winding has only one parallel branch thus it is a serial winding
2) $a_= \in (1; p)$ and it is a combined windings with serial and parallel parts
3) $a_= = p$ and the result will be a parallel winding
4) $a_= > p$ and the winding will be multiply parallel

During the process of design of a DC winding it may happen that although y_k is an integer, its value is unsuitable and the winding dissolves into multiple galvanic units. This situation occurs when the number of commutator lamellar is commensurable with the commutator pitch. Such a commutator forms groups of lamellae connected to a single galvanic unit whereas the remaining lamellae can be connected only to other galvanic insulated unit. The total number of independent galvanic units of the winding may be calculated as a greatest common divisor of the number of lamellae and the commutator pitch, i.e.

$$\kappa_1 = GCD(K; y_k) \quad . \tag{4.8}$$

The division of the winding to multiple galvanic units does not mean, that the winding cannot be used. After an analysis using star of slots and phasor polygon it is possible to determine points on these galvanic units with equal potential and connect them using equipotential connections. The winding then cannot be designed only in case when it is not possible to introduce equipotential connections or the winding units reduce to exactly identical potential. In this case the winding is considered to be a degenerated winding – the real number of parallel winding branches reduces and the resulting winding does not correspond to requirements of the assignment.

4.4 Classification and Nomenclature of AC Windings

The AC windings may be derived from DC winding by so called "clipping"[6]. The characteristic variables of AC windings are the number of winding phases *m*, mathematical number of winding phases *m'* and the number of slots per pole and phase *q*:

$$q = \frac{Q}{2pm} \quad . \tag{4.9}$$

The mathematical phases are then formed by phase sections supplied in both polarities – i.e. sections corresponding with physical phases and sections corresponding with physical phases but powered in opposite direction. This means, that the number of mathematical phases *m'* is always twice as high as the number of physical phases *m* (if the opportunity to create mathematical phases is used). The process of clipping of a DC winding to AC winding is performed in three phases. On base of the number of pairs of parallel DC winding branches we get the number of coil segments

$$S_c = m' a_{=} \quad . \tag{4.10}$$

These segments are then divided between all phases and we obtain the amount of coil segments per phase of an AC winding

$$S_p = \frac{S_c}{m} = \frac{m' a_{=}}{m} \quad . \tag{4.11}$$

Using the total number of coils we can finally determine the number of coils in a segment

$$K_1 = \frac{K}{S_c} = \frac{K}{m' a_{=}} \quad , \tag{4.12}$$

whereas in case of two layer windings the number of coils in a segment K_1 is identical to the number of slots per pole and phase *q*, nevertheless in case of single layer winding the number of coils is one half, thus the K_1 drops to one half of *q*. The created coil segments may be then connected on base of the numbers of coils in each segment connected to serial parallel or combined connections and it is possible to form AC winding parallel branches $a_{\sim}$, which is a value that does not have generally any relation to the number of pairs of parallel DC winding branches $a_{=}$. The values of $a_{\sim}$ may then be from one up to the number of machine poles. In case of $a_{\sim} = 1$ the winding is in purely serial connection. If $a_{\sim}$ is in the interval between 1 a $2p$, then it is a combined connection, in case of $a_{\sim} = 2p$ the winding is purely parallel. In relation to increase of the number of parallel winding branches a risk of equalizing currents increases.

As a helping tool it is possible to use a segment schema instead of saw schema. In this schema it is possible to create parallel branches on base of polarity and number of coils in each segment. The abscissae in this schema are then oriented and located according to the rotation direction of each mathematical phase (see 4.12). In case of a three phase winding this corresponds with sequence U-W'-V-U'-W-V', in case of five phase winding it is U-X'-V-Y'-W-U'-X-V'-Y-W'. Each abscissa corresponds with a coil section and it is numbered with the number of coils in each section.

6 But it is also possible to create non-clipped AC winding. The condition for the design is that the number of commutator lamellae of fictive DC winding is a multiple of the number of phases of final AC winding. The resulting winding will be connected as appropriate polygon and it will have a very low winding factor.

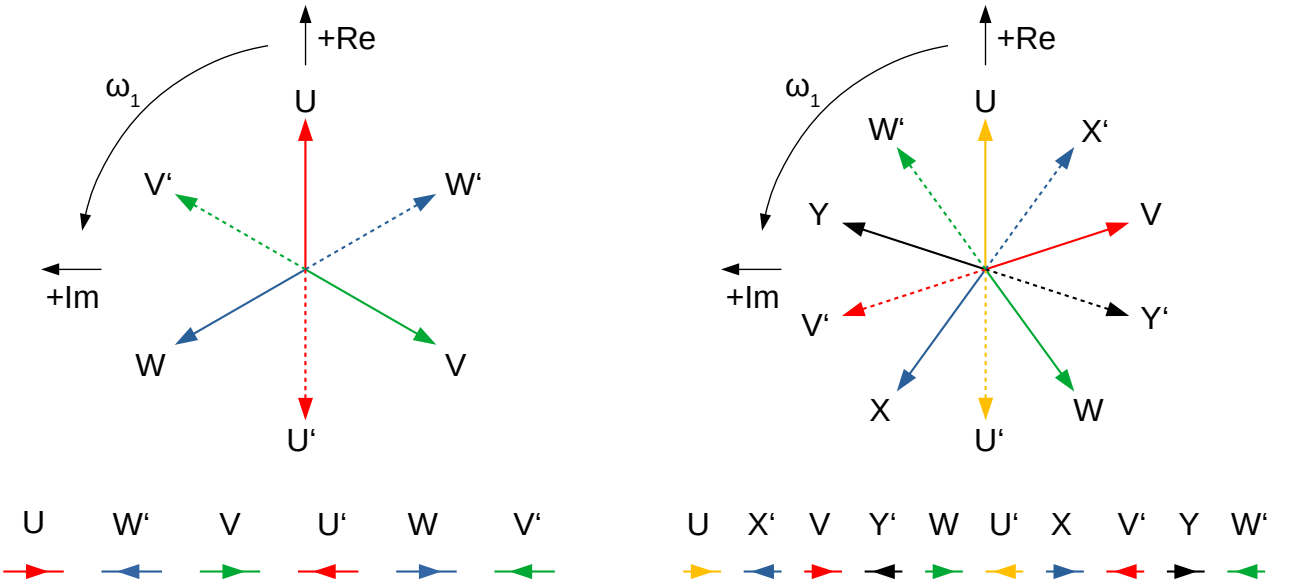


Fig. 4.12: Phasors of mathematical phases and their orientation in segment schema

The Fig. 4.13 shows examples of possible winding connections with K_1 = 2.5 coils per segment and S_c = 12 coil segments. In case the K_1 is a fraction the numbers of coils in segments switch so their average value corresponds with the value of K_1. In this case it is necessary to interchange coil segments with three and two coils in sequence according to Fig. 4.12 to achieve average value equal to 2.5. This sequence, as mentioned before, results from the order of mathematical phases nad their rotation in complex coordinate system. The segments of each phase are then connected to elementary groups to have an identical number of coils in each group. These croups may be then connected in series or in parallel. From the segment schema, it is possible to derive the saw schema and final winding drawing.

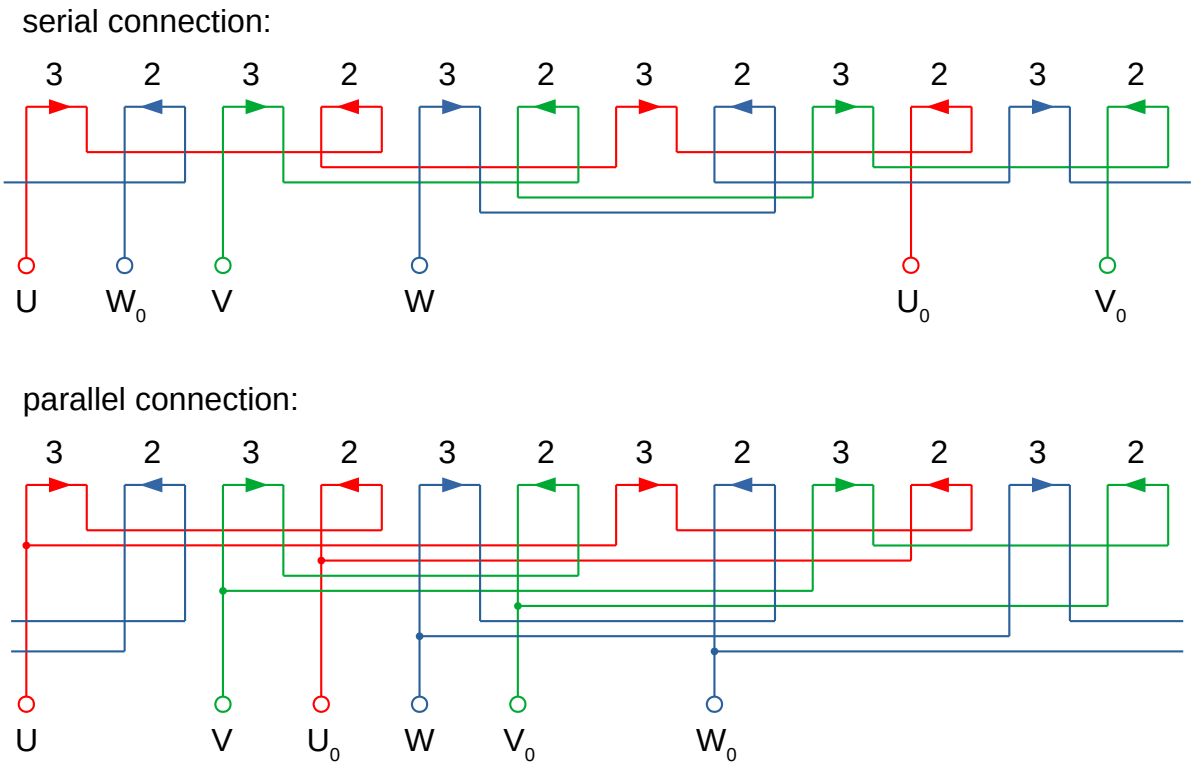


Fig. 4.13: Possible winding connection for windings with K_1 = 2,5 and S_c = 12

As an alternative it is possible to design an AC winding directly from required number of slots per pole and phase, number of winding phases and number of machine poles, which lead to

$$Q = 2\,pmq \tag{4.13}$$

slots. From this point it is possible to derive coil pitches and pole pitch, similarly to a DC winding. The clipping of the winding may be then performed using Tingley's schema.

In this case the chosen variable is the number of slots per pole and phase q. In general it may be expressed as an integer (suitable for motors; easier for manufacture) or as a fraction

$$q = \frac{q_0}{c} \quad , \tag{4.14}$$

where, if a symmetrical winding should be designed, the denominator of the fraction must not be a multiple of the amount of winding phases m. The windings which have a fractional number of slots per pole and phase q are generally called fractional slot windings. These windings show a richer composition of harmonic components in the air gap and thus they have a higher differential leakage flux ratio and they form more parasitic torque components. On the other side, thanks to higher numerator of q_0, the have a better quality of induced voltage and they are more suitable for electric generators. It is necessary to note, that single-layer windings with odd q also behave as fractional slot windings.

From the number of slots per pole and phase point of view it is further possible to divide the windings to traditional distributed windings ($q \geq 1$) and tooth windings ($q<1$). The tooth windings exhibit with exceptionally high values of differential leakage flux factors which makes the suitable only for machines with large air gap and low inductance, i.e. permanent magnet machines (PMSM, PMSG, BLDC etc.).

Especially in case of tooth windings it is advantageous to use the before mentioned process of winding clipping using Tingley's schema. As an example let us choose a $2u = 2$ layered winding with $2p = 8$ poles, $m = 3$ phases and $q = 3/8$ slots per pole and phase. This winding has

$$Q = 2\,pmq = 8.3 \cdot \frac{3}{8} = 9 \tag{4.15}$$

slots, whereas for tooth windings the coil pitch is always chosen as $y_{1s} = 1$. The coil pitch calculated in number of coil sides is then

$$y_1 = 2u\,y_{1s} + 1 = 2.1 + 1 = 3 \tag{4.16}$$

coil sides. The Tingley's schema will have $R = 2p = 8$ rows and $C = q_0 m = 3.3 = 9$ columns. In the schema each $c = 8^{th}$ field will be filled (see putrefaction of q in (4.14)). Each slot then corresponds with one slot of the machine. The front coil sides are always put in the area of one phase, which belongs to q_0 columns, whereas in case of $m = 3$ phase winding the front coil sides in areas of odd poles correspond to phases U-W'-V and in even poles they correspond to phases U'-W-V' (according to sequence in Fig. 4.12).

Based on above described process it is possible to build a Tingley's schema shown in Tab. 4.2. The incidence of each coil side to its respective phase the results from the placement of the front coil side in area of a certain phase. The incidence of back coil side with its phase is then given by defined coil pitch.

From Tingley's schema, it is then possible to derive, that the coil 1-4 will belong to phase U, coil 3-6 to phase V, coil 5-8 to phase V' (since the front coil side of this coil (number 5) is located under an even pole, which reverses the phase V direction to phase V') etc. The resulting segment schema is then shown in Fig. 4.14.

	U U'			W' W			V V'		
p = 1	1 2								3 4
p = 2								5 6	
p = 3							7 8		
p = 4						9 10			
p = 5					11 12				
p = 6				13 14					
p = 7			15 16						
p = 8		17 18							

Tab. 4.2: Tingley's schema of a winding with q = 3/8

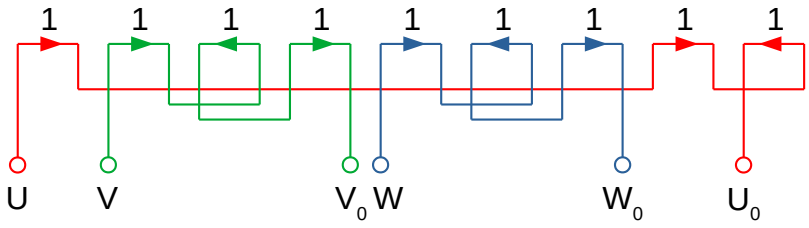


Fig. 4.14: Segment schema of a winding with q = 3/8

4.5 Winding Overhangs

The winding overhangs have, from the winding function point of view, only a function of connections between front and back coil sides. Except tooth windings in all cases the crossings of winding overhangs is very complicated which makes placement of winding overhangs into steel impossible. This means that they are placed only in the air or on non-magnetic supports. Due to this fact they do not contribute to generation of torque nor back EMF, thus they are passive parts of windings only. Withal they contribute to generation of losses either by their electrical resistance or through leakage magnetic field they generate. This is why it is suitable to manufacture the winding overhangs as short as possible.

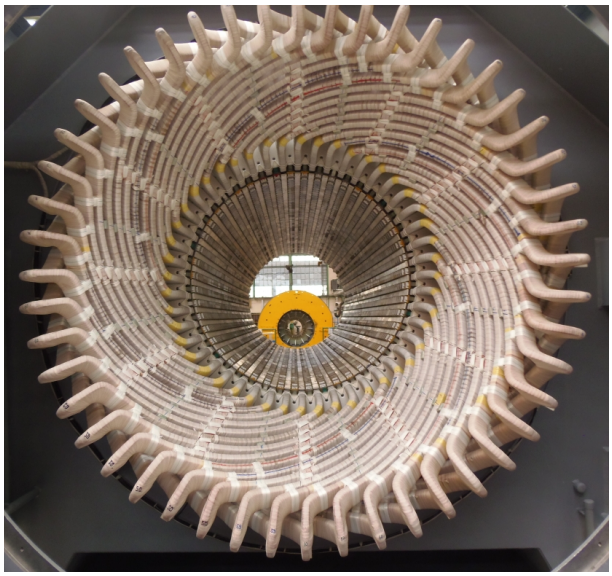


Fig. 4.15: Turbo generator winding overhangs

In case of low voltage machines with coils formed by round wires all conductors touch and – if needed – insulation layers between coils of different phases are used. In case of machines with winding made of rectangular wires a certain insulation distance c is used, which is in case of low voltage machines slightly higher than one or two millimetres. This distance ensures flow of cooling air around winding overhangs. In case of high voltage machines the insulation distance is derived from rated voltage of the machines according to

$$c = 4 + \frac{U_n[kV]}{2} \quad [mm]. \tag{4.17}$$

To keep constant distance between neighbouring winding overhangs it is in case of distributed windings necessary to form the windings overhangs according to equidistant curves. In case of purely axial winding overhangs (see Fig. 4.16) the forming curve is a spiral which projects to a cylindrical plane as a straight line. These winding overhangs may be then drawn as shown in Fig. 4.17. The angle between this spiral and base of the cylinder may be then derived from the width of the winding bar b_b, necessary insulation distance c ans slot pitch t_s using Fig. 4.17 as:

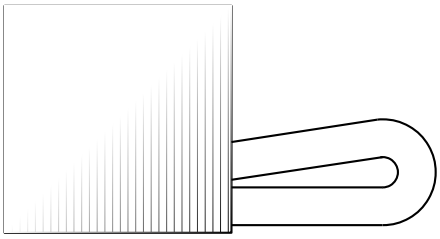


Fig. 4.16: Shape of axial winding overhang

$$\alpha_o = \operatorname{asin} \frac{b_b + c}{t_s} \quad . \tag{4.18}$$

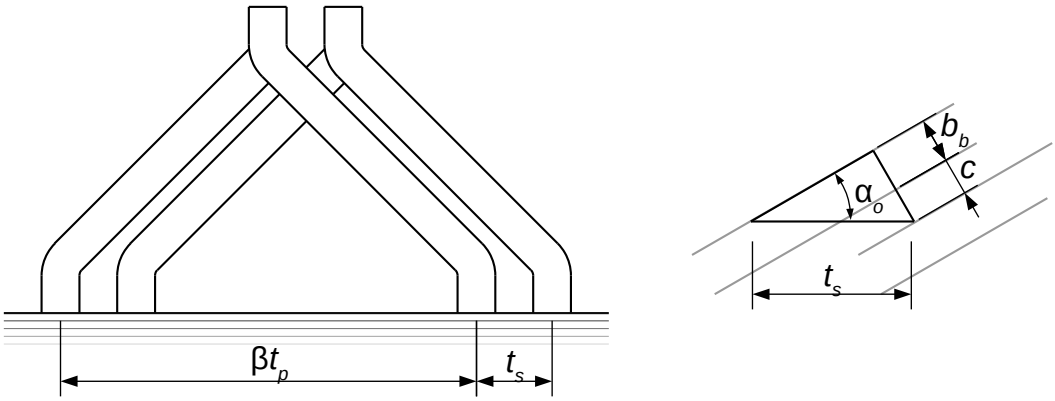


Fig. 4.17: Projection of axial winding overhangs and determination of minimal possible angle between winding overhangs and stator stack

In case of different winding overhang types, where the overhangs are deflected from cylindrical plane the spiral deforms and in front view they form a shape of an involute. Since axial winding overhangs are used only in case of armatures of DC machines it is possible to consider other types of winding overhangs ans involute overhangs. Examples of involute overhangs are shown in Fig. 4.18. The angle between winding overhangs and cylindrical plane α is then commonly between units of degrees up to 15 degrees in case of axially deflected overhangs and approximately 25 degrees to 35 degrees in case of partially radial winding overhangs.

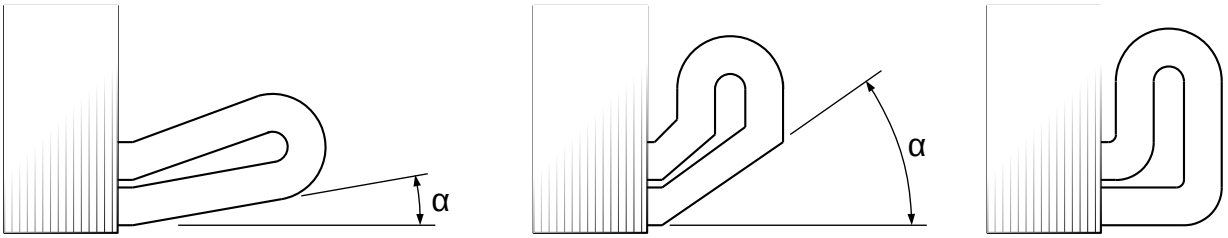


Fig. 4.18: Involute winding overhangs: axially deflected (left), partially radial (middle) and radial (right)

The involute formed by winding overhangs is a curve which is drawn by a secant which rolls off the circle. Since the distance of points on the circle is explicitly given, the distance between two neighbouring involutes corresponds with the distance on the circle and the drawn lines are therefore equidistant. The distance between these lines are then given by the bar width b_b and the insulation distance c. For Q winding slots (and winding overhangs) the circumference of forming circle (involute base circle) is:

$$o = Q(b_b + c) \qquad (4.19)$$

and the diameter of base circle is then

$$d_0 = \frac{Q(b_t + c)}{\pi} \quad . \qquad (4.20)$$

Since the insulation distance between neighbouring winding overhangs is in almost in all cases smaller than the tooth width, the diameter of the base circle d_0 is smaller than the armature inner diameter D_1. In other case there would be no mathematical solution.

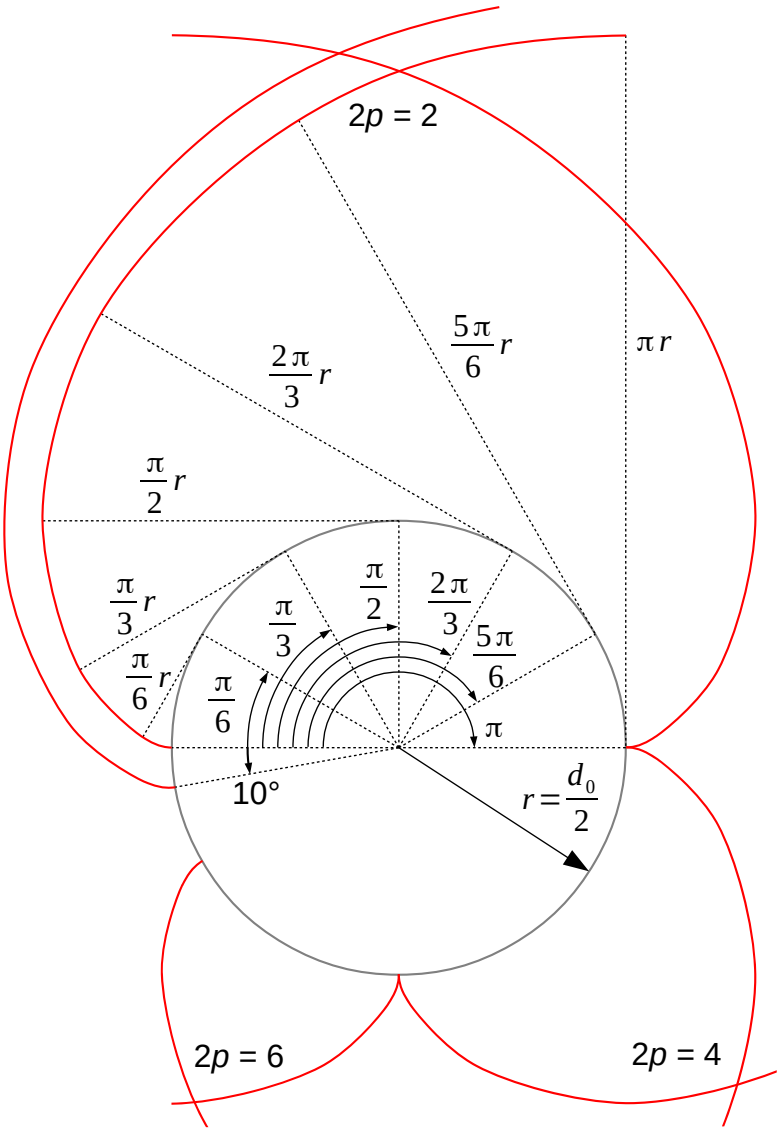


Fig. 4.19: Shapes of involute winding overhangs for two, four and six pole machine

In case of deflected winding overhangs the involute projects to a cone plane under angle α (see Fig. 4.20, practical performance is obvious from Fig. 4.1). The involute is here formed from virtual radius R described by

$$\sin\alpha = \frac{r}{R} \qquad (4.21)$$

and similarly as in previous case the radius of base circle is

$$R=\frac{Q\left(b_b+c\right)}{2\pi\sin\alpha} \quad , \tag{4.22}$$

and its diameter is

$$D_0=\frac{Q\left(b_b+c\right)}{\pi\sin\alpha} \quad . \tag{4.23}$$

As noted before – the above shown calculations are valid only for (outer) stator armatures, therefore in case of (inner) rotors of electrical machines only spiral winding overhangs are used.

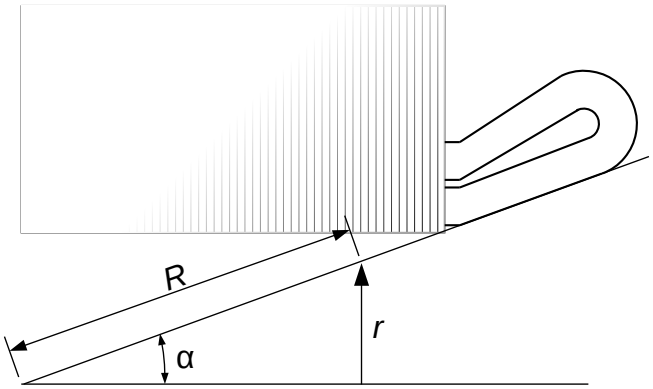


Fig. 4.20: The projection of an involute to cone plane

5 Magnetic Circuits of Rotary Electric Machines

Parts of an electric machines which are dedicated to leading of magnetic flux, are in general called magnetic circuits. In dependence of type of the machine the magnetic flux may be direct or alternating, thus this part of the magnetic circuit may be manufactured as a monolithic part or made of insulated steel sheets. The insulation layer then can be performed as an oxide layer or using lacquer. In some cases even parts which lead direct magnetic flux are manufactured from steel sheets – the reasons may include reduction of appearing losses, technology or economy of the manufacture. In these cases non-insulated steel sheets are often used.

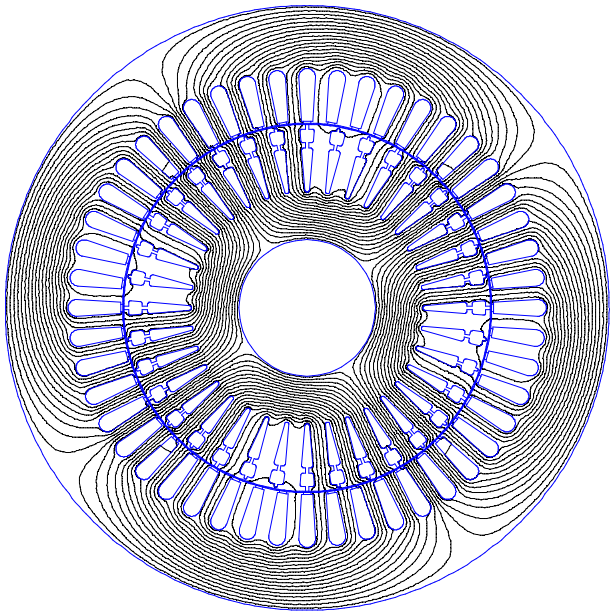


Fig. 5.1: Magnetic field of an induction machine

Nowadays, it is necessary to pay attention even on parts of a machine which appear – from electromagnetic point of view – to be used by direct magnetic flux only. In case of a machine fed from power electronics converter there is (in case when no filtering is used) a current ripple which causes also oscillations of the magnetic flux which further generates additional losses in the magnetic circuits – both hysteresis and eddy currents. This is why it may be only recommended to use the insulated electrical steel sheets also in these applications.

Parts of a machine which are supposed to lead the magnetic flux include among steel parts also the air gap (whose presence is from mechanical point of view necessary) and permanent magnets. All these parts therefore should be precisely designed to with corresponding attention.

5.1 Magnetic Circuit Materials

The major part of the volume of the magnetic circuit is formed by magnetically conducting components made of electrical steel sheets. The term “electrical steel sheet” is commonly understood as a steel sheet mage of iron alloy including approximately 3 to 5 per cent of silicon. The effect of inclusion of the silicon is the increase of electrical resistance of the sheets resulting in reduction of eddy current losses. Since the inclusion of silicon influences also mechanical properties of electrical steel sheets the percentage of silicon is commonly below five per cent otherwise the resulting sheet would be fragile and it would have also worse magnetic properties.

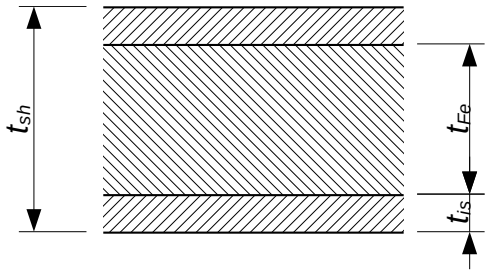


Fig. 5.2: A sketch of double side insulated electrical steel sheets

Standard electrical steel sheets (either non-oriented according to EN 10106 or oriented) are manufactured in thicknesses 0.35 *mm*, 0.5 *mm* a 1.0 *mm* and they are equipped either by single or double side insulation layer. This insulation layer has almost in all cases similar thickness thus only the ratio of its thickness in relation to the sheet thickness changes. This is commonly expressed by lamin-

ation fill factor k_{Fe} which expresses the percentage of the thickness of the steel (and so of volume) in the total thickness of the steel sheet including insulation (see Fig. 5.2 – t_{sh} is the total thickness of the steel sheet, t_{is} is the insulation thickness and t_{Fe} is the thickness of pure steel sheet). In case of mentioned steel sheet thicknesses the standardized lamination fill factors are k_{Fe} = 0.95, 0.97 and 0.98.

With the development of electrical machines the standard electrical steel sheets came to the border of their usability which leads to development of steel sheet types which are not standardized yet or for which the standards are currently developed. The most renown examples are made from Arnold Magnetics Co. which manufactures non-oriented electrical steel sheets under trademark Arnon. These steel sheets have lower specific losses due to higher volume of silicon and smaller thickness (e.g. Arnon 5 sheets are 0.005 (0.127 *mm)* inches thick). A similar way of development was chosen by Voestalpine which provides electrical steel sheets named as Isovac NO30-15 with 0.3 *mm* thickness. These steel sheets are currently standardized in EN 10303.

An alternative way was chosen in development of steel sheets called Hiperco. These steel sheets are manufactured by multiple manufacturers (e.g. Carpenter Electrification) and in contrast to common approach which uses addition of silicon for lowering losses the Hiperco is an alloy made of iron, cobalt and vanadium. This results (in combination with smaller thicknesses) to specific losses close to Arnon steel sheets but thanks to the volume of cobalt these steel sheets have significantly higher saturation point – while standard electrical steel starts to saturate at approximately 1.5 *T*, the Hiperco may be used with almost linear properties up to 2 *T*. This material is therefore very advantageous for manufacture of highly saturated rotary electric machines and transformers.

An independent chapter is formed by usage of soft mould composite materials. These may be based either on traditional iron-silicon alloy or on Hiperco basis. Their usage is very limited nowadays (limited by properties and price of 3D print or moulding) and in relation to losses arising in these materials their usage is currently focused more on prototypes of electric machines.

5.2 The Mechanism of Generation of Iron Core Losses

The main part of losses generated in magnetic components are the hysteresis losses, i.e. losses which arise while passing the alternating magnetic flux through ferromagnetic material. In microscopic scale the magnetic domains change their orientation which generates “friction” generating heat inside of this material. Depending on strength of the outer magnetic field these domains may merge or dissolve, which further increases the generation of heat.

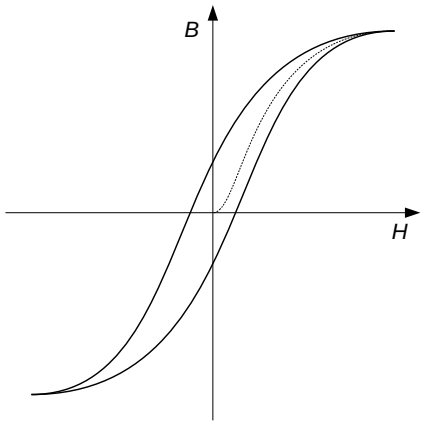


Fig. 5.3: Hysteresis loop of soft magnetic steel

This phenomenon depends on energy necessary for change of magnetization direction of the ferromagnetic material, i.e. to magnetic energy whose density is

$$w_m = \int B\,dH \quad . \tag{5.1}$$

This equals to the area of the hysteresis loop created while changes of magnetization direction. From this point of view it is obvious that for usage of a (ferro)magnetic material in time alternating magnetic field the area of the hysteresis loop must be possibly smallest thus it is necessary to use a magnetically soft steel. The area of the hysteresis loop then depends on square of magnetic flux density and during one power supply period it is drawn once. Thus for calculation of the hysteresis losses the following relation will be valid:

$$\Delta p_h = k_h f B^2 \quad , \tag{5.2}$$

where k_h is the coefficient of hysteresis losses.

The second component of losses arises as an after-effect of the conductivity of electrical steel sheets. It is caused by eddy currents which are generated in steel sheets due to induced voltage. In general it may be calculated from Poynting's vector whereas the result may be written as

$$\Delta p_v = \frac{J^2}{\gamma_{Fe}} \quad , \tag{5.3}$$

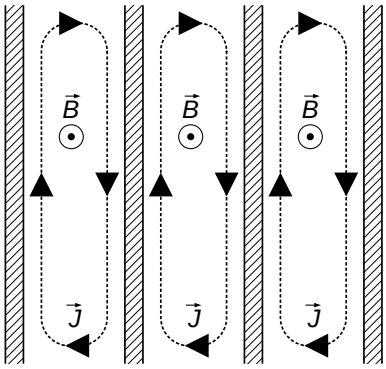


Fig. 5.4: Eddy currents in electrical steel sheets

where the induced current density J is proportional to the induced voltage into each sheet

$$J \sim f B \tag{5.4}$$

thus the result is a relation

$$\Delta p_e = k_e f^2 B^2 \quad , \tag{5.5}$$

where k_e is the coefficient of eddy current losses. The total losses are then given by a sum of both components, i.e.

$$\Delta p_{Fe} = \Delta p_h + \Delta p_e = k_h f B^2 + k_e f^2 B^2 \quad [7], \tag{5.7}$$

which is generally known as Jordan's equation. A problem of this equation is that it is complicated to separate both components of losses, especially coefficients k_h and k_e from the measurement. This measurement is often performed at a certain reference frequency f_{ref} and at a certain reference mag-

7 In some FEM software the iron core losses are being modelled using

$$\Delta p_{Fe} = k_h f B^2 + k_e f^2 B^2 + k_{exc} f^{1,5} B^2 \quad , \tag{5.6}$$

where k_{exc} are the "excess losses." Considering the fact, that this component of the equation corresponds best with the real loss distribution according to magnetic flux density and frequency. This number results highest from k_h, k_v and k_{exc}.

netic flux density B_{ref}, which provides a single value of reference iron core losses Δp_{ref}. Because of this reason a simplified form

$$\Delta p_{Fe} = \Delta p_{ref} \left(\frac{f}{f_{ref}} \right)^{1,5} \left(\frac{B}{B_{ref}} \right)^{2} \quad , \tag{5.8}$$

which averages the frequency exponents of both loss components is used. This relation corresponds very well with the behaviour of traditional electrical steel, but new materials have both types of losses extremely unbalanced, thus it is more suitable to use so-called Steinmetz' equation for iron core losses

$$\Delta p_{Fe} = \Delta p_{ref} \left(\frac{f}{f_{ref}} \right)^{\alpha} \left(\frac{B}{B_{ref}} \right)^{\beta} \quad , \tag{5.9}$$

where α and β are general exponents, which need to be derived on base of measurement.

For currently available materials, the exponent α is most commonly in range between 1.3 and 1.5, while coefficient β is almost in all cases close to two. In the praxis it is possible to obtain the value of Δp_{ref} from the measurement using Epstein's frame or from the data sheet of selected steel sheets, which often includes complete frequency characteristics of losses.

Another factor significantly influencing the iron core losses is the machining technology, i.e. the whole technology of processing of steel sheets. Among the most common way of machining of steel sheet parts (stamping) nowadays also laser or string cutting is used. These technologies lead to various sheet damages like burrs or insulation overheating. Although it is possible to compensate these effects (e.g. by additional annealing and insulation) such actions are expensive and they slow down the manufacture.

All these effects are in terms of magnetic circuit design considered by technological coefficient of yoke and teeth machining k_{tt} and k_{ty}. These coefficients consider a proportional increase of losses in given part of the magnetic circuit and their values vary according to damages due to machining in each part. For thinner parts of magnetic circuits (teeth) they are in range between 1.6 and 2.0, for wider parts of magnetic circuits (yokes) they are commonly in range of 1.3 to 1.6. A more precise determination of these coefficients results from the experience of the machine manufacturer with selected technology and provider. The total yoke losses are then

$$\Delta P_y = k_{ty} m_y \Delta p_y \quad , \tag{5.10}$$

where k_{ty} is the technological factor of yoke iron core losses,
m_y is the mass of the yoke
and Δp_y are the proportional losses in the yoke.

In a very similar way it is possible to express the losses in teeth of the machine as

$$\Delta P_t = k_{tt} m_t \Delta p_t \tag{5.11}$$

with identical meaning of each variable.

5.3 Design of Magnetic Circuit

The design of magnetic circuit is based on well known equations

$$\Phi = \oint B\,dS \quad , \tag{5.12}$$

and

$$\Theta = \oint H\,dl \quad , \tag{5.13}$$

whereas the relation between magnetic flux Φ and magnetomotive force drop on the magnetic circuit Θ may be determined on base of Hopkinson's law

$$\Phi = \Lambda\,\Theta \quad , \tag{5.14}$$

where Λ is the magnetic conductance of the magnetic circuit,

nevertheless thanks to strongly non-linear characteristic of steel it is more common to read the values from the B-H curve of used steel sheets. Each part of the magnetic circuit is then designed on certain values of magnetic flux density to keep relative low value of losses and low value of magnetomotive force drop. E.g. in case of induction machines the magnetomotive force is related to power factor of the machine, in case of synchronous machines it is bound to design of excitation.

5.3.1 Magnetic Field in Teeth of an Electric Machine

From the point of view of examination of magnetic field in machine teeth there are two extreme cases – teeth of a machine equipped with distributed winding and teeth of a machine equipped with tooth winding. While in case of machines with distributed winding it is possible to consider the tooth as a very narrow object in comparison to wavelength of the magnetic filed in the air gap, in case of machines equipped with tooth winding the dimensions of the tooth pitch are comparable to magnetic field wavelength.

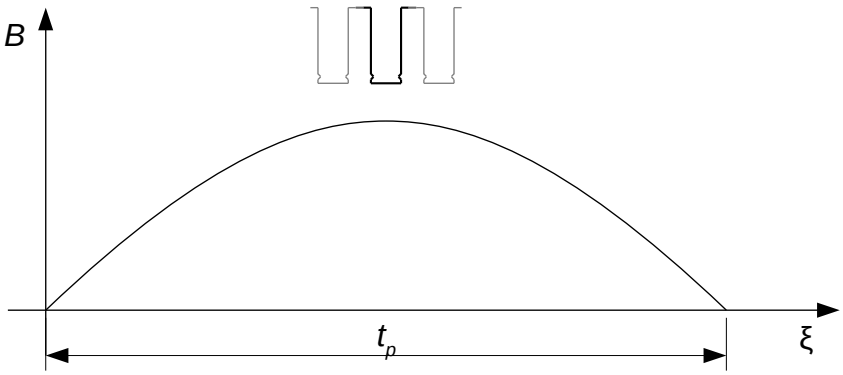


Fig. 5.5: Magnetic load of a tooth of distributed winding

Thus, in case of distributed winding the magnitude of the magnetic flux density in the tooth results from magnitude of the air gap magnetic flux density and tooth pitch, as shown in Fig. 5.5. The magnetic flux, which enters the tooth has a magnitude of

$$\Phi_{tp} = B_\delta t_s l_{Fe} \quad , \tag{5.15}$$

which corresponds with tooth magnetic flux

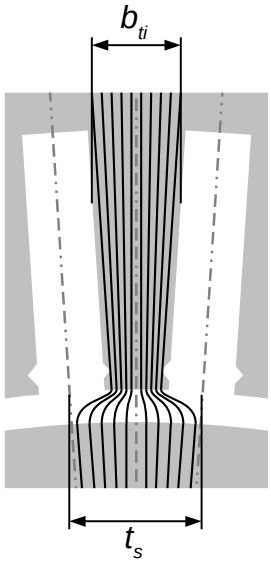


Fig. 5.6: Magnetic flux through non-saturated tooth

$$\Phi_t = \Phi_{tp} = B_t b_t k_{Fe} l_{Fe} \quad . \tag{5.16}$$

The tooth magnetic flux density is then

$$B_t = \frac{\Phi_t}{b_t k_{Fe} l_{Fe}} = \frac{t_s}{b_t k_{Fe}} B_\delta \quad . \tag{5.17}$$

This relation corresponds to reality only in case when he teeth are not saturated, i.e. approximately to magnetic flux density of 1.7 *T*. Since this value the permeability of the iron starts to decrease. This pulls a part of the magnetic flux out of the tooth to the slot space which results in "lightening" of the tooth from the magnetic flux.

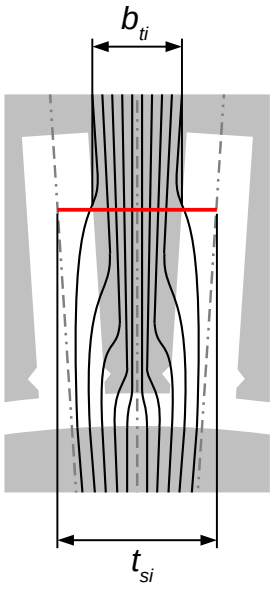


Fig. 5.7: Desaturation of a tooth due to leakage of magnetic flux to a slot

The magnetic flux through slot pitch may be then determined as a sum of real value of the magnetic flux through tooth and magnetic flux through slot

$$\Phi_{ts} = \Phi_t + \Phi_s \quad , \tag{5.18}$$

which gives

$$\Phi_{ts} = B_t b_t k_{Fe} l_{Fe} + B_s b_s l_{Fe} \quad . \tag{5.19}$$

The magnetic flux Φ_{ts} may be substituted from (5.16) but in this case let us designate the magnetic flux density in tooth as B' – as apparent tooth magnetic flux density:

$$B_t' b_t k_{Fe} l_{Fe} = B_t b_t k_{Fe} l_{Fe} + B_s b_s l_{Fe} \quad . \tag{5.20}$$

From this relation it is possible to express the real tooth magnetic flux density as

$$B_t = B_r' - \frac{b_s}{b_t k_{Fe}} B_s \quad . \tag{5.21}$$

If we substitute the magnetic flux density in a slot by magnetic field strength according to

$$B_s = \mu_0 H \tag{5.22}$$

we obtain the functional prescription for determining of real tooth magnetic flux density:

$$B_t(H) = B_t' - \mu_0 \frac{b_s}{b_t k_{Fe}} H \tag{5.23}$$

The fraction

$$k_d = \frac{b_s}{b_t k_{Fe}} \tag{5.24}$$

is then commonly used as stator teeth desaturation factor. The real value of the magnetic flux density in tooth can be then determined by graphical construction shown in Fig. 5.8. In this construction an intersection of function $B_t(H)$ with stator steel B-H curve is found. The result is then real value of magnetic field strength H_t and magnetic flux density in tooth B_t. With respect to most precise description of magnetic field in tooth the magnetic flux density and magnetic field strength is commonly determined at three levels of the tooth – in wedge area, in the middle and at the slot bottom.

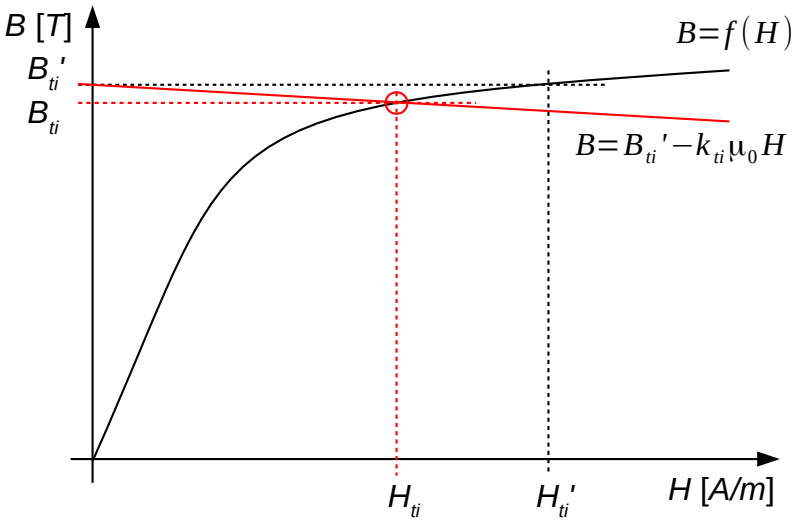


Fig. 5.8: Determination of real tooth magnetic flux density

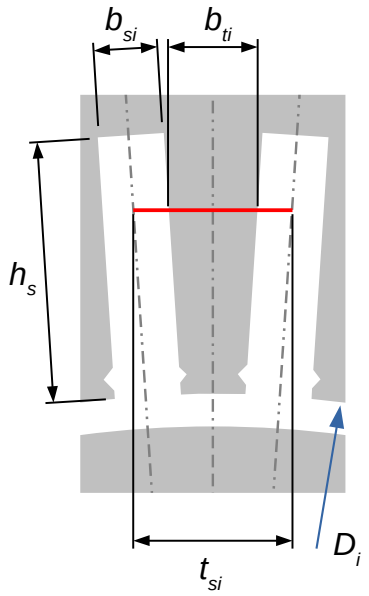


Fig. 5.9: Geometrical dimensions of a tooth

In terms of machine design this is reflected by usage of indices i = 1, 2, 3 for each part of the tooth. This leads to triple calculation during which it is necessary to determine desaturation factors for each layer

$$k_{ti} = \frac{b_{si}}{b_{si} k_{Fe}} = \left| b_{si} = t_{si} - k_{Fe} b_{ti} \right| = \frac{t_{si}}{b_{ti} k_{Fe}} - 1 \quad . \tag{5.25}$$

To be able to calculate the tooth magnetomotive force drop all determined values average according to

$$H_{ta} = \frac{H_{t1} + 4H_{t2} + H_{t3}}{6} \quad . \tag{5.26}$$

This leads to teeth layer magnetomotive force drop

$$\Theta_t = \oint H\, dl = H_{ta} h_t \quad , \tag{5.27}$$

where h_t is the tooth height.

Across the literature this effect is considered in a variety of solutions. To be able to omit the desaturation factor in some literature a separate B-H curve for teeth is presented (e.g. [4]), which uses a presumption of similarity between electric machines – i.e. presumption, that in case of optimal design the desaturation factors will result very similar thus also the magnetic field effects will be very similar. Another alternative is so-called intersectional diagram, which allows determination of real magnetic flux density on base of known combination of apparent magnetic flux density and desaturation factor.

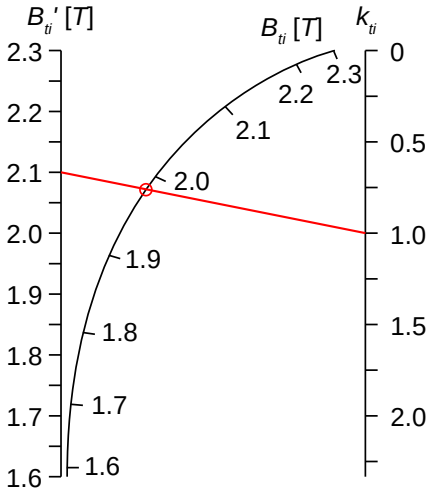


Fig. 5.10: Intersectional diagram

In case of a tooth winding the situation is more complicated. Since different types of tooth windings have different relation between tooth pitch and pole pitch it is suitable to examinate each type of winding separately, especially using finite element method. In general it is possible to say that the magnetic flux through one tooth is approximately as large as the air gap magnetic flux ($\Phi_z \approx \Phi_\delta$), but there is a significant magnetic flux leakage between teeth thus consideration of the whole air gap magnetic flux may lead to significantly overlarged magnetic circuit. After correct determination of the tooth magnetic flux density B_t the remaining design approach is identical to distributed winding.

5.3.2 Magnetic Field Distribution in the Armature Yoke

Since the magnetic field enters the yoke through tooth layer, its examination is more complicated than in case of other parts of the machine. In general, it is possible to easily obtain the amplitude of the magnetic flux density in the yoke from the knowledge of air gap magnetic flux, i.e. from

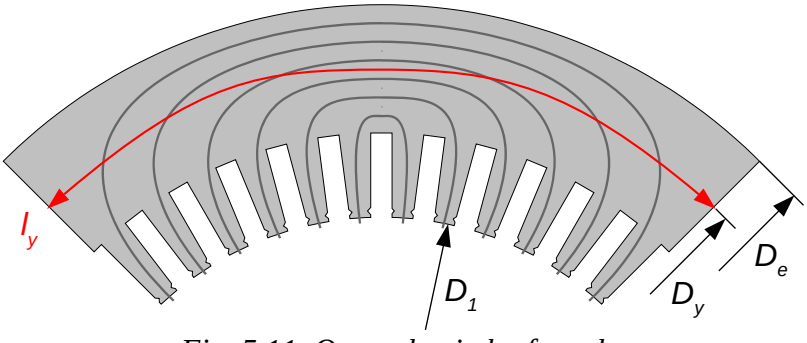


Fig. 5.11: One pole pitch of a yoke with related flux lines and dimensions

$$\Phi_y = \frac{\Phi_\delta}{2} = \oint B_y \, dS \quad , \tag{5.28}$$

which leads to

$$\Phi_y = B_y \, h_y \, k_{Fe} \, l_{Fe} \quad , \tag{5.29}$$

where the yoke height is (in case of stator)

$$h_y = \frac{D_e - (D_1 + 2\,h_s)}{2} \quad . \tag{5.30}$$

The amplitude of the magnetic flux density in the yoke then results

$$B_y = \alpha_\delta B_\delta \frac{t_p}{2\,h_y k_{Fe}} \quad . \tag{5.31}$$

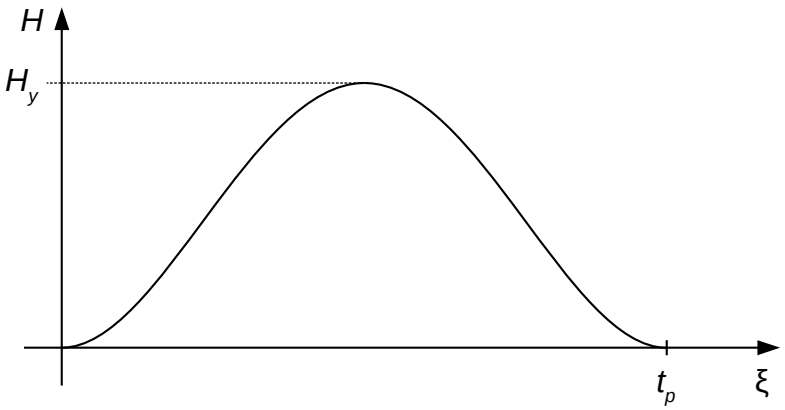


Fig. 5.12: Magnetic field strength curve in centre of a yoke

Due to transmission of the magnetic flux into the yoke through teeth its layout is not uniform and the values of yoke magnetic field strength H_y and corresponding magnetic flux density B_y are located almost only in the centre of the yoke. Following a virtual line in the middle of the yoke the real layout of the magnetic field strength will be similar to a harmonic function distorted by its third harmonic component (see Fig. 5.12).

Real shape of the yoke magnetic field strength curve may be examined using construction shown in Fig. 5.13. The presumption is that the yoke magnetic flux density has a sinusoidal space dependency, which is in the figure drawn as one quarter of a sine wave on coordinates between $t_p/2$ and 0. In thze same scale the B-H curve of used steel sheets is

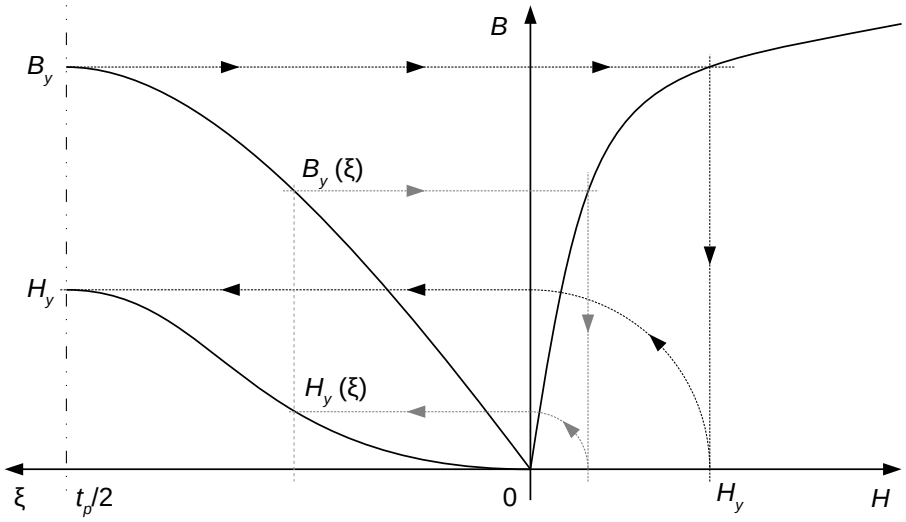


Fig. 5.13: The construction of magnetic field strength curve in the yoke as depending on position

drawn on the right side. For each coordinate ξ on the periphery of the machine a corresponding value of the yoke magnetic field strength is obtained. It is drawn over the *y* axis to the same quadrant as the magnetic flux density. The result is a deformed curve of the yoke magnetic field strength. To achieve correct value of yoke magnetomotive force drop in form of

$$\Theta_y = \int H_y \, dl = H_y l_y \tag{5.32}$$

it is necessary to know the average value of the yoke magnetic field strength H_y. The length of the yoke is then (for outer stator)

$$l_y = \frac{\pi\left(D_1 + 2h_s + h_y\right)}{2p} \quad . \tag{5.33}$$

It is obvious that the presented approach is time consuming, hence instead of calculation in form of (5.32) a reduced length of the yoke length l_{yred} is used while using maximal value of the magnetic field strength H_y

$$\Theta_y = H_y l_{yred} \quad , \tag{5.34}$$

The reduced yoke length uses a coefficient of correction of the yoke magnetic field strength k_y, which may be obtained using nomograms presented in literature. For this purpose a ratio between h_j and t_y is used, whereas the yoke pole pitch is (for stator yoke)

$$t_y = \frac{\pi\left(D_1 + 2h_s\right)}{2p} \quad , \tag{5.35}$$

thus ut is pole pitch measured at the bottom of stator slots. The reduced yoke length l_{yred} is (after reading of k_y from Fig. 5.14)

$$l_{yred} = k_y \frac{t_y}{2} \quad . \tag{5.36}$$

Even in this case it is necessary to note that the approach is specific for each available literature and it is necessary to strictly follow the approach of chosen literature. E. g. [4] includes specific characteristic of the steel for yokes, which results again from similarity between electric machines.

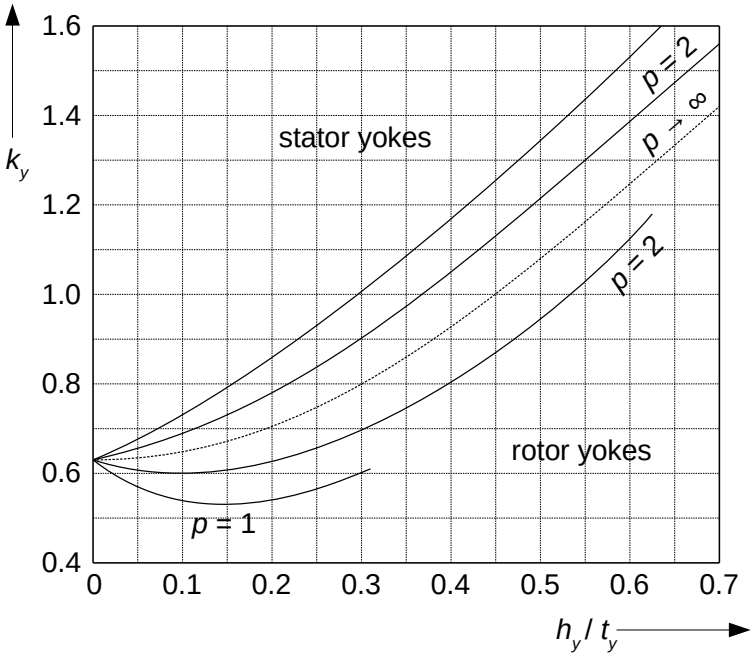


Fig. 5.14: Diagram for reading of the magnetomotive force correction factor k_y (translation from [3])

5.3.3 Magnetic Field of Excitation Poles and Yoke

Since the excitation poles of DC machines and synchronous generators have significantly different dimensions than teeth it is necessary to apply slightly different approach to design of these parts of the magnetic circuit. While in case of teeth it is possible to consider field effect only using desaturation factor in case of excitation poles the situation complicates and the leakage magnetic field increases. This projects also to the necessity of modification of their design, when a sum of main and leakage magnetic flux must be considered. The leakage magnetic flux is respected through magnetic flux leakage factor k_σ, which gives a ratio between leakage and main magnetic fluxes

$$k_\sigma = \frac{\Phi_\sigma}{\Phi_\delta} \quad . \tag{5.37}$$

The total magnetic flux at the root of the pole will be

$$\Phi_p = \Phi_\delta + \Phi_\sigma = (1 + k_\sigma)\,\Phi_\delta \quad , \tag{5.38}$$

where the magnetic flux is in general

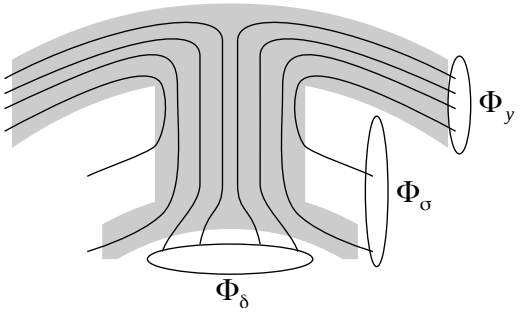


Fig. 5.15: Magnetic field of DC machine excitation poles

$$\Phi_p = \oint B_p \, dS = B_p \, b_p \, k_{Fe} \, L_p \quad , \tag{5.39}$$

since the length of the pole body may be slightly different in comparison to the length of the stator stack. For required value of the pole magnetic flux density it is necessary to reach pole width

$$b_p = \frac{(1 + k_\sigma)\,\Phi_\delta}{B_p \, k_{Fe} \, L_p} \quad . \tag{5.40}$$

The magnetic flux in te pole divides to two parallel patch leading through yoke, to chieve required value of the yoke magnetic flux density B_j it is possible to write

$$h_y = \frac{(1 + k_\sigma)\,\Phi_\delta}{2\,B_y \, k_{Fe} \, L_p} \quad , \tag{5.41}$$

whereas in comparison to armature yoke the magnetic flux goes through a massive yoke and it comes from a single pole, thus it is possible to obtain the corresponding magnetomotive force drop directly from the B-H curve of used material.

The leakage magnetic flux itself can be determined using known geometry and excitation through-Hopkinson's law. The magnetic flux lines considered for calcuation of the leakage magnetic flux are shown in Fig. 5.16 and except flux lines between poles and pole shoes also leakage between pole shoes and pole winding overhangs are considered. Thus, from Hopkinson's law point of view, the magnetomotive force of the excitation winding is known, i.e.

$$F_{ex} = N_{ex} I_{ex} \quad . \tag{5.42}$$

Considering conductance of the leakage paths Λ_σ the leakage magnetic flux will be equal to

$$\Phi_\sigma = \Lambda_\sigma F_{ex} \quad . \tag{5.43}$$

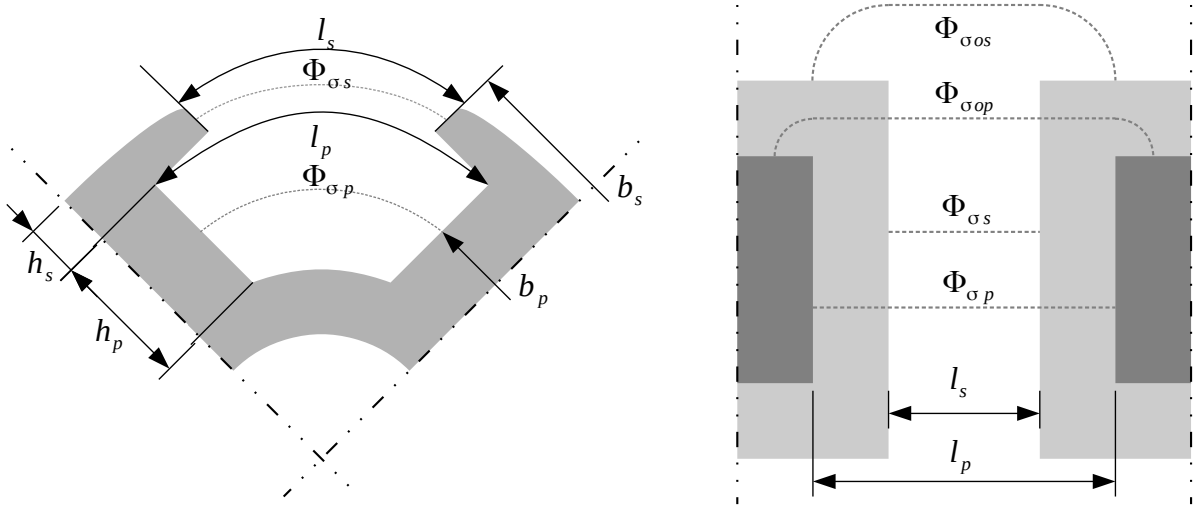


Fig. 5.16: Magnetic flux lines of leakage magnetic field of excitation poles

Since the area between the poles is from electromagnetic point of view equivalent to machine slots it is possible to write for the inter-pole leakage paths directly (equivalent to machine slots)

$$\Lambda_p = \mu_0 \frac{h_p}{3 l_p} L_p \tag{5.44}$$

and for conductance between pole shoes (again equivalently to slot openings)

$$\Lambda_s = \mu_0 \frac{h_s}{l_s} L_s \quad , \tag{5.45}$$

where l are the lengths between poles and pole shoes
and L are axial lengths of poles and pole shoes respectively.

The magnetic field between overhangs of excitation poles and pole shoes must be examined separately as it is a more complicated problem. In this case the magnetic flux line may be substituted by two quadrants axially going out of poles/pole-shoes. They are tangentially connected by segments of flux lines of lengths l_p and l_s. For an element of magnetic flux we can hen write

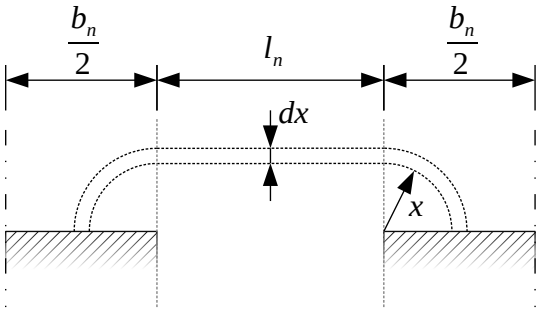


Fig. 5.17: Magnetic flux lines connecting pole shoes and magnetic flux element dx

$$d\Lambda_{os}=\mu_0\frac{dS}{l}=\mu_0\frac{h_s}{\frac{\pi}{2}x+l_s}dx \quad , \tag{5.46}$$

which leads to an integral

$$\Lambda_{os}=\mu_0 h_s\int_0^{\frac{b_s}{2}}\frac{1}{\frac{\pi}{2}x+l_s}dx \quad . \tag{5.47}$$

After calculation we obtain

$$\Lambda_{os}=\mu_0 h_s\frac{2}{\pi}\left[\ln\frac{\pi}{2}x+l_s\right]_0^{\frac{b_s}{2}} \quad , \tag{5.48}$$

and after substitution of boundaries the result is

$$\Lambda_{os}=\mu_0 h_s\frac{2}{\pi}\left[\ln\left(\frac{\pi b_s}{4}+l_s\right)-\ln l_s\right]=2\frac{\mu_0 h_s}{\pi}\left[\ln\left(\frac{\pi b_s}{4l_s}+1\right)\right] \quad . \tag{5.49}$$

Using equivalent approach and considering the coefficient of triangular magnetic field for pole body we obtain

$$\Lambda_{op}=\frac{2\mu_0 h_p}{3\pi}\left[\ln\left(\frac{\pi b_p}{4l_p}+1\right)\right] \quad . \tag{5.50}$$

The resulting magnetic conductance of leakage paths is then

$$\Lambda_\sigma=\Lambda_p+\Lambda_n+2\left(\Lambda_{čp}+\Lambda_{čn}\right) \quad . \tag{5.51}$$

Now it is possible to determine the value of leakage magnetic flux using (5.43) and the leakage magnetic flux coefficient according to (5.37). Using similar approach it is also possible to determine the leakage magnetic fluxes in permanent magnet synchronous machines, which is necessary for successful design of permanent magnet excitation.

5.3.4 Air Gap Magnetic Field

Although the air gap is formed by a magnetically linear environment, the layout opf the magnetic field here is most complicated and affected by a whole set of factors. The most important are

- division of winding into slots
- width of slot openings
- magnetic circuit saturation, especially teeth layer

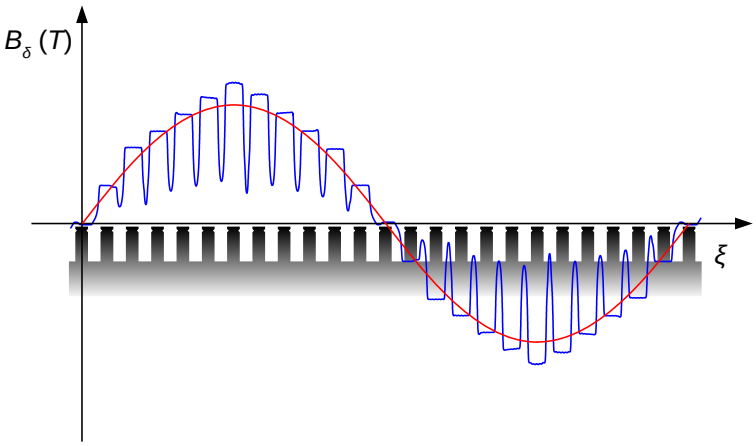


Fig. 5.18: A comparison of ideal layout of the air gap magnetic flux density with FEM results

The division of winding into slots creates discrete changes of the magnetic flux density along the air gap, which is generally known as a "step-curve." This curve is further affected by slot openings, which introduces further pulsations, which appear as a set of higher order harmonic components in the air gap magnetic field. The unused energy of harmonic components is then similar to leakage magnetic flux and it is reflected in form of differential leakage flux coefficient τ_{dif}. Its correct calculation should result either from knowledge of Görges pattern or from harmonic analysis of the air gap magnetomotive force. But, the literature also mentions more or less accurate empiric relations to obtain a value of the differential leakage flux coefficient.

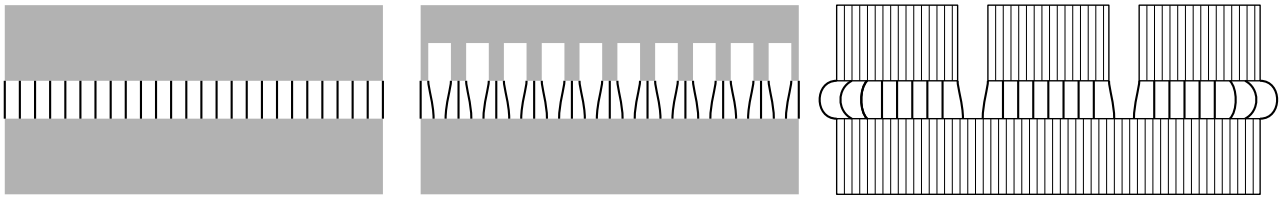


Fig. 5.19: Air gap magnetic flux lines between two smooth surfaces, smooth and slotted surface and between segmented stator and massive rotor

Among harmonic components the slot openings also project in extension of air gap magnetic flux lines and in increase of the air gap magnetomotive force drop, while this effect may be observed in both axial and radial cross-sections of the machine (see Fig. 5.19). This phenomena is reflected via Carter's factor, which expresses the extension of air gap magnetic flux lines, but except slot effects it also allows application for segmented stator/rotor.

The derivation of the Carter's factor may be shown on an analysis of magnetic fluxes through one slot pitch, as shown in Fig. 5.20. The magnetic flux going through a slot pitch is in an ideal case given by the air gap magnetic flux density B_δ and its value is

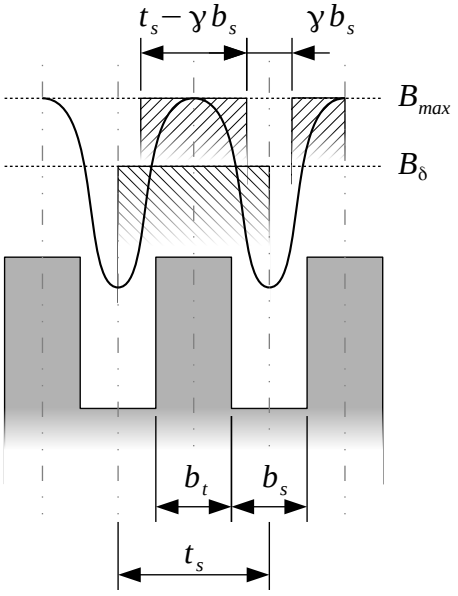


Fig. 5.20: Magnetic flux density pulsations resulting from slotting

$$\Phi_{ts} = B_\delta t_s l_{Fe} \quad . \tag{5.52}$$

If an increase of the magnetic flux density ripple to B_{max} is considered, it is necessary to reduce the width of the area, which leads this magnetic flux to $(t_d - \gamma b_d)$ and it may be written as

$$\Phi_{ts} = B_{max} (t_s - \gamma b_s) l_{Fe} \quad . \tag{5.53}$$

Now let us define the Carter's factor as a ratio between maximal and average magnetic flux density values B_{max} and B_δ

$$k_C = \frac{B_{max}}{B_\delta} = \frac{t_s}{t_s - \gamma b_d} \quad . \tag{5.54}$$

In case of semi-closed slots the magnitude of the flux ripples decreases and the slot width from relation (5.54) is being replaced by the width of the slot opening b_o

$$k_C = \frac{t_s}{t_s - \gamma b_o} \quad . \tag{5.55}$$

The coefficient γ is then across literature being expressed differently, whereas one of most common expressions is

$$\gamma = \frac{b_o}{b_o + 5\delta} \quad , \tag{5.56}$$

which may in case of small air gaps fail. In these cases it is suitable to use a more complex relation

$$\gamma = \frac{2}{\pi} \left\{ \operatorname{atan}\left(\frac{b_o}{2\delta}\right) - \frac{\delta}{b_o} \ln\left[1 + \left(\frac{b_o}{2\delta}\right)^2\right] \right\} \quad .^{8} \tag{5.57}$$

As obvious, the Carter's factor is derived as a coefficient of a slotted surface against smooth one. In case of doubly slotted machines (induction machines) it is necessary to derive separately Carter's factors for stator and the rotor, whereas the result is a multiplication of both values.

As shown a similar effect can be expected in case of segmented machines, i.e. machines with radial cooling channels. In this case the edge effects extend the air gap and it is possible to use the previous relations with following modifications:

- the slot pitch verges to the length of a single stator segment l_s and neighbouring ventilation channel l_v

8 Again it is necessary to emphasise some caution in work with the literature – the presented relations are derived for Carter's factor as presented in [3], which corresponds with original Carter's work [7]. The commonly available Czech literature ([4], [8]) presents slightly modified way of calculation of the Carter's factor and the coefficient γ thus it is not possible to combine both approaches (and related calculations).

$$t_s \rightarrow l_s + l_v \tag{5.58}$$

- the width of the slot opening verges to the width of the cooling channel

$$b_o \rightarrow l_v \tag{5.59}$$

The Carter's factor for ventilation channels is then

$$k_{Cv} = \frac{l_s + l_v}{l_s + l_v - \gamma l_v} = \frac{l_s + l_v}{l_s + (1-\gamma) l_v} \tag{5.60}$$

using coefficient

$$\gamma = \frac{l_v}{l_v + 5\delta} \quad . \tag{5.61}$$

The effective length of the stator stack is then

$$l_{ef} = \frac{l}{k_{Cv}} \quad , \tag{5.62}$$

where the total length of the stator l is

$$l = n_s l_s + (n_s - 1) l_v \quad , \tag{5.63}$$

where n_s is the number of stator stack segments,
l_s is the length of the segments
and l_v is the width of ventilation channels.

Another effect influencing the air gap dimensions is the border effect. In comparison to Carter's factor, which acts especially in radial dimension, the border effect axially extends the air gap and length of the machine (see Fig. 5.21). As a result the length of the machine appears to be

$$l_i = l_{Fe} + \delta \quad . \tag{5.64}$$

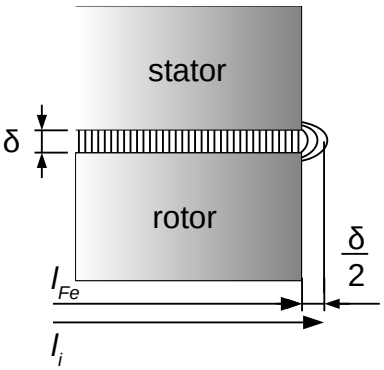


Fig. 5.21: Border effects at the end of the air gap

The air gap length considering Carter's factor is denoted by an apostrophe

$$\delta' = k_C \delta \tag{5.65}$$

and it influences the air gap magnetomotive force drop, which results from air gap magnetic flux density as

$$\Theta_\delta = H_\delta \delta' = \frac{1}{\mu_0} B_\delta k_C \delta \quad . \tag{5.66}$$

5.4 Saturation of the Magnetic Circuit and Related Characteristics

The last effect, which influences the properties of the magnetic circuit is the saturation of the magnetic circuit. The saturation is commonly expressed as no-load characteristic of the machine, especially in case of machines with controllable excitation and induction machines. Historically the no-load characteristic has been drawn for 100 %, 115 % and 130 % of the air gap magnetic flux density B_δ and interpolated for other values. Nowadays it can be relatively easily drawn in whole interval of possible values using numeric software. From known no-load characteristic (denoted as ch_0 in Fig. 5.22) and air gap characteristic (a tangent to no-load characteristic at the beginning of the coordinate system) the magnetic circuit saturation factor k_{sat} may be derived.

The procedure of determination of the saturation factor starts with determination of the no-load characteristic – i.e. for 100 %, 115 % and 130 % of the air magnetic flux density the magnetomotive force drop on the whole magnetic circuit is calculated and by interpolation the whole characteristic ch_0 is obtained. The magnetomotive force corresponds in case of synchronous machines (for which these characteristics are most commonly constructed) to excitation, thus the x axis is marked as F_m.

In the next step it is possible to get the air gap characteristic from the tangent to the no-load characteristic at the beginning of the coordinate system. Considering a sine-wave curve of the air gap magnetomotive force, it is possible to project it to the fourth quadrant as a sine curve with magnitude of F_{m100} and then using ch_0 determine the corresponding value of $B_{\delta 100}$. Using air gap characteristic it is possible to determine the value of B_{1r}, i.e. a value of the air gap magnetic flux density in case of desaturated magnetic circuit.

Consequently it is possible to find the air gap magnetomotive force F_δ on the crossing of connection between value $B_{\delta 100}$ with the air gap characteristic. This results in magnetic circuit saturation factor

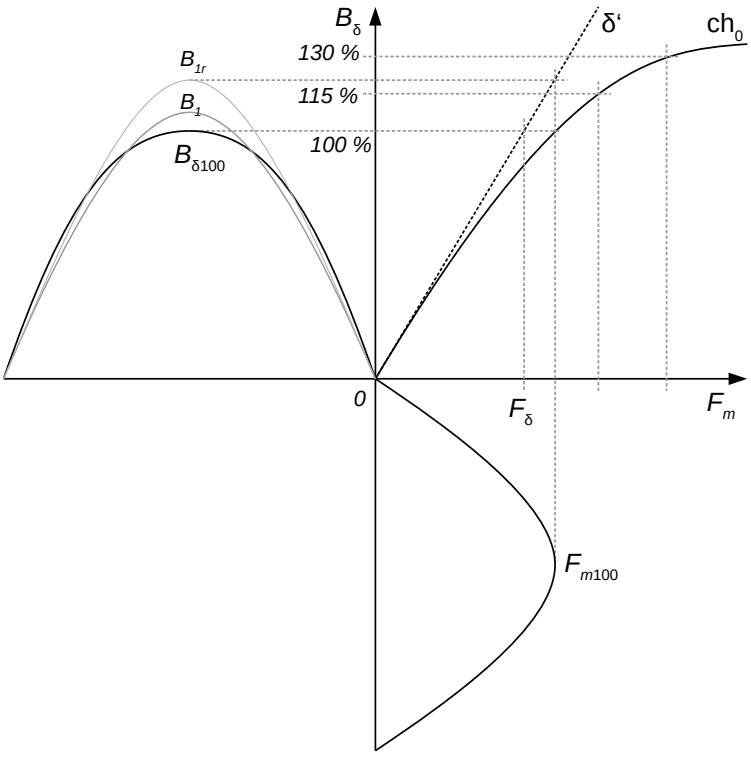


Fig. 5.22: The determination of the saturation factor from the no-load characteristic

$$k_{sat} = \frac{F_{m100}}{F_{\delta}} \quad . \tag{5.67}$$

To obtain a full analysis, it is also possible to draw the air gap magnetic flux density using “mirroring” of the magnetomotive force curve over the no-load characteristic. The magnetic flux density is slightly flattened, which may be further used for more accurate determination of magnetic field shape coefficient k_B and pole coverage factor α_δ. As an example also fundamental harmonic component of the air gap magnetic flux density B_1 is also shown in Fig. 5.22.

The magnetic circuit saturation factor is further used for modification of the air gap size in relation to saturated equivalent circuit parameters. In this case it is designated by two apostrophes and its value is

$$\delta'' = k_{sat}\,\delta' = k_{sat}\,k_C\,\delta \quad . \tag{5.68}$$

6 Equivalent Circuit Parameters

A precise calculation of equivalent circuit parameters is an important part of the design for two main outputs – calculation of losses and for the purpose of validation of the phasor diagram, since using phasor diagram it is possible to verify the choice of parameters of the machines (power factor, overloadability etc.) as well as correct design of e.g. excitation.

In case of resistance, which is frequency dependent, the literature uses approximately identical approach, while only minor differences appear in the interpretation of some particular results. A different situation relates to machine inductances. The inductances are often not calculated separately and instead of them only reactances are obtained (e.g. [4], [3], [6]). Historically this approach is given by the fact that it was presumed that all machines will be supplied from the power grid, thus the working frequency of the machine will be constant. Thus also resulting multiplication of the angular frequency of the grid and inductance will be also constant, thus the value of reactances is a sufficient information.

With the growth of the amount of machines supplied from power converters the term “reactance” forms more an obstacle and it is suitable to calculate the inductances only. They are (at least in terms possibilities of analytical calculation) independent by frequency and they serve as an important input for the purpose of simulation and control of the machine. Because of this reason the inductances are used in further text as wide as possible and reactances are used only in cases where their usage has a reasonable background.

6.1 Winding Resistances

The calculation of winding resistances is relatively simple and the most demanding part of the calculation is accuracy of calculation of the winding wire length. The resistances are commonly calculated for two temperatures – for 20 degrees Celsius and for rated machine temperature[9]. The most common materials used for winding wires are copper and in some specific application aluminium. As an additional material (e.g. for double caged armatures of induction machines) also copper alloys like bronze and brass are used.

From above mentioned materials the best conductivity belongs to copper (γ_{Cu} = 58.5 *MS/m* at 20 degrees Celsius) whose thermal resistance coefficient is α_{Cu} = 0.00429 K^{-1}. Its disadvantage is relatively high mass density (ρ_{Cu} = 8900 kg/m^3) which leads to a large fraction of copper mass. In case of aluminium the conductivity is lower (γ_{Al} = 35.4 *MS/m* at 20 degrees Celsius) and it has also slightly higher thermal coefficient (α_{Al} = 0.0044 K^{-1}) nevertheless thanks to its lower density (ρ_{Cu} = 2700 kg/m^3) it is suitable for use in applications requiring low machine mass (aerospace etc.).

In the past the aluminium was commonly used for casting of squirrel cage rotors whereas its main advantage was its low viscosity in liquid state and low melting temperature. These factors made the manufacture cheap and easy. The forced transition to squirrel cages made of copper[9], which has higher melting temperature and it is very viscose, led to increase of demands on the manufacture and it also increased the prices of such machines.

9 In some cases there is an additional reference temperature defined to have comparable data across e.g. traction machines.

The relation between resistivity of the material at temperature ϑ and reference temperature ϑ_0 is at common temperatures expressed by relation

$$\rho_\vartheta = \rho_0\left[1+\alpha\left(\vartheta-\vartheta_0\right)\right] \quad , \tag{6.1}$$

which may be modified to relation of conductivity

$$\gamma_\vartheta = \frac{\gamma_0}{1+\alpha\left(\vartheta-\vartheta_0\right)} \quad . \tag{6.2}$$

The resistance may be then determined on base of well known relation

$$R = \frac{1}{\gamma}\cdot\frac{l}{S} \quad , \tag{6.3}$$

where γ is the conductivity of the material at given temperature,
l is the total phase conductor length,
and S is its cross section.

The length of the conductor is given by the number of winding turns in series N_s and length of the winding turn l_c, which is composed of slot part and winding overhang part

$$l_c = 2\left(l_s + l_o\right) \quad . \tag{6.4}$$

The length of the slot part (linear) corresponds with the length of the stator stack with possible additional cooling channels increased by some additional extension. Thus extension is also forms by a linear part just before its bending to the shape of the winding overhang and its size is a purely technological element and it can be in order of millimetres or centimetres. It is affected among others by possibilities of forming of precise coil overhang shape, but also by presence of press boards at the and of the stator stack. Generally the length of the linear par may be written as

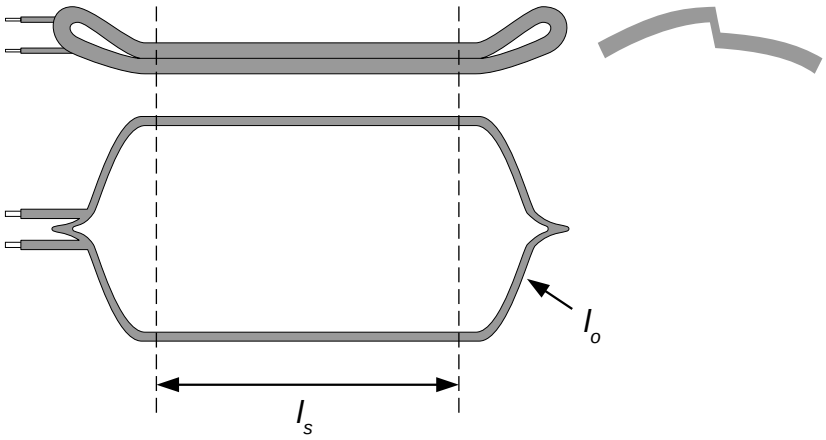


Fig. 6.1: Shape of a lap winding coil

$$l_s = n_{is} l_{is} + \left(n_{is}-1\right) l_v + 2\, l_{of} \quad , \tag{6.5}$$

where l_{of} is the length of the linear offset of the coil.

The length of the wining overhang may be then determined simply from known geometry of the coil shape. In case of windings made of round wires the winding overhangs are formed by arc segments while in case of pre-formed coils the coil shape corresponds to a coil shown in Fig. 6.1 with known angle between coil overhang and the stator stack α_o. The average length of the winding overhang may be then determined using (considering radial extension of winding overhangs α and half-circular shape of the coil loop R_c)

$$l_o = \frac{\pi(D_1 \pm h_s)\beta}{2p\cos\alpha_o \cos\alpha} + \pi R_c \quad , \tag{6.6}$$

where the "+" sign must be applied for slots on outer part of the air gap (outer stators) and the "-" sign for slots on inner part of the air gap (inner rotors).

The cross-section of a phase wire is then affected by the winding topology, i.e. the used number of parallel wires n_p or the number of parallel winding branches ($a_\sim$ for AC windings, $2a_=$ in case of DC windings). Considering both effects the relation (6.3) verges to

$$R = \frac{1}{\gamma} \cdot \frac{N_s l_c}{a_\sim n_p S_w} \quad , \tag{6.7}$$

where S_w is the cross-section of an elementary winding wire.

In case of AC power supply additional eddy currents loading the wires by additional losses are generated. In comparison to DC resistance according to (6.7) the resistance increases. This effect is expressed by coefficient $k_\sim$ - a coefficient expressing the increase of losses by using AC power supply. This coefficient may be neglected in case the winding wire height is smaller than the penetration depth at given frequency, where the penetration depth is

$$a = \sqrt{\frac{2}{2\pi\mu_0\gamma f}} \quad [10]. \tag{6.8}$$

The calculation of the resistance increase coefficient for a conductor in a slot $k_\sim$ results from analysis of eddy currents of a conductor in a slot [10] and it uses proportional penetration depth

$$\zeta = \frac{h_v}{a} \quad , \tag{6.9}$$

and the value of the resistance increase coefficient is

$$k_\sim = \zeta \frac{\sinh 2\zeta - \sin 2\zeta}{\cosh 2\zeta - \cos 2\zeta} \quad . \tag{6.10}$$

10 For copper at 20 degrees Celsius and 50 *Hz* frequency the penetration depth is 9.35 *mm*.

The resulting effective winding resistance while leading AC current is then

$$R_{\sim} = k_{\sim} R \quad . \tag{6.11}$$

6.2 Machine Inductances

The inductances of an electric machine play a crucial role regarding its behaviour thus it is necessary o pay attention while estimation of machine inductances. They affect e.g. dynamic behaviour of synchronous machines (while damping pulsations) but they also affect the magnitude of current ripples while feeding the machine from semiconductor converters. A suitably chosen value of inductance then affects also its overloadability and power factor as the inductance is a main parameter of the machine as a power consuming element.

6.2.1 Magnetizing Inductance

The magnetizing inductance expresses a mutual connection between stator and rotor, whereas it is in any form present in case of all electric machines. A will be shown later, its value is tightly bound to the air gap size, whereas it may be also affected by presence of permanent magnets. The magnetizing inductance value may be derived from magnetic field of one single winding turn, which generates a rectangular magnetic field with amplitude of magnetomotive force

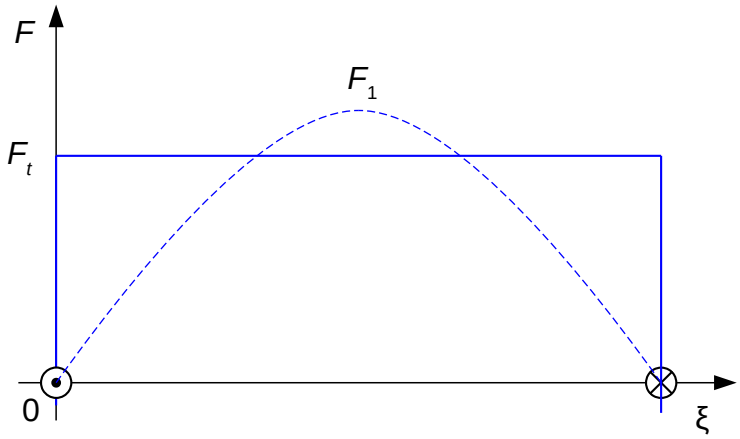


Fig. 6.2: Magnetic field of a single coil turn

$$F_t = I_m \quad . \tag{6.12}$$

The amplitude of fundamental harmonic component of this field is

$$F_1 = \frac{4}{\pi} I_m \quad , \tag{6.13}$$

whereas in reality the winding is formed by N_s winding turns in series, which together have fundamental winding component winding factor k_{w1} and they are spread over $2p$ poles. For one whole phase may be therefore written

$$F_{m1} = \frac{4}{\pi} \cdot \frac{N_s k_{w1} I_m}{2\,p} \quad . \tag{6.14}$$

In case of generally *m*-phase machine the amplitude of the magnetomotive force increases *m*/2-times, thus the relation (6.14) verges to

$$F_m = \frac{m}{\pi} \cdot \frac{N_s k_{w1} I_m}{p} \quad , \tag{6.15}$$

which is the amplitude of armature rotary magnetic field. Knowing electromagnetic length of the air gap δ‘, it is possible to write (neglecting saturation effects of the magnetic circuit)

$$H_\delta = \frac{F_m}{\delta'} \tag{6.16}$$

and the spacial layout of the magnetic field strength in the air gap is

$$H(\xi) = H_\delta \cos \xi \quad . \tag{6.17}$$

Now it is possible to derive the magnetizing inductance of the machine from magnetic energy in the air gap, whereas the magnetic filed energy density is

$$w_m = \int B\,dH = \mu_0 H^2 = \mu_0 H_\delta^2 \cos^2 \xi \quad . \tag{6.18}$$

The total magnetic field energy in the air gap is then

$$W_m = \int_{V_\delta} w_m\,dV = \int_0^{l_i} \int_0^{\delta'} \int_0^{p2\pi} w_m(\xi)\,d\xi\,dr\,dz \quad . \tag{6.19}$$

After calculation the air gap magnetic field energy is

$$W_m = \frac{1}{2}\mu_0 \left(\frac{m}{\pi} N_s k_{w1} I_m \right)^2 \frac{t_p l_i}{p\delta'} \quad . \tag{6.20}$$

The magnetic field energy in the air gap is for one phase

$$W_{m1} = \frac{1}{2} L_\mu I_m^2 \quad , \tag{6.21}$$

whereas in case of *m* phases it is

$$W_m = \frac{m}{2} W_{m1} = \frac{m}{4} L_\mu I_m^2 \quad . \tag{6.22}$$

Using comparison with (6.20) we obtain

$$L_{\mu} = 2\mu_0 \frac{m}{p}\left(\frac{N_s k_{w1}}{\pi}\right)^2 \frac{t_p l_i}{\delta'} \quad . \tag{6.23}$$

The value derived in (6.23) then corresponds with non-saturated magnetizing inductance value. For obtaining its saturated value, it is necessary to use the air gap length considering saturation δ“.

6.2.2 Leakage Inductance

The leakage inductance of machine winding expresses total energy of magnetic field which is not used for generation of the torque. This corresponds to leakage magnetic fields in slot and around winding overhangs, but also to harmonic components of magnetic field, which are not utilized to generation of torque. Thus it is necessary to calculate separately:

- slot leakage inductance
- winding overhang leakage inductance
- differential leakage inductance of magnetic field higher order harmonic components

The slot leakage is composed of magnetic field of a conductor in a slot (as shown in Fig. 6.3) and leakage magnetic field going through slot opening. For a single conductor in a slot it might be derived

$$L_{\sigma w} = \mu_0 \frac{h_1}{3 b_s} l_{Fe} + \mu_0 \frac{h_o}{b_o} l_{Fe} \quad . \tag{6.24}$$

But, this form is valid only for one shape of the slot, thus a more general expression is commonly used

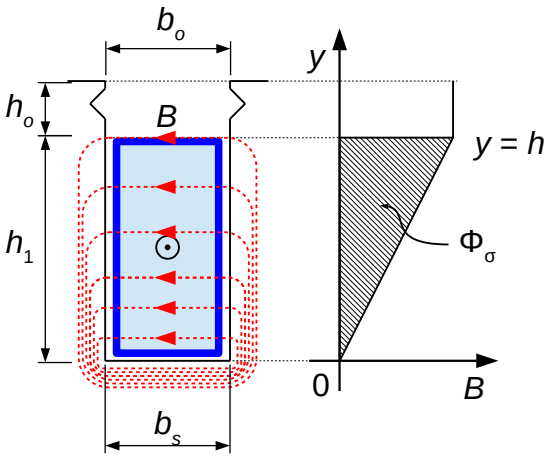


Fig. 6.3: Leakage magnetic field in a slot

$$L_{\sigma w} = \mu_0 l_{Fe}(\lambda_s + \lambda_o) \quad , \tag{6.25}$$

where λ_s is the slot leakage factor
and λ_o is the slot opening leakage factor.

The inductance of a whole coil is given by a square of the number of the coil wires in series

$$L_{\sigma c} = L_{\sigma w} N_w^2 \quad , \tag{6.26}$$

whereas the number of coil wires in series may be written as

$$N_w = 2 N_c = 2 \frac{N_s}{2pq} = \frac{N_s}{pq} \quad . \tag{6.27}$$

One phase has then

$$K_f = \frac{Q}{m} = \frac{2\,pmq}{m} = 2\,pq \tag{6.28}$$

coils, thus the total value of the leakage inductance of slot part will be

$$L_{\sigma d} = K_f L_{\sigma w} N_w^2 = 2\,pq\,L_{\sigma w}\left(\frac{N_s}{pq}\right)^2 = 2\mu_0 \frac{N_s^2}{pq}(\lambda_s + \lambda_o) l_{Fe} \quad . \tag{6.29}$$

This relation is generally valid for single layer windings and tooth windings with coil sides beside each other, whereas the coefficients λ_s and λ_o are tabled in the literature according to the slot shape. In case of double layer three phase windings[11] these coefficients are extended by coil pitch factors

$$k_\beta' = \frac{1}{4}(1 + 3\beta) \tag{6.30}$$

and

$$k_\beta = \frac{1}{4}(1 + 3k_\beta') \quad , \tag{6.31}$$

thus for double layer three phase windings the slot leakage inductance is

$$L_{\sigma s} = 2\mu_0 \frac{N_s^2}{pq}(\lambda_s k_\beta + \lambda_o k_\beta')\, l_{Fe} \quad . \tag{6.32}$$

The calculation may be extended by winding overhangs leakage factor in a very similar way. The magnetic field in the area of winding overhangs is very complicated and except free space around winding overhangs it may enter constructional parts of the machine. This corresponds with complexity of its calculation, thus simplified relations are commonly used. One of most common is e.g.

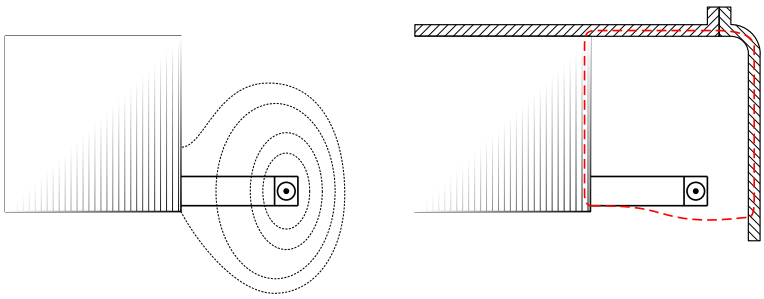


Fig. 6.4: Leakage magnetic field around winding overhangs

$$\lambda_o = 0.34\frac{q}{l}(l_o - 0.64\beta t_p) \quad . \tag{6.33}$$

The last component of the inductance is the differential leakage flux factor, which is tightly bound to the magnetizing inductance of the machine. If we mark the sum of coefficients of the slot leakage and slot opening leakage as λ_{so}, the final relation for calculation of leakage inductance is

11 In case of polyphase windings with $m > 3$ please refer appropriate literature.

$$L_\sigma = 2\mu_0 \frac{N_s^2}{pq}(\lambda_{so} + \lambda_o) l_{Fe} + \tau_{dif} L_\mu \quad , \tag{6.34}$$

where for single layer windings we have

$$\lambda_{so} = \lambda_s + \lambda_o \tag{6.35}$$

and for more layers

$$\lambda_{so} = \lambda_s k_\beta + \lambda_o k_\beta' \tag{6.36}$$

while in case of usage of magnetic wedges the slot opening factor must be multiplied by relative permeability of used wedges (commonly about $\mu_r \rightarrow 3$ [11]).

6.3 „Iron Resistance“

The only element of the equivalent circuit, which cannot be directly measured is so-called “iron resistance“, which represents the losses arising in the magnetic circuit in equivalent circuit of the machine. In equivalent circuits it is commonly being laid in parallel to the back EMF and it symbolizes iron core losses by a resistance with equivalent I^2R losses. Thus if relation

$$\Delta P_{Fe} = m R_{Fe} I_{Fe}^2 \quad , \tag{6.37}$$

should be equal to

$$I_{Fe} = \frac{U_i}{R_{Fe}} \tag{6.38}$$

from Ohms law, we obtain

$$\Delta P_{Fe} = m \frac{U_i^2}{R_{Fe}} \quad . \tag{6.39}$$

Thus the iron resistance results

$$R_{Fe} = m \frac{U_i^2}{\Delta P_{Fe}} \quad . \tag{6.40}$$

7 Losses in Electric Machines

The calculation of losses is a crucial step for calculation of efficiency as well as for the purpose of calculation of thermal rise of the machine, since all generated losses – directly or not – cause the heating of the machine. This affects degradation of other parts of the machine – insulation ageing, degradation of bearing lubricant and together with thermal stretchability it also stresses mechanical components of the machine.

The exact composition of losses is specific according to the machine type, its topology and duty type. Losses appearing in all types of electric machines are I^2R losses (Joule losses, ΔP_j), mechanical losses (ΔP_m), iron core losses (ΔP_{Fe}) and commonly losses related to armature slotting, i.e. either pulsation losses (ΔP_p) or surface losses (ΔP_s). Losses related to specific types of machines then include filed winding losses (ΔP_f – synchronous and DC machines with electric excitation), permanent magnet losses (ΔP_{PM} – permanent magnet machines) an in case of machined fed from the power converter also related PWM losses (ΔP_{PWM}). Since there is some uncertainty of calculation of some kinds of losses and also some manufacturing imperfections occur also some "additional" losses are considered (ΔP_{add}), which are expressed in dependence on the size and power of the machines.

7.1 I^2R (Joule) losses

Losses caused by leading of the current through the winding are commonly designated "I^2R losses" (which describes well their calculation), although foreign literature uses also the term Joule losses. In general they can arise in any winding of an electric machine, nevertheless for the design purposes the I^2R losses arising in the armature of the machine are distinguished from field winding losses (synchronous or DC machines) by designation ΔP_j vs. ΔP_f. Both types of losses result from the resistance of the winding and for the purpose of determination of efficiency and thermal rise they are calculated for rated temperature resistance[12]. The losses in the armature of generally m-phase machines are calculated according to

$$\Delta P_j = m R_{\sim} I^2 \quad , \tag{7.1}$$

where $R_{\sim}$ is the winding resistance at a certain frequency.

In the armature of DC machines the situation is simpler and the I^2R losses can be calculated as

$$\Delta P_j = R_a I_a^2 \quad . \tag{7.2}$$

The field winding I^2R losses are then in similar way

$$\Delta P_f = R_f I_f^2 \quad . \tag{7.3}$$

12 In some cases there is an additional reference temperature defined to have comparable data across e.g. traction machines.

The losses arising in brushes while leading the current may be also considered I^2R losses. These losses, since the resistance of the brushes is relatively high, form a non-negligible part of losses and thy are calculated from brush voltage drop as

$$\Delta P_b = U_b I_a \quad , \tag{7.4}$$

where the voltage drop on a brush can be determined according to brush material and its value should not exceed $U_b = 1\ V$.

7.2 Iron Core Losses

The iron core losses were partially described in relation to the description of the magnetic circuit in chapter 5.2. This type of losses relates generally to any part of electrically and magnetically conducting parts of the magnetic circuit of the machine. According to the principle of generation of each loss component they can be divided to losses related to the main magnetic flux and losses arising due to slot harmonic components in massive as well as in sheeted parts of machine.

7.2.1 Losses Generated by Magnetizing Magnetic Flux

The losses generated by the main magnetic flux arise in all parts of the machine which are utilized by the main magnetic flux and its value changes in time – i.e. especially in armature teeth and yoke. With reference to the chapter 5.2 we can summarize that these losses are separately calculated for armature teeth as

$$\Delta P_t = k_{tt} m_t \Delta p_t \quad , \tag{7.5}$$

where k_{tt} is the technological factor of teeth iron core losses (k_{tt} = 1.5 … 2)
m_t is total teeth mass
and Δp_t is the iron core loss density at given frequency t and magnetic flux density B_t as

$$\Delta p_t = \Delta p_{ref} \left(\frac{f}{f_{ref}} \right)^{\alpha} \left(\frac{B}{B_{ref}} \right)^{\beta} \quad , \tag{7.6}$$

where Δp_{ref} is the iron core loss coefficient for reference values of frequency and flux density
α is the exponent of frequency, for common electrical steel sheets $\alpha \approx 1.5$
and β is the exponent of magnetic flux density, for common electrical steel sheets $\beta \approx 2$.

In the same way the iron core losses for yoke are calculated

$$\Delta P_y = k_{ty} m_y \Delta p_y \quad , \tag{7.7}$$

where k_{ty} is the technological factor of teeth iron core losses (k_{ty} = 1.3 … 1.7)
m_y is total mass of the yoke
and Δp_y is the iron core loss density at given frequency t and magnetic flux density B_j obtained using (7.6).

7.2.2 Pulsation Losses

The pulsation losses arise in slotted parts of the machine where two slotted parts move against each other. A typical example if such a system are induction machines where the rotor armature rotates in stator armature – both of them are slotted and each of them generates pulsations of the air gap magnetic flux density. These pulsations move with each part and they generate flux ripples in the opposite part – the pulsations generated by stator slotting generate ripples in rotor teeth et vice versa – pulsations generated by rotor teeth cause flux ripples in stator teeth. These pulsations cause quick changes in teeth magnetization and thus they generate additional component of iron core losses in teeth.

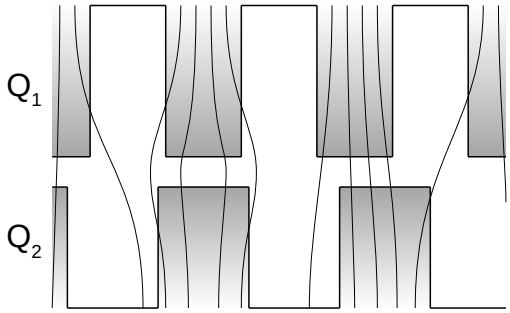


Fig. 7.1: Magnetic flux lines between stator and rotor teeth

The pulsation losses are one of loss component, which is determined in each literature different, in most cases using empiric relations. In comparison with measurement the relations mentioned in [3] correspond very well, whereas the pulsation losses in the stator are calculated as

$$\Delta P_{puls1} = 8.3\,\Delta p_e \left(\frac{Q_2 n}{10000}\right)^2 \left(\frac{B_{p1}}{B_{ref}}\right)^2 m_{t1} \quad , \tag{7.8}$$

where Δp_e is the eddy current loss coefficient at reference frequency and magnetic flux density, whereas it is possible to use value of $\Delta p_e = 0.5\,\Delta p_{ref}$,
Q_2 is the number of rotor slots,
n is the speed of the machine in revolutions per minute,
m_{t1} is the mass of stator teeth,
B_{ref} is the reference value of magnetic flux density
and B_{p1} is the amplitude of magnetic flux density pulsations in stator teeth calculated as

$$B_{p1} = \frac{t_{s2}}{2\,t_{s1}} k_{C1}\left(k_{C2} - 1\right) B_{t1} \quad , \tag{7.9}$$

where t_{s1} is the stator slot pitch,
t_{s2} is the rotor slot pitch,
k_{C1} is the stator Carter factor,
k_{C2} is the rotor Carter factor
and B_{t1} is the stator teeth magnetic flux density.

In the same way the rotor pulsation losses are

$$\Delta P_{puls2} = 8.3\,\Delta p_a \left(\frac{Q_1 n}{10000}\right)^2 \left(\frac{B_{p2}}{B_{ref}}\right)^2 m_{t2} \tag{7.10}$$

with pulsation magnitude

$$B_{p2}=\frac{t_{s1}}{2t_{s2}}k_{C2}\left(k_{C1}-1\right)B_{t2} \quad . \tag{7.11}$$

Similar loss generation mechanism occurs also in case of some types of synchronous machines (machines equipped with damper, cylindrical rotor machines), reluctance machines with flux barriers and in direct current machines equipped with compensation winding.

7.2.3 Surface Losses

Similarly to pulsation losses the surface losses are generated by slot effects. In this case the slots do not create pulsations in opposite slotted surface but they form a travelling wave over a massive surface. This wave generates eddy currents and losses. This surface may be a massive pole shoe (salient pole rotor synchronous machine, DC machine) or a massive rotor (cylindrical rotor synchronous machines) Also in case of this type of losses the approaches of different references differ and they cite mostly empiric relations. A very often used for is

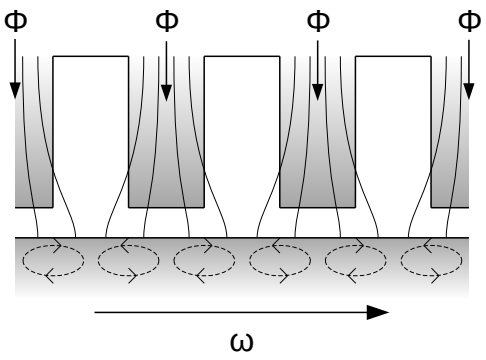


Fig. 7.2: Eddy currents in massive rotor surface

$$\Delta P_s=\sqrt{\frac{\gamma}{2\pi\mu}}S_{ps}t_s^2B_p^2f_p^{1.5} \quad , \tag{7.12}$$

where γ is the conductivity of pole shoe material,
μ is the pole shoe permeability,
S_{ps} is the total area of pole shoes,
t_s is the slot pitch of opposite armature,
and B_p is the pulsations amplitude calculated as

$$B_p=\left(1-\frac{1}{k_C}\right)B_\delta \quad , \tag{7.13}$$

where k_C is the Carter factor
and B_δ is the amplitude of the air gap magnetic flux density.

The pulsations frequency is similarly to case of pulsation losses

$$f_p=\frac{Qn}{10000} \quad , \tag{7.14}$$

where Q is the number of lots of opposite armature
and n is the rotational speed of the rotor.

Since the ratio between conductivity and permeability of the pole shoe material may be very hard to de fine, it is often used as a dedicated number k_s – coefficient of surface losses, which modifies (7.12) to

$$\Delta P_s = k_s S_{ps} t_s^2 B_p^2 f_p^{1.5} \quad , \qquad (7.15)$$

material	k_s [-]
construction steel	23.3
grey cast iron	17.3
low silicon steel (2 mm)	8.6
low silicon steel (0.5 mm)	2.5
high silicon steel (0.5 mm)	1.5

Tab. 7.1: Values of surface losses factors according to used materials (translation from [3])

Common values of this coefficient are shown in table 7.1.

7.3 Permanent Magnet Losses

Although permanent magnets are considered a purely passive part of the magnetic circuit which generates no losses, in reality they have their own conductivity, thus they are able to generate eddy currents. These eddy currents may be generated by slotting of the machines (in case of surface mounted permanent magnets) as well as by magnetic flux pulsations generated by current ripples from semiconductor power supplies. However the source is the eddy currents may be calculated using eddy current analysis and they result for a certain harmonic component

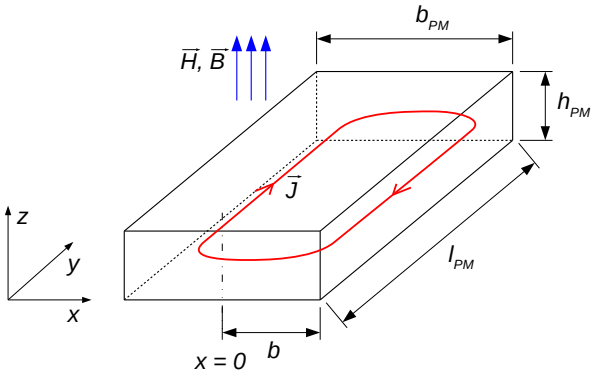


Fig. 7.3: Eddy currents induced into permanent magnet volume

$$\Delta P_{PM\nu} = \frac{1}{16} \cdot \frac{\alpha_\nu^2}{\zeta_\nu} B_\nu^2 \gamma_{PM} \omega_\nu^2 b_{PM}^2 \left(\frac{\sinh \zeta_\nu - \sin \zeta_\nu}{\cosh \zeta_\nu - \cos \zeta_\nu} \right) b_{PM} l_{PM} h_{PM} \quad , \qquad (7.16)$$

where α_ν is the harmonic component coverage factor (in interval $2/\pi$ … 1 according to its wavelength),
ω_ν is the angular speed of the harmonic component,
B_ν is the magnitude of pulsations of the harmonic component,
and ζ_ν is the proportional penetration depth of the harmonic component according to

$$\zeta_\nu = \frac{b_{PM}}{a_\nu} \quad , \qquad (7.17)$$

where b_{PM} is the width of the permanent magnet
and a_ν is the penetration depth

$$a_\nu = \sqrt{\frac{2}{\omega_\nu \gamma_{PM} \mu_{PM}}} \quad . \qquad (7.18)$$

The remaining parameters are parameters of the permanent magnet itself – its conductivity γ_{PM}, permeability μ_{PM}, length l_{PM} and height h_{PM}. It is obvious, that using this approach only losses in one permanent magnet and for one harmonic component may be calculated, thus it is necessary to make a sum over the number of permanent magnets and harmonic components:

$$\Delta P_{PM} = n_{PM} \sum_{\nu,\mu} \Delta P_{PM\,\nu,\mu} \quad , \tag{7.19}$$

where n_{PM} is the total number of permanent magnets in the machine
and ν, μ are designations of orders of time and spatial harmonic components.

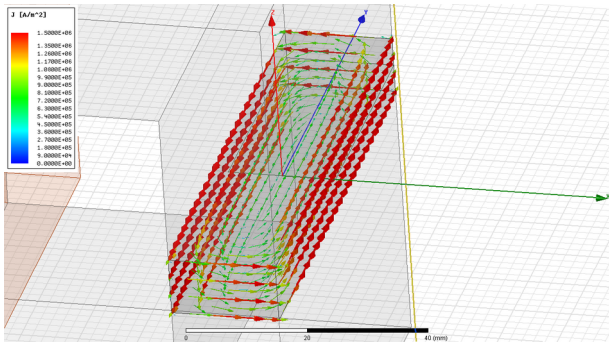


Fig. 7.4: Eddy currents in a permanent magnet (finite element analysis)

From the equation (7.16) one more conclusion can be recognized – and it is a dependence of permanent magnet losses on its width and volume. Because of this reason it is suitable to manufacture the permanent magnets as segmented, which leads to similar way of reduction of losses as in cae of electrical steel sheets. This inspired Arnold Magnetics to introduce laminated permanent magnets, i.e. permanent magnets made of thin electrically insulated segments [12].

Considering calculation demands on estimation of permanent magnet losses (necessary knowledge of air gap magnetic field, power supply etc.) they are often evaluated empirically as one per cent of the output power or using simplified relations [13].

7.4 Mechanical Losses

The mechanical losses belong to most complicated losses for calculation, since they depend on many parameters, which are by their nature heavily describable. This results in uncertainty in evaluation of mechanical losses and in a large variability of relations used for their calculation. These losses include all mechanical interactions in the machine, which lower its output power – rotor air friction, fan friction, bearing friction and friction of brushes on commutator or slip-rings. All these mechanism are affected by surface roughness, viscosity of cooling medium and properties of chosen bearing. The result is then very hardly describable system.

7.4.1 Rotor Movement Caused Losses

There is a while set of relations which try to approximate the losses caused by rotor movement (see e.g. [4], which includes a few of them), but a really qualified estimation may be base only on measurement performed on a set of similar machines. As one of compromising relations the equation from [3] may be mentioned:

$$\Delta P_m = k_m D\left(l + 0{,}8^3 \cdot 0{,}6\, t_p\right) v^2 \quad , \tag{7.20}$$

where k_m is the mechanical loss coefficient,
D is the rotor diameter,
l is the rotor length,
t_p is the pole pitch
and v is the surface speed of the rotor, i.e.

$$v = \frac{\pi D n}{60} \quad . \tag{7.21}$$

The rotor geometry and the cooling type are respected through the mechanical loss coefficient. Its approximate values are shown in table 7.2 where the highest values correspond with machines having a radial fan on the shaft, medium values to machines with axial fans and the lowest value belongs to hydrogen cooled machines, which is given by its low viscosity.

cooling type	k_m [-]
TEFC, fan on shaft	15
opened machine with fan on shaft	8 – 10
cylindrical rotor air cooled	5
cylindrical rotor hydrogen cooled	< 3

Tab. 7.2: The values of mechanical losses factors for different cooling types (translation from [3])

7.4.2 Losses Caused by Brush Friction

In comparison to previous components of losses the brush friction losses are relatively easy to be calculated, wince if we use relation

$$\Delta P_{bf} = F_b v_c \quad , \tag{7.22}$$

where F_b is the brush friction force
and v_c is the commutator peripheral speed

$$v_c = \frac{\pi D_c n}{60} \quad , \tag{7.23}$$

where D_c is the commutator diameter
and n is the number of machine revolutions per minute,
we can substitute the friction force by

$$F_b = k_t S_b p_b \quad , \tag{7.24}$$

where k_t is the brush friction coefficient (commonly between 0.15 – 0.5; mostly below 0.2),
S_b is the brush cross-section
and p_b is the brush pressure (set in interval from 15 to 70 kPa).

Then we obtain

$$\Delta P_{bf} = k_t S_b p_b v_c \quad . \tag{7.25}$$

This relation results from measurable values and it is easily verificable.

7.5 Additional Losses

The additional losses are determined purely empirically except cases when it is necessary to determine losses in some critical part. In these cases the finite element method is commonly used (e.g. in case of turbo alternator press boards etc.). An empiric estimation of additional losses is simple as

$$\Delta P_{add} = (0{,}2 \ldots 1\,\%)\, P_n \quad , \tag{7.26}$$

where P_n is the rated machine power.

The choice of percentage depends mainly on the size of the machines, whereas the lower values are considered for turbo generators, 0.5 per cent for large machines and 1 per cent for small and medium size motors.

7.6 Pulse-Width Modulation Losses

The losses generated by pulse-width modulation belong to one of most complex elements of losses, since the voltage impulses cause insulation heating by displacement current, current ripples resulting in winding eddy currents and magnetic flux pulsations superimposing to main magnetic flux and heating the magnetic circuit. Their exact determination is very demanding and in many cases for evaluation of PWM losses the experience from previous measurements on certain machine with certain control type is used.

A general approach to analysis of machines supplied from semiconductor power sources is described in CLC/TS 60034-25 [14], whereas one of the conclusions is that the losses may increase by 20 per cent. The total losses in a machine fed by power converter considering PWM losses may be then estimated as

$$\Delta P_{PWM} = 1.2\, \Delta P_{sin} \quad , \tag{7.27}$$

where ΔP_{sin} is the sum of losses calculated for sine-wave power supply.

7.7 Machine Efficiency

The total efficiency of the machine is given by ratio between output and input power, i.e.

$$\eta = \frac{P}{P_{\text{in}}} = \frac{P}{P + \Delta P} \quad , \tag{7.28}$$

where ΔP is the sum of losses at rated temperature and power unless stated else. Depending on power supply type the efficiency or losses can give either sine wave of PWM value.

8 General Approach for Design of an Electric Machine

While looking to Appendices 1 to 3 it is obvious, that the general approach for electric machine calculation is from a large part common for all electric machines and it differs more or less in machine type specific parts. It is also necessary to note that shown approach is focused on design of a machine with required rated parameters. By a modification of operation order it is possible to modify the sequence to obtain a machine with maximal output power while filling given space although its rated parameters are not known before the calculation. This approach is often used in electric traction, where the machine space is very limited and it is requested to achieve optimal usage of given space.



Fig. 8.1: Winding wires

The main input for approaches shown in Appendices 1 to 3 are the rated parameters of the machine, which may be supplemented by further limitations – maximal machine diameter, its maximal length, overloadability or maximal current in a certain duty cycle. These values are commonly binding, nevertheless some of the change during the design of the machine together with changes of the dimensions or equivalent circuit parameters. A typical example is the power factor of the machine, which is in certain cases more advantageous to have its lower value than originally requested.

As can be seen from shown flow charts, the whole procedure is affected by a set of parameters – from designer's parameters like some factors obtained from the experience, through material coefficients like saturation, up to "boundary conditions" giving a cooling type of the machine. A whole set of these parameters is being changed and corrected during the calculation, hence it depends mainly on designer's experience how exactly is he able to estimate these coefficients at the beginning of the design process.



Fig. 8.2: Winding while embedding to slots

Among all of these parameters it is necessary to decide about the fundamental machine parameters like its number of poles and slots, from which the winding design results. Further it is possible to estimate the dimensions of the machine. At this point it is necessary to iterate the values of the air gap magnetic flux density or linear current density to have an integral number of conductors in a slot, in case of double layer winding further dividable by two. In case of large armature currents it is also necessary to decide about possible parallel winding branches.

In the next stage it is necessary to derive the design of the armature magnetic circuit on base of known winding parameters (number of slots, number of conductors in a slot, number of parallel

wires, insulation layers etc.) and cooling circuit (radial/axial cooling ducts). On base of resulting magnetic flux densities it is then necessary to decide on manufacturability of the magnetic circuit, which in case of extreme deviations leads to necessity of modification of e.g. linear current density value or the number of machine slots.

The next step is related to the machine type and to design of a component, which is electromagnetically bound to the armature. In case of DC and synchronous machines it is related to the field winding design (on stator or on rotor), in case of induction machines it is related to the design of rotor armature. Even in this case an important result is the manufacturability of the resulting design, which could lead back to recalculation of the power equation and change of dimensions (machine diameters) or electromagnetic parameters - air gap magnetic flux density or linear current density.

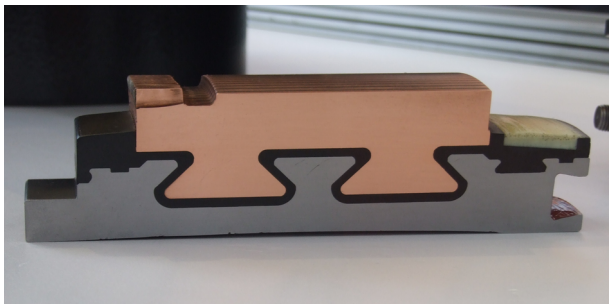


Fig. 8.3: Commutator cross-section

After finishing the electromagnetic design with both stator and rotor windings it is possible to calculate the equivalent circuit parameters. This is a purely analytical process leading to the construction of the phasor diagram including also the calculation of resistances which are necessary for calculation of losses. Using phasor diagram it is possible to verify the power factor of the machine and its back EMF value, which, in case that they do not correspond with inputs of given iteration, lead to modification of these inputs and recalculation of the electromagnetic design.

The following loss calculation is crucial both for calculation of the efficiency of the machine and also for following thermal and ventilation calculations. In case that some of these steps does not correspond with input variables, it is – again – necessary to recalculate the whole design with appropriately modified variables.

The last step which influences the electromagnetic design is the thermal and ventilation calculation. From given losses an equivalent thermal circuit is constructed and it is supplemented by cooling conditions in each part of the machine. The result is thermal rise of the machine, which should again correspond with expected thermal class of the insulation. In case the thermal rise is too low or too high it is necessary to modify the design to achieve an optimally designed and non-overheating machine.

The result is a knowledge of the machine on both geometric an electromagnetic, which is necessary for creation of machine documentation.

During the whole design process it is suitable to perform verification using calculation software. In case of simpler problems this may include Matlab or GNU/Octave which can help to determine some coefficients during the calculation of the machine. For more complicated tasks it is suitable to use the finite element method (FEMM, ANSYS), which allow also the verification of equivalent circuit parameters of selected load states.

9 Specific Parts of DC Machine Design

The design of a direct current machine is one of most complex and demanding designs of all electric machines. Its full calculation includes designs of:

- armature winding (with optional equalizing connections of 1st and 2nd order)
- stator and rotor magnetic circuits
- excitation
- interpoles
- compensation winding
- commutator
- brushes

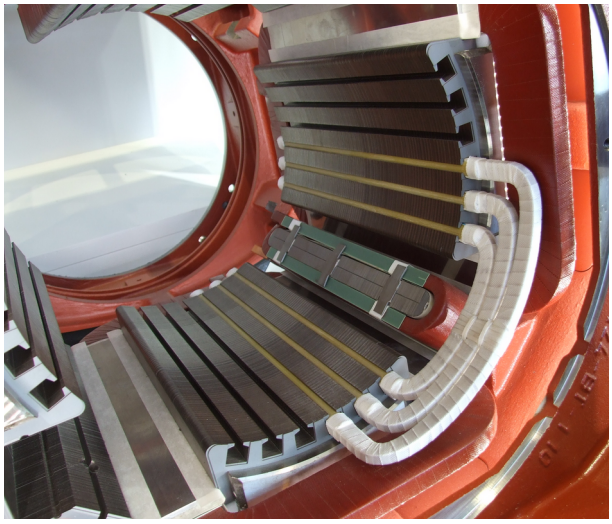


Fig. 9.1: Stator of a DC machine with interpoles and compensation winding

Depending on size of the machine the design of smaller machines is being simplified where interpoles and compensation windings are not used.

The requirements for calculation of a DC machine should include following information:

rated power of the machine	P_r [W]
rated armature voltage	U_r [V]
rated speed	n [rpm]
duty type	motor/generator
excitation type	field winding connection[13]/permanent magnets
cooling type	IC code
protection class	IP code
construction and mounting arrangement	IM code

These may be further supplemented by additional specific requirements like dimensions, efficiency or winding temperature rise.

9.1 Calculation of Fundamental Dimensions of the Machine

Based on given requirements it is then possible to choice of designer's parameters, i.e. parameters necessary for the electromagnetic calculation itself. The values of linear current density A is commonly in case of DC machines chosen in range of 20 000 to 40 000 A/m, whereas according to the insulation class and cooling type it is possible to step outside these borders. The air gap magnetic

13 In case of externally excited machines also field winding voltage U_f [V].

flux density B_δ is commonly chosen between 0.6 and 1.05 *T*, where lower values correspond with smaller machines and higher values with large machines equipped with compensation winding and interpoles.

The electromagnetic coefficients α_δ and k_B have been already mentioned in chapter 2 and regarding to a will of achieving possibly flattest air gap magnetic flux density the electromagnetic pole coverage factor is being chosen up to 0.7 and in case of small machines stamped of whole steel sheets it can achieve even higher values. This corresponds also to high mechanical pole coverage factor α_m, which is commonly between 0.7 and 0.8. The magnetic field shape factor k_B is in case of DC machines commonly around one, usually slightly higher (1.03 to 1.05).

The value of the electromotive force factor k_E must be estimated on base of supposed duty type of the machine – in case of generators it is between 1.0 and 1.1, in case of motors between 0.9 – 1.0. Since it is a ratio defined by

$$k_E = \frac{U_i}{U_r} \quad , \tag{9.1}$$

it is possible to estimate it on base of back EMF value determined from presumed current value and from the armature resistance as

$$U_i = U_r + R_a I_r + U_b \quad , \tag{9.2}$$

where R_a is the armature resistance,
I_r is the armature rated current
and U_b is the voltage drop on brushes.

The choice of the number of pole-pairs can be base on two independent views. The first one is the resulting frequency of the magnetic field in the armature, which is commonly (traditionally) chosen to be near to 50 *Hz*, even if this is not a hard condition. The the number of pole-pairs is

$$p \approx \frac{60 f}{n} \quad . \tag{9.3}$$

The second point of view is formed by possibilities of the manufacturer, who may limit the dimensions of manufactured pole and also the pole pitch. Regarding this fact the number of poles is chosen as

$$2p = \frac{\pi D_2}{t_{p2}} \quad , \tag{9.4}$$

where t_{p2} is the excitation pole pitch.

Historically the limit was commonly between t_{p2} = 300 to 400 *mm*.

The last parameter to be chosen is the winding current density J, which is chosen in range of 4 to 6 A/mm^2 depending on armature cooling type. The reason of choosing such a low current densities is the fact that the armature winding is relatively poorly cooled, especially in area of winding overhangs, where it is fixed by multiple bonding layers, which worsens the transmission of heat to outer air.

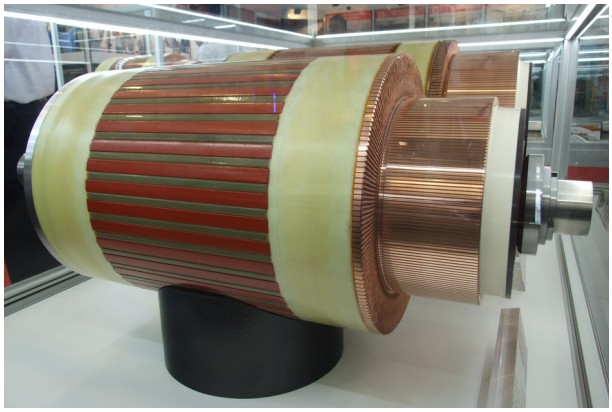


Fig. 9.2: DC machine armature with well visible fixation of the winding overhangs

In the design of the winding the limiting factor is the voltage between adjacent lamellae U_l, which should be lower than 20 V and for smooth machine operation it is commonly chosen between 12 and 15 V. This voltage is divided between

$$K_p = \frac{K}{2p} \tag{9.5}$$

lamellae, hence for achieving sufficiently low voltage between lamellae it is necessary to use

$$K = 2p\frac{U}{U_l} \tag{9.6}$$

lamellae. Now it is possible to derive the minimal number of slots as

$$Q = \frac{K}{u} \quad . \tag{9.7}$$

This number is being adjusted further as for elimination of magnetic “gluing” of rotor teeth against main poles the number of slots per pole t_{ps} is being chosen to be an integer increased by ½ and in case of larger machines it is chosen to be $t_{ps} \geq 10$. Except the topological design of the winding itself, one of important outputs is the winding pitch factor k_y, which is further used for calculation of machine dimensions from the power equation.

In case of DC machines the power equation is in form

$$P_i = C D_1^2 l_i n \quad , \tag{9.8}$$

where one of the input dimensions may be previously given. If a given outer machine diameter of the machine D_e is requested, it is necessary to choose D_1 according to experience of using relations mentioned in the literature [4]. The inner power of the machine then results from electromotive force factor as

$$P_i = k_E P_n \quad . \tag{9.9}$$

Using known value of machine total current I_t, which results from linear current density

$$I_t = \pi D_1 A \tag{9.10}$$

or

$$I_t = V \frac{I}{2a_=} = V_s 2a_= \frac{I}{2a_=} = 2N_s 2a_= \frac{I}{2a_=} = 2N_s I \quad , \tag{9.11}$$

where V is the total number of armature conductors
and V_s is the number of conductors in series,

it is possible to derive the necessary number of armature winding turns in series, which results from comparison of (9.10) and (9.11)

$$N_s = \frac{\pi D_1 A}{2I} \quad . \tag{9.12}$$

This must result an integral number, otherwise it is necessary to round it and modify the linear current density value and perform a new calculation to achieve correct result.

In the same way it is possible to express the total current through the machine using the number of conductors in a slot V_c as

$$I_t = V_c Q \frac{I}{2a_=} \quad , \tag{9.13}$$

which gives by comparison with one of results of (9.11)

$$V_c = \frac{4a_= N_s}{Q} \quad , \tag{9.14}$$

which must be again an integral number, which must be further dividable by the number of coil sides in a slot $2u$, otherwise it is necessary to modify the value of the linear current density A again.

The number of a single coil turns may be derived from

$$N_c = \frac{V_c}{2u} \quad . \tag{9.15}$$

After determination of the winding topology it is possible to perform the design of armature magnetic circuit, whereas the starting point is formed by slot dimensions which result from chosen current density. The slot dimensions are then given by a sum of wire dimensions and used insulation

layers, whereas the wire cross-section results directly from armature current I_r, number of pairs of parallel winding branches $a_=$ and chosen winding current density J:

$$S_{Cu} = \frac{I_r}{2 a_= J} \quad , \tag{9.16}$$

whereas the conductor itself may be chosen from EN 60317 standard. In case when no wire cross-section is available, it is possible to introduce more parallel winding wires n_p and wind them together.

In terms of dimensioning of the magnetic circuit, it is again necessary to take into account the used cooling type of the machine. As approximate values it is possible to use magnetic flux densities 2.2 to 2.5 *T* in area of rectangular slot bottom, 1.7 – 2.0 *T* in area of armature between teeth with parallel walls. The magnetic flux densities in the armature yoke should not exceed 1.3 to 1.4 *T*, whereas lower values correspond with machines with larger pole pitch.

9.2 The design of DC Machine Excitation

The magnetic flux densities for excitation poles loaded by direct current magnetic flux the common values are between 1.5 and 1.7 *T* and in case of cast iron they are lowered to 1.1 to 1.2 *T*. In case of alternating magnetic flux and excitation poles made of electrical steel sheets, the chosen values are slightly higher, i.e. between 1.2 and 1.4 *T*.

The air gap size is in case of DC machines chosen according to empiric relations, although these relations are not obligatory. From the air gap size choice point of view, the important parameter is that the value of magnetomotive force is proportional to the air gap size, thus with increasing air gap length the excitation current and necessary number of excitation coil turns increase. The lower limit is approximately 0.2 *mm*, which relates to very small machines with stiff rotor and small bearing clearances. From empiric relations it is possible to mention

$$\delta > \frac{D_1}{1000} \tag{9.17}$$

or

$$\delta = k_\delta t_{p1} \frac{A}{B_\delta} \cdot 10^{-6} \quad , \tag{9.18}$$

where the coefficient k_δ is chosen between 0.3 and 0.5 for machines between compensation winding and 0.2 to 0.3 for machines equipped with compensation winding. For the purpose of construction of the machine the air gaps smaller than 5 *mm* are rounded to tenths of millimetre, larger air gaps to halves of millimetre.

For the purpose of excitation of DC machines traditional methods are used (i.e. serial, shunt and external excitation) as well as permanent magnets are. In their case almost all types of permanent

magnets are used – ferrites in case of small machines, neodymium-iron-boron (NdFeB) in common machines and in some special applications samarium-cobalt (SmCo) or AlNiCo. In relation to mentioned methods the design of permanent magnets is simplest part and it is practically the design of external excitation.

The principle of the design is the solution of magnetic circuit where the permanent magnet acts as a real voltage source. Its magnetomotive force must be equal to the sum of magnetomotive force drops over the whole magnetic circuits and it must also overcome its own reluctance. The magnetomotive force supplied by the permanent magnet is

$$F_{PM} = H_{c\vartheta} h_{PM} \quad , \tag{9.19}$$

where $H_{c\vartheta}$ is the coercive force of the permanent magnet[14] at rated temperature
and h_{PM} is the height of permanent magnets.

This permanent magnet has also its inner reluctance, which causes magnetomotive force drop of

$$\Theta_{PM} = H_{PM} h_{PM} \quad , \tag{9.20}$$

where H_{PM} is the magnetic field strength in permanent magnets.

It is necessary to determine the magnetic field strength H_{PM} from magnetic flux through permanent magnets including interpole leakage

$$\Phi_{PM} = (1 + k_\sigma)\Phi_\delta \quad , \tag{9.21}$$

where the dimensions of the permanent magnets can be substituted

$$\Phi_{PM} = B_{PM} b_{PM} l_{PM} \tag{9.22}$$

or

$$\Phi_\delta = \alpha_\delta B_\delta t_p l_i \quad , \tag{9.23}$$

which gives, after substitution and modification, the magnetic flux density in the permanent magnet

$$B_{PM} = (1 + k_\sigma)\alpha_\delta B_\delta \frac{t_p l_i}{b_{PM} l_{PM}} \tag{9.24}$$

from which the magnetic field strength in permanent magnets results

14 It is necessary to distinguish between intrinsic coercive force H_{ci} and "external" coercive force H_c. For the purpose of design of the machine magnetic circuit the H_c is the important one, whereas the value of H_{ci} is important when analysing the possible risk of permanent magnet demagnetization. The difference between both values is well recognizable from data sheets [15].

$$H_{PM}=\frac{B_{PM}}{\mu_{PM}} \quad , \tag{9.25}$$

whereas the permeability of the permanent magnets may be determined from rated parameters of chosen type of permanent magnets at room temperature as

$$\mu_{PM}=\frac{B_{r\,20}}{H_{c\,20}} \quad . \tag{9.26}$$

The condition of solvability of this problem is that the permanent magnet flux density and its magnetic field strength must be lower than its remanence and coercive force ($B_{r\vartheta}$ and $H_{c\vartheta}$) at rated temperature.

For a known design of a magnetic circuit it is possible to calculate the total magnetomotive force drop

$$\sum \Theta=\Theta_{y1}+\Theta_{y2}+2\left(\Theta_t+\Theta_p+\Theta_\delta\right) \quad , \tag{9.27}$$

which must be equal to magnetomotive force of permanent magnets

$$2F_{PM}=2\Theta_{PM}+\sum \Theta \quad , \tag{9.28}$$

which gives, after calculation, the height of permanent magnets

$$h_{PM}=\frac{\sum \Theta}{2\left(H_{c\vartheta}-H_{PM}\right)} \quad . \tag{9.29}$$

As seen from (9.29) the magnetic field strength in permanent magnets must be lower than their coercive force at rated temperature to obtain physically correct solution. Similarly for $H_{PM} \rightarrow H_{c\vartheta}$ the permanent magnets result very thick, thus it is suitable to change the width of permanent magnets or the air gap magnetic flux density.

A very similar approach is used for design of external excitation. An additional input is in this case the field winding voltage, which is commonly standardized in series U_f = 65, 110, 220 or 440 *V*, but also other values may be used [16]. The main problem is then to design a winding to have a resistance, which would correspond with relation

$$U_b=R_b I_b \quad , \tag{9.30}$$

where field winding coils having N_f turns connect into resies and their resistance is then

$$R_f=\frac{1}{\gamma_{Cu\vartheta}}\cdot\frac{2p N_f l_f}{S_f} \quad , \tag{9.31}$$

where l_f is the average length of field winding turn
and S_f is the cross-section of the field winding wire.

After substitution to (9.30) the multiplication of $N_f I_f$ appears having a meaning of one field winding coil magnetomotive force which must be equal to magnetomotive force drop on magnetic circuit of the machine, thus we have

$$U_f = \frac{1}{\gamma_{Cu\vartheta}} \cdot \frac{2 p l_f}{S_f} \sum \Theta \tag{9.32}$$

and the suitable wire cross-section is

$$S_f = \frac{2 p l_f \sum \Theta}{\gamma_{Cu\vartheta} U_f} \quad . \tag{9.33}$$

An equivalent design is used also in case of shunt excitation, while in this case the field winding voltage is considered to be 90 per cent of the terminal voltage, i.e. in case of shunt excitation the relation (9.33) verges to

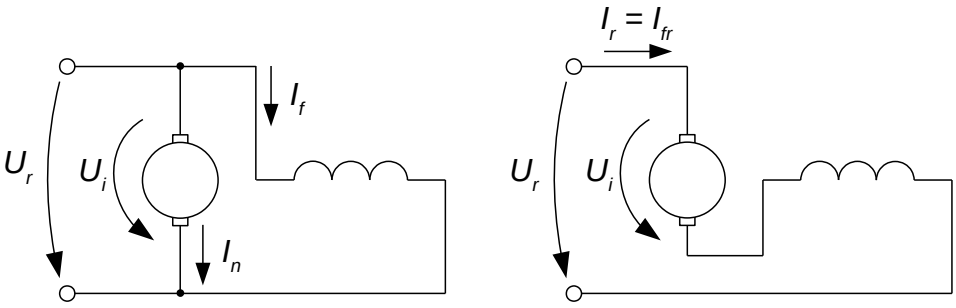


Fig. 9.3: Shunt (left) and serial (right) connection of field winding

$$S_f = \frac{2 p l_f \sum \Theta}{0.9 \gamma_{Cu\vartheta} U_f} \quad . \tag{9.34}$$

In case of serial excitation the field winding current is identical to the rated current of the machine, thus it is necessary to derive the number of field winding turns from the value of the rated current. Considering slight demagnetization due to armature reaction the sum of magnetomotive force drops is being increased by 5 per cent, i.e. the number of field winding turns results

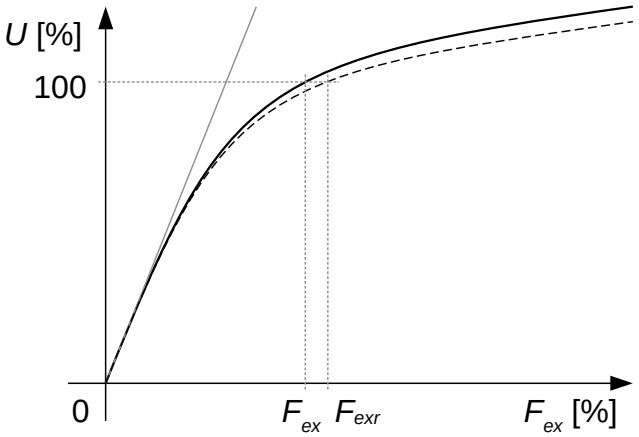


Fig. 9.4: Deformation of no-load characteristic due to demagnetization effects

$$N_f = 1.05 \frac{\sum \Theta}{I_r} \tag{9.35}$$

and the winding cross-section is designed according to required current density to

$$S_f = \frac{I_r}{J_f} \quad , \tag{9.36}$$

whereas the current density of the field winding is commonly set to 1.5 to 3.5 A/mm^2.

9.3 The Design of Interpoles and Compensation Winding

As a more common optional component of DC machines the interpoles are used. The interpoles are supposed to suppress remaining reactive voltage of the armature and thus improve the commutation of the machine by achieving zero air gap magnetic flux density between main poles. To achieve a perfect compensation the magnetomotive force of interpoles must be proportional to the armature magnetomotive force, hence they are connected in series with the armature winding. Consequently the compensation should be linear in whole working range of the current, i.e. even interpoles must be dimensioned to work in non-saturated part of the B-H curve of their material. This is why their rated magnetic flux density is being chosen only between 1.1 to 1.3 *T*. As a result of the machine design the interpoles result relatively thin and high, so the interpole winding is located as near to the air gap as possible to reduce the leakage magnetic flux of the interpoles (expressed by k_σ), which is often higher than 1. Such a high value of the interpole leakage flux coefficient is given by relatively large air gap between interpoles and armature, which is often being chosen 1.5 to twice as long as the mechanical air gap, as well as by the nearby main poles. The magnetomotive force to compensate then results from the presence of compensation winding in the machine and if the machine is not equipped by the compensation winding, the remaining magnetomotive force to be compensated is

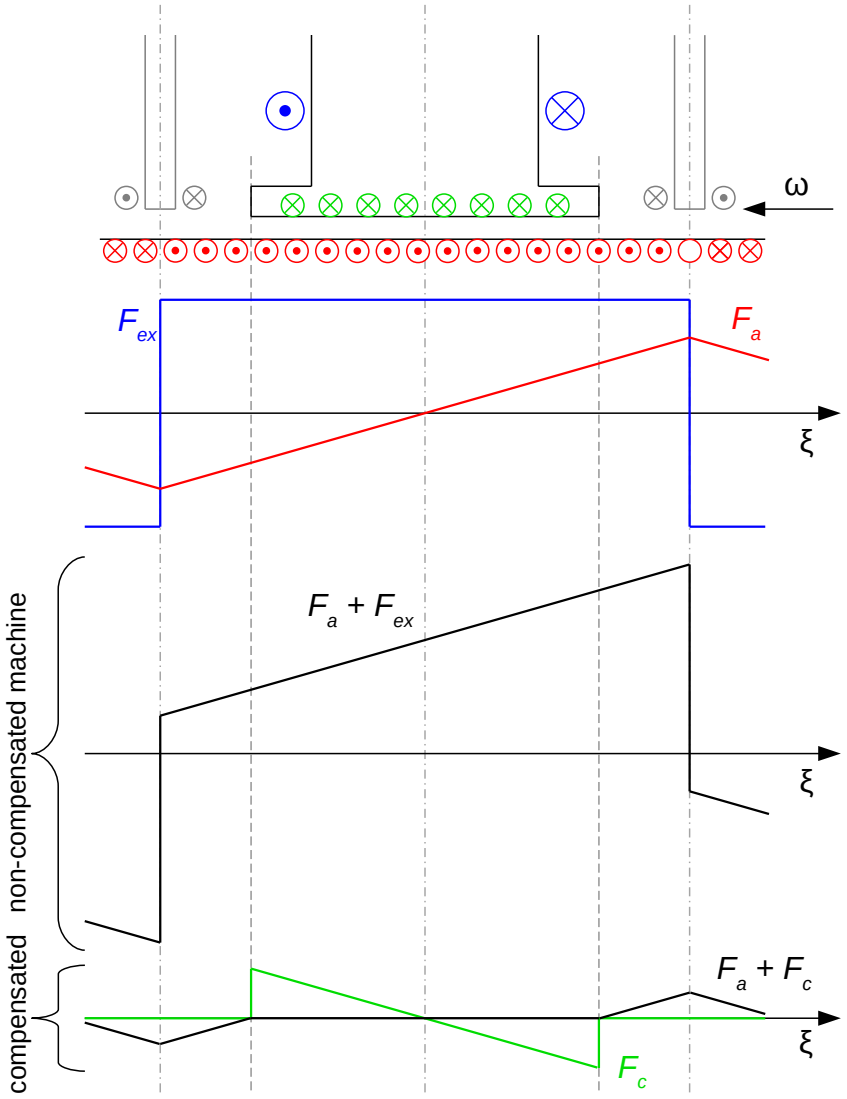


Fig. 9.5: Magnetomotive force curves for each machine winding

$$F_{an}=\frac{1}{2}At_p \quad , \tag{9.37}$$

while in case the machine is equipped by compensation winding its value is

$$F_{ac}=\frac{1}{2}(1-\alpha_\delta)At_p \quad . \tag{9.38}$$

The reactive magnetomotive force is then given by time variation of the current in commutating coil

$$u_r=L\frac{di}{dt} \quad , \tag{9.39}$$

which may be transcribed to differential in form of

$$U_r=L\frac{\Delta I}{\Delta t} \quad , \tag{9.40}$$

where ΔI is the current difference, i.e. transition from value $+I_r$ to $-I_r$,
Δt is the commutation time T_c
and L is the inductance of commutating coil, which may be calculated analogically to (6.25) as

$$L=\mu_0\lambda_c N_c^2 l_{Fe} \quad , \tag{9.41}$$

where λ_c is the commutating coil reluctance factor
and N_c is the number of its turns.

The reactive voltage is then given by

$$U_r=2\mu_0\lambda_c N_c^2 l_{Fe}\frac{I_r}{T_k} \quad . \tag{9.42}$$

The rated current may be substituted from modification of (9.12)

$$I_r=\frac{\pi D_1 A}{2N_s} \quad , \tag{9.43}$$

where the number of winding turns in series is given by the number of coil sides in a slot, number of slots and the number of coil turns, i.e.

$$N_s=uQN_c \quad . \tag{9.44}$$

After substitution to (9.43) we obtain

$$I_r = \frac{\pi D_1 A}{2 u Q N_c} \quad , \tag{9.45}$$

where the multiplication of the number of slots and the number of coil sides in a slot has a meaning of commutator lamellae and the ratio of armature circumference to the number of lamellae gives the lamellae pitch on the surface of the commutator

$$t_l = \frac{\pi D_1}{u Q} \quad . \tag{9.46}$$

After substitution of (9.45) into (9.42) we get

$$U_r = 2 \mu_0 \lambda_c N_c^2 l_{Fe} \frac{t_l}{T_c} \cdot \frac{A}{N_c} \quad , \tag{9.47}$$

where the number of coil turns reduces and the ratio between lamellae pitch and the commutation time gives the velocity of the brushes on the commutator. The result is then

$$U_r = \mu_0 \lambda_c N_c l_{Fe} v A \quad , \tag{9.48}$$

where the commutating coil reluctance factor is approximately

$$\lambda_c \simeq \frac{h_s}{b_s} + 2 \frac{l_o}{l_{Fe}} \quad . \tag{9.49}$$

The value of the magnetic reluctance factor together with permeability of the vacuum may be then substituted by so called Hobart factor

$$\xi = \frac{1}{2} \mu_0 \lambda_c \quad , \tag{9.50}$$

whose value is in range of $(4 - 8).10^{-6}$. Using this factor the expression (9.48) verges to

$$U_r = 2 \xi N_c l_{Fe} v A \quad . \tag{9.51}$$

This voltage must be induced into commutating coil by its movement, i.e.

$$U_r = 2 N_c B_c l_{Fe} v \quad , \tag{9.52}$$

which gives the necessary magnetic flux density under interpole

$$B_c = \xi A \quad , \tag{9.53}$$

whereas this relation is often being modified (due to leakage fluxes) to

$$B_c = \left(1 + \frac{U_b}{U_r}\right) \xi A \quad , \tag{9.54}$$

where U_b is the voltage drop on the brushes.

At this magnetic flux density the magnetomotive force drop in the air gap is

$$\Theta_i = \frac{B_k}{\mu_0} \delta_i \tag{9.55}$$

and the necessary magnetomotive force of the interpoles is

$$F_i = F_{an|ac} + \Theta_i \quad , \tag{9.56}$$

and the necessary number of interpole coil turns is

$$N_i = \frac{F_i}{I_n} \tag{9.57}$$

and the cross-section of the wire is being chosen from current density, which is in range of 2 to 4 A/mm^2.

Since there is a large influence of manufacturing tolerances and the calculation itself it is necessary to adjust the interpoles after installation on a finished machine. This is being performed through magnetic or non-magnetic interlayers between the interpole and the yoke. They are installed in the area between the interpole and yoke to keep constant air gap under the interpole.

The design of the compensation winding is derived from the principle of its function, which is compensation of the armature magnetomotive force. This is proportional to the armature current, thus the compensation winding is connected to series to the armature. It is being placed into slots in main pole shoes, which are opened or semiclosed, whereas it is necessary to achieve identical linear current density of the compensation winding as of the armature. For a compensated machine it is valid, that the residual magnetomotive force to be compensated is

$$F_{ac} = F_a + F_c = \frac{1}{2} A t_p - \frac{1}{2} \alpha_\delta A t_p = \frac{1}{2} (1 - \alpha_\delta) A t_p \quad , \tag{9.58}$$

where F_a is the armature magnetomotive force
and F_c is the magnetomotive force of compensation winding.

The compensation winding is commonly performed in completely serial connection, i.e. the parallel branches are not used. On the pole shoe an even number of slots for compensation winding is being used (for the purpose of usage of pole composition of coils) and their slot pitch must be different from the armature slot pitch. By successful compensation it is possible to lower the saturation of pole shoes and lower the field winding demands.

9.4 Commutator Design

The design of the commutator and the number of commutator lamellae is bound with the armature winding design, whereas it is necessary to consider a limitation of 20 V which is the maximal acceptable voltage between neighbouring lamellae. From the knowledge of the lamellae number and presumed commutator diameter, the lamellae pitch results

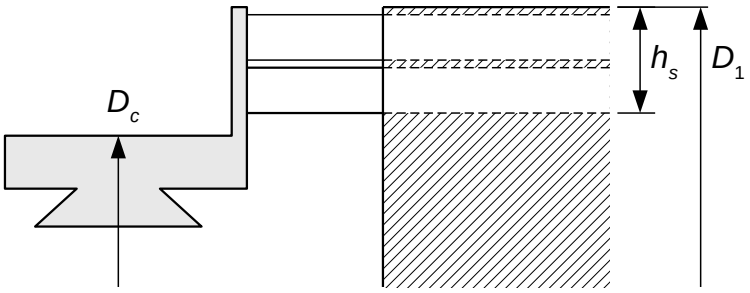


Fig. 9.6: The relation between armature and commutator diameters

$$t_c = \frac{\pi D_c}{K} \quad . \tag{9.59}$$

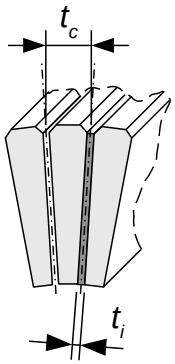


Fig. 9.7: Width of commutator lamellae and of insulation

The diameter of the commutator is in case of small machines chosen to achieve a direct connection from the commutator lamellae to the armature coils, i.e. its diameter is

$$D_c = D_1 - 2h_s \quad . \tag{9.60}$$

In other cases the commutator diameter is commonly chosen between 0.6 to 0.8 of the armature diameter. The thickness of insulation between lamellae is then chosen according to the voltage and size of the machine between 0.2 to 0.4 *mm* in case of small machines and 0.7 to 1.0 *mm* in case of medium size low voltage machines and 1.2 to 1.5 *mm* in case of large high voltage machines. The width of the lamella is commonly about 3 *mm* at its bottom. The maximal commutator length is 300 to 400 *mm*.

The dimensions of the brushes are standardized and it is necessary to choose them according to the resulting brush current density, which is commonly between 8 to 10 A/cm^2. The current per brush set is then

$$I_p = \frac{I}{p} \tag{9.61}$$

thus the necessary brush cross-section is

$$S_b = \frac{I_p}{J_b} \ , \tag{9.62}$$

where J_b is the brush current density.

If there is no brush available in target dimensions, it is possible to choose multiple parallel brushes. Because of manufacturing reasons at least 5 *mm* space is being used between parallel brushes whereas brushes of each polarity should be placed interleaved. On base of the number of brushes in a set N_b the length of the commutator lamella results

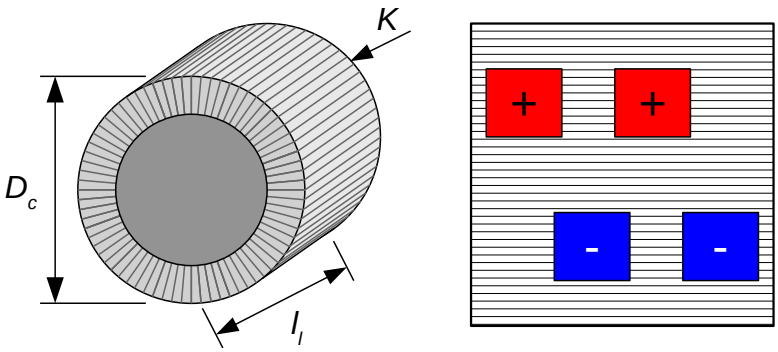


Fig. 9.8: Commutator dimensions and brushes overlap

$$l_l = (N_b + 0{,}5) l_b + (N_b - 1) i + (25 \div 50) \quad [mm] \ , \tag{9.63}$$

where l_b is the length of a single brush
and i is the insulation distance between the brushes.

The brush itself should be overlapping over at least two commutator lamellae, whereas its width is in general proportional to the number of the coil sides in a slot layer u.

10 Specific Parts of Design of Synchronous Machines

Synchronous Machines form the core of the energy generation industry and even through increasing fraction of alternative energy resources the usage of synchronous machines a key part for transformation of mechanical energy into electrical energy while its generation. Similarly to DC machines which have have achieved maximal sophistication in terms of electromagnetic design (interpoles, compensation winding etc.) the synchronous machines have achieved maximal sophistication in terms of used technology, whereas the synchronous machines were manufactured with combined water-hydrogen cooling thanks to which the greatest manufactured machine has achieved a power of 2 000 000 000 Watts. This machine was manufactured and tested in 2008 by Siemens [17]. Even through clear connection of synchronous machines with power industry, their use is still expanding and especially due to possibility of active excitation control they gain increasing attention in automotive industry [18].

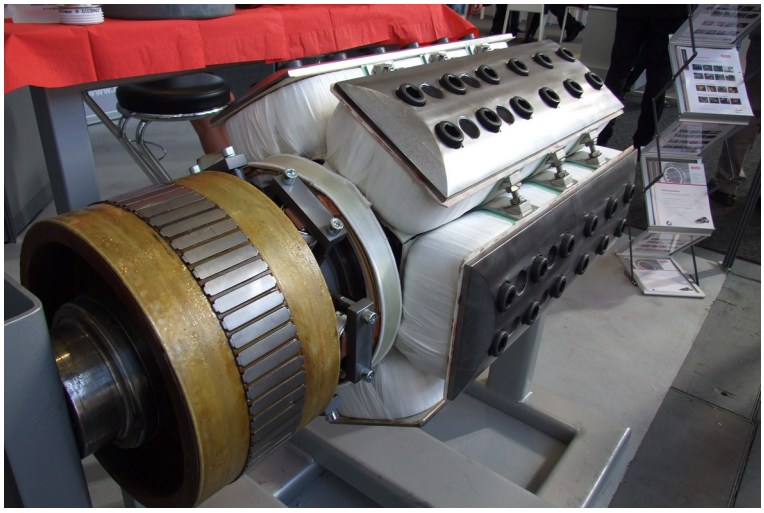


Fig. 10.1: The rotor of a synchronous machine equipped with salient poles and exciter (in front)

Similarly as in case of direct current machines the design may include some optional parts, but in general the components of the electromagnetic design include:

- armature winding
- magnetic circuits of stator and rotor
- excitation
- field winding power supply system
- damper

Depending on final application of the machine there is a large amount of variation and some components do not have to be included at all. The input values for the design should included following information:

rated power of the machine	P_r [W], optionally S_r [VA]
rated voltage	U_r [V]
rated speed	n [ot/min]
rated frequency	f [Hz]
duty type	motor/generator/compensator
excitation type	permanent magnets/winding (incl. field winding voltage)

excitation power supply	slip rings/contactless (exciter/rotary transformer)
protection type	IP code
cooling type	IC code
construction and mounting	IM code

These and possible further requirements (maximal diameter, length, efficiency, temperature rise, requirement of X_{dn} in case of generators etc.) then influence the choice of designer variables for the purpose of start of the machine design

10.1 Determination of Fundamental Machine Dimensions

The synchronous machines are one of most variable machines regarding their size and power, thus there is also a large variability in choice of designer's parameters. As already mentioned in chapter 2, in case of largest machines equipped with hydrogen cooling, which is commonly supplemented by direct water cooling, the synchronous machines may achieve values of linear current density up to 200 *kA/m*. With smaller machines and worse cooling technology this value drops down to 20 *kA/m*, which corresponds to small totally enclosed synchronous machines. In case of largest machines the air gap magnetic flux density may reach up to 1.1 *T* and with decreasing dimensions again it drops down to 0.6 *T*, whereas in case of smallest synchronous machines excited by ferrite permanent magnets it can go down under 0.3 *T*.

Similarly as in case of direct current machines it is necessary to consider the context of electromagnetic and mechanical pole coverage factor, whereas in case of synchronous machines there is an additional element of pole shoe curvature, which is used for shaping of the air gap magnetic flux density. While the mechanical pole coverage factor α_m can move within range of 0.6 to 0.8, the electromagnetic pole coverage factor α_δ is commonly located only in range between 0.63 to 0.75. The electromotive force factor k_E may be defined similarly as in case of direct current machines on base of the equivalent circuit, but in this case it is necessary to consider the phasor nature of all variables, i.e. the induced voltage value will be

$$\bar{U}_i = \bar{U} - R_a \bar{I}_r - j X_{a\sigma} \bar{I}_r \quad , \tag{10.1}$$

and the electromotive force coefficient will be given by the ratio between sizes of the phasors U_i and terminal (phase) voltage U

$$k_E = \frac{U_i}{U} \quad . \tag{10.2}$$

The electromotive force factor is commonly chosen between 0.9 (motors) to 1.1 (generators), nevertheless since the total magnetic flux through the machine is given by the terminal voltage and the excited magnetic flux may be easily controlled, it is possible to consider $k_E = 1$[15]. In case of perman-

15 Because of this reason it is not referred in relation to synchronous machines in some literature at all.

ent magnet synchronous machines the range of the electromotive force coefficient is even larger and it is necessary to consider the optimal control of the machine.

In case of machines fed from the power grid the number of machine pole pairs is bound to their speed and power grid frequency according to

$$p = \frac{60 f}{n} \quad , \tag{10.3}$$

in case of machines fed from semiconductor converters the number of pole pairs is chosen with respect to losses and machine dimensions, in some case also with respect to possibility of introduction of the tooth winding into design of the machine, which leads, especially in case of larger machines, to large numbers of poles.

The last parameter related to machine size is used current density. The value of the current density starts at 3 A/mm^2 in case of machines with worst cooling (high-voltage machines without water cooling of the stator winding) up to 15 A/mm^2 in case of well cooled machines.

From the winding design point of view different requirements are laid on generators and on motors. Whereas in case of generators the main requirement is the quality of the back EMF, in case of motors the main requirement is smooth torque. In case of large generators the total harmonic distortion of the voltage is required to be $THD_U \leq 2.5$ % in case of smaller machines $THD_U \leq 5$ %. This requirement is reflected in choice of large mounts of slots per pole and phase q ($q \rightarrow 7$ to 10), or, if it is not possible to use such a high value of physical number of slots per pole and phase, at least a fractional winding with such a large numerator q_0 is chosen ($q_0 \rightarrow 7$ to 10 while keeping low value of denominator $c \leq 5$). This leads to a large number of harmonic components while examination of Görges pattern, which is not suitable for motors [19].

In case of motors it is suitable to achieve possibly lowest volume of subharmonic components in the air gap. Thus an integral number of slots per pole and phase is being chosen to avoid generation of subharmonic components even though q may have a relatively low value.

A specific case are permanent magnet synchronous machines. In case of these machines the tooth windings are often used ($y_{1s} = 1$), which have q smaller than one. These windings generate a large amount of harmonic components[16]. Nevertheless since the height of permanent magnets adds to the air gap length δ, these machines are more tolerant against air gap harmonic components than other machines.

Depending on available space it is possible to determine the initial number of slots on base of slot pitch according to

$$Q = \frac{\pi D_1}{t_{s1}} \quad , \tag{10.4}$$

16 It is also necessary to note, that the volume of harmonic components in the stator magnetomotive force is further related to larger value of the differential leakage flux coefficient τ_{dif}, which affects the value of leakage inductance. Depending on chosen topology of the tooth winding the total inductance of the machine increases, whereas the leakage inductance may be higher than armature inductance.

which is the modified to be dividable by the number of machine phases and all previously mentioned requirements to be met.

In contrast to DC machines, in case of AC machines the coil pitch is generally chosen to be shorter than the pole pitch to reduce harmonic components in magnetomotive force and back EMF (in case if three phase windings optimally $\beta \approx 5/6$). In case of three phase machines the number of slots per pole is often chosen as a multiple of six, so the coil pitch is chosen as multiple of five which leads to optimal coil pitch shortening.

Based on chosen designer's parameters it is possible to determine the Esson's factor and from power equation

$$S_i = C D_1^2 l_i n \tag{10.5}$$

also the dimensions of the machine. These may be somehow limited (requirement of axial height, outer dimensions, etc.). The rated current through machine then results from terminal apparent power

$$I_r = \frac{S_f}{m U_{pn}} \quad . \tag{10.6}$$

This current may be further divided into parallel branches, whereas their theoretical maximal number is equal to the number of machine poles. Their usage must be considered well as all imperfections during machine manufacture may lead to equalizing currents in the winding and additional losses. A current through one parallel branch I_a and so through one mathematical conductor may be determined from machine total current, which is

$$I_c = \pi D_1 A = m 2 N_s a_\sim I_a \quad , \tag{10.7}$$

which gives

$$I_a = \frac{\pi D_1 A}{2 m N_s a_\sim} \quad . \tag{10.8}$$

Thus the number of winding turns in series is then

$$N_s = \frac{\pi D_1 A}{2 m a_\sim I_a} = \left| I_a = \frac{I}{a_\sim} \right| = \frac{\pi D_1 A}{2 m I} \quad , \tag{10.9}$$

which may be used for determination of the number of machine conductors

$$V = m 2 a_\sim N_s \quad . \tag{10.10}$$

Thus, per one slot we have

$$V_s = \frac{2ma_{\sim}N_s}{Q} = \frac{2ma_{\sim}N_s}{2pmq} = \frac{a_{\sim}N_s}{pq} \qquad (10.11)$$

conductors. This must be an integral number dividable by the number of coil sides in a slot. If this requirement is not met, it is necessary to modify the number of conductors in a slot V_s, which leads to modification of the number of winding turns in series N_s and also to modification of the linear current density A. This projects to the value of Esson's factor C and further to machine dimensions.

A verification of correctness of determined number of winding turns may be performed using the back EMF value, from which we have

$$N_s = \frac{U_i}{4k_B k_{v1}\Phi_\delta f} \quad . \qquad (10.12)$$

If the resulting value is different, there is an error in calculation and it must be checked.

In the next step it is possible to perform the design of the magnetic circuit. It is derived from calculation of necessary winding space and possible saturation of the magnetic circuit. As limiting values the magnetic flux densities in tooth tips B_{t1} in range of 1.7 to 2.3 T are chosen for rectangular slots (and trapezoidal teeth), or in range of 1.7 to 2 T for rectangular teeth. From the yoke saturation point of view the magnetic flux densities are chosen lower because of its length in case of machines with lower number of poles (1.3 to 1.4 T for two pole machines), higher values are chosen for machines with higher number of poles (from eight pole machines in range between 1.6 to 1.7 T). For rotor poles and rotor yokes the values are similar to DC machines – between 1.3 to 1.5 T for poles, 1.4 to 1.6 T for rotor yokes.

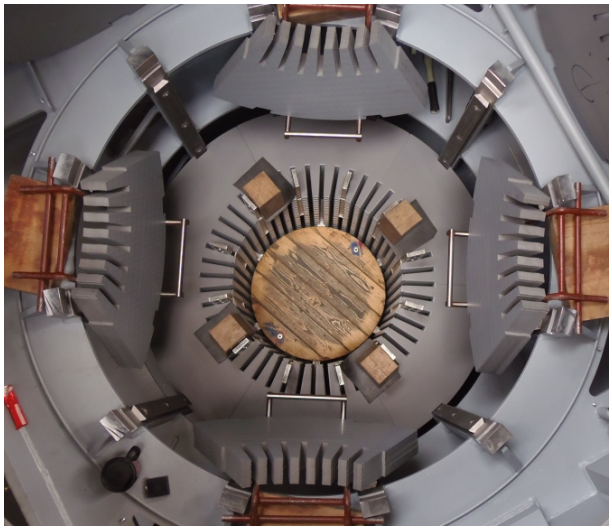


Fig. 10.2: Magnetic circuit of a turbo generator during manufacture

The air gap length is commonly in case of synchronous machines chosen with relation to required inductance value, although even in this case there is a certain lower limit which is given by manufacturing technology, mechanical properties and losses in pole shoes. Consequently it is necessary to respect the fact, that the value of direct axis inductance drops with increasing air gap length, which leads to necessity of stronger excitation (see machine phasor diagram). If no inductance requirement is given, the air gap length is chosen according to empiric relation:

$$\delta = (0{,}3 \div 0{,}5)\, t_p \frac{A}{B_\delta} \cdot 10^{-6} \quad [m] \qquad (10.13)$$

If there is a requirement on a certain value of the direct axis inductance or reactance, the following relation is used

$$\delta = 40\frac{t_p A}{B_\delta (x_d - x_\sigma)\cdot 10^{-6}} \quad [m], \tag{10.14}$$

where x_d and x_σ are the per unit values of direct and leakage reactance of the machine.

poles	x_d [%]
2	200 – 230
4	170
12	120
72	92

Tab. 10.1: Reference values of d-axis reactances of generators

The values of direct axis reactances are often required in power industry by the customer because of short-circuit behaviour of the machine. Commonly required values are shown in table 10.1.

10.2 The Design of Excitation of Synchronous Machines

The synchronous machines can be, in general, divided to two large groups – electrically excited synchronous machines and permanent magnet synchronous machines. In case of electrically excited synchronous machines there are two main rotor topologies – cylindrical rotor, which has excitation winding placed in slots, and salient pole rotor, which has excitation winding formed to coils wound on poles[17]. A common part of these machines is the excitation, which may be performed using slip rings or as contactless excitation. In this case the excitation is performed via rotary transformer or via primary and secondary exciter, whereas the primary exciter is commonly a permanent magnet generator and the secondary exciter is again a synchronous generator with inverse construction and controllable excitation. Between the secondary exciter and excitation winding a rectifier is located. The excitation control is therefore made in the circuit between primary and secondary exciter.

The large cylindrical rotors are made of one single piece of steel, into which slots for excitation winding are milled. They are most commonly located on 2/3 of rotor periphery, whereas the remaining third belongs to wide teeth – rotor poles. The diameter of these machines is limited by mechanical strength of the rotor and excitation winding fixation to approximately 1.2 *m*, which leads in case of large machines to a large rotor bearing pitch. In this case the rotor is relatively flexible, whereas its flexibility is non-homogeneous. In the pole axis the rotor is stiffer than in teeth area, thus for achieving homogeneous stiffness transversal cuts are made into the wide teeth (so-called Lafoon's slots [20]).

In case of salient pole synchronous machines these poles are made as massive parts, eventually the pole shoes are made of electrical steel sheets or whole poles and pole shoes are composed of electrical steel sheets. Into these pole shoes a squirrel cage may be implemented (complete or in sections) – so-called damper – whose task is to damp the sways of the rotor during load changes.

The permanent magnet synchronous machines are then very variable regarding placement of permanent magnets. However their rotor should be, with respect to usage of semiconductor power supplies, made of electrical steel sheets. According to the art of permanent magnet placement of the ro-

17 Historically, the designation of turbo generator merges with cylindrical rotor machines and hydro generator with salient pole machines. Considering the fact, that it is possible to construct also multiple pole machines with cylindrical rotors, which offers also several advantages, this designation may be in many cases misleading.

tor they have properties more similar to cylindrical rotor machines (permanent magnets mounted on the rotor surface) or salient pole machines (machines with buried permanent magnets).

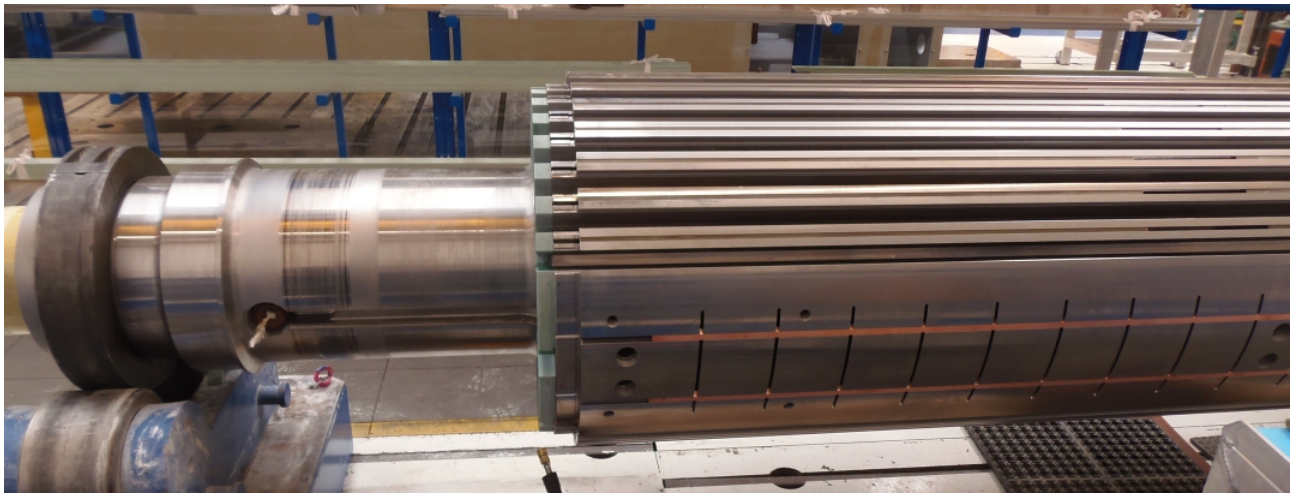


Fig. 10.3: Rotor of a turbo generator with well visible Lafoon's slots

In case of electrically excited synchronous machines, it is necessary to consider two components, which must be overcome by the excitation – on the one hand the voltage drop on the leakage inductance and on the other hand the armature reaction, which may have different value in *d* and *q* axes.

The saturation of the magnetic circuit is considered through construction of no-load characteristic of the machine (i.e. calculation of the magnetic circuit for 100 %, 115 % and 130 % of air gap magnetic flux) from magnetomotive force drops on each part of the magnetic circuit of the machine

$$\Theta = \sum_i \Theta_i = 2\left(\Theta_p + \Theta_{ps} + \Theta_\delta + \Theta_t\right) + \Theta_{y1} + \Theta_{y2} \quad , \tag{10.15}$$

where Θ_p is the magnetomotive force drop on poles,
Θ_{ps} is the magnetomotive force drop on pole shoes,
Θ_δ is the magnetomotive force drop on the air gap,
Θ_t is the magnetomotive force drop on teeth
and Θ_{yx} are magnetomotive force drops on stator and rotor yoke.

Using this characteristic it is possible to determine the flattening of the air gap magnetic field so, that the no-load characteristic in the I. quadrant (see fig. 10.4) is supplemented by vertical addition of magnetomotive force of the stator to the IV. Quadrant. It has a sinusoidal shape with magnitude

$$F_a = \frac{m}{\pi} \frac{N_s k_{w1}}{p} I_m \quad . \tag{10.16}$$

The, step by step the magnetic flux density corresponding to the magnetomotive force curve is determined to obtain real curve of the air gap magnetic flux density form which the fundamental harmonic component B_1 is obtained. Now let us mark the amplitude of the deformed curve as the amplitude of the fundamental harmonic component B_1‘ of a curve, whose shape is identical to the real shape of the air gap magnetic flux density, but its magnitude drops in ratio

$$B'(\xi)=\frac{B_1'}{B_1}B(\xi) \quad .$$
(10.17)

Using reverse approach it is possible to obtain via no-load characteristic the saturated value of F_a‘. From the ratio between the armature magnetomotive force F_a and it saturated value F_a‘ it is possible to determine the armature magnetic field shape factor

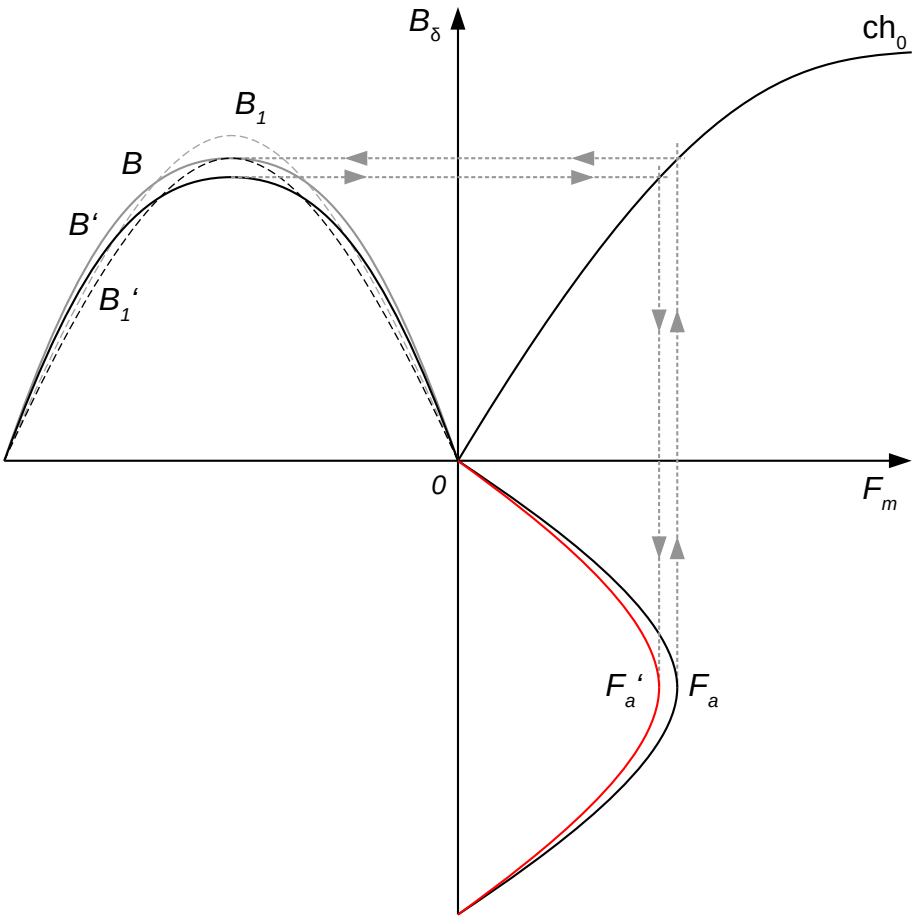


Fig. 10.4: The determination of deformed shape of the magnetic flux density

$$C_1=\frac{F_a}{F_a'} \quad .$$
(10.18)

The excitation of the synchronous machine may be then calculated using procedure shown in fig. 10.5. The fundamental part is again the no-load characteristic of designed machine, which is in the *y*-axis marked in per-unit values of terminal voltage, whereas to the 100 per cent value the values of per unit voltage drops on stator resistance and leakage inductance are added using phasor sum. The phasor sum is projected over the no-load characteristic to a line perpendicular to the induced voltage. To this point the value F_a‘ is added on a line parallel to stator current. The distance between ending point of this construction and the origin of the coordinate system then gives the value of required excitation at given load

In case of salient pole machines it is necessary to consider the variability of the air gap, which is mathematically respected using decomposition of the armature magnetomotive force F_a‘ to components F_d and F_q. If we fix the inner power factor angle of the machine to ψ = 90°, the stator magnetic field will be aligned with rotor magnetic field and it is possible to define both components as

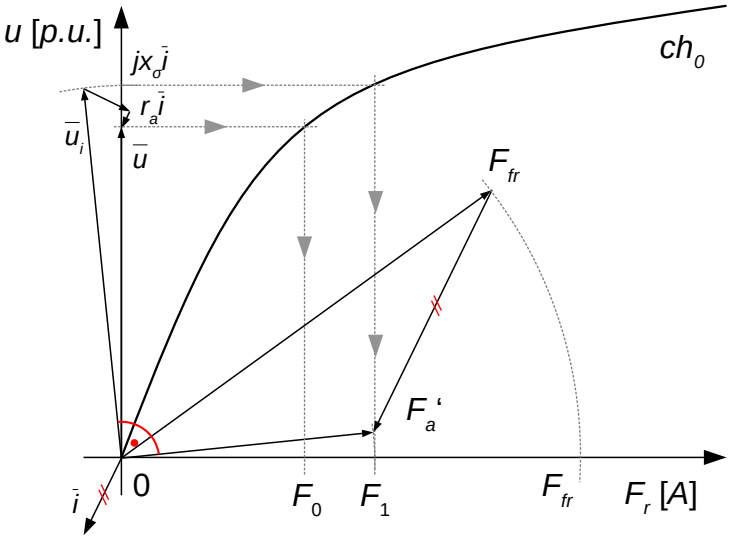


Fig. 10.5: The determination of excitation magnetomotive force for a machine with cylindrical rotor

$$\begin{aligned} F_d &= F_a' \sin\psi \\ F_q &= F_a' \cos\psi \end{aligned} \quad . \tag{10.19}$$

To achieve possibly most sinusoidal magnetic field shape, a curvature of the pole shoes is performed to achieve the air gap length according to

$$\delta(\xi) = \frac{\delta_{min}}{\cos\xi} \quad , \tag{10.20}$$

where δ_{min} is the mechanical air gap size.

This is relatively demanding regarding the manufacture of the rotor, therefore the curvature is in praxis made using arc segment only. The parameters of this arc are determined from maximal air gap length δ_{max}, which is ion the edges of the pole shoes set to 1.5 to 2 times of the mechanical air gap length. The pole shoe futher does not cover the whole pole pitch, which introduces futher deformation of the magnetic field, which is very hard to be analytically expressed. This is why the magnetic field shape factors in *d* and *q* axis are used to determine the total value of the armature reaction in each axis

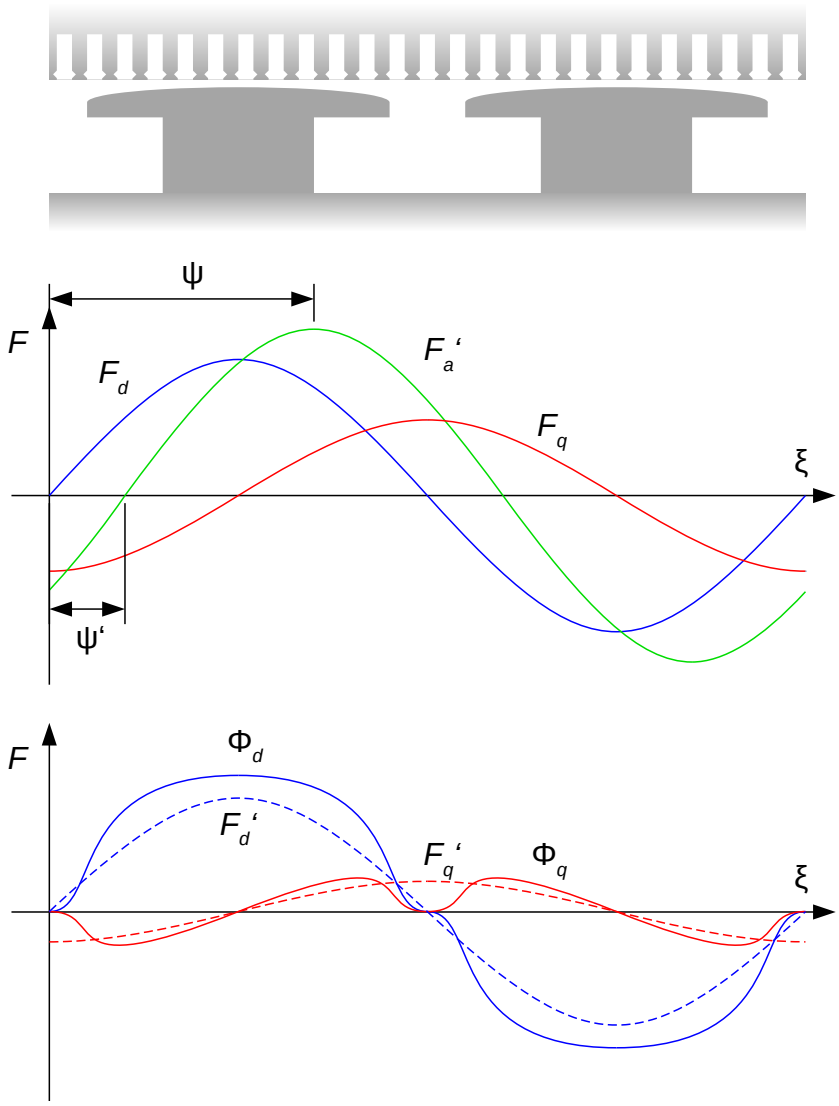


Fig. 10.6: Dissolution of the armature reaction magnetomotive force to d and q components

$$\begin{aligned} F_d' &= C_{d1} F_d = C_{d1} F_a' \sin\psi \\ F_q' &= C_{q1} F_q = C_{q1} F_a' \cos\psi \end{aligned} \quad , \tag{10.21}$$

where C_{d1} is commonly a value between 0.7 to 0.85 and C_{q1} has a value between 0.4 and 0.6.

The values of magnetic field deformation factors depend on mechanical pole coverage factor α_m and ratio $\delta_{max}/\delta_{min}$, whereas for common machines these values are often tabulated [4], [3]. In specific cases it is necessary to perform their examination using numeric software or finite element method.

The practical construction for the purpose of determination of magnetomotive force for required load is developed from construction mentioned in case of cylindrical rotor machines. The base is again the no-load characteristic ch_0, which is drawn in voltage per units on the *y*-axis and in real units of magnetomotive force on the *x*-axis (see fig. 10.7). The construction of a phasor diagram is put on the *y*-axis, whereas to the terminal voltage the voltage drops on stator resistance and leakage reactance in per units are added as phasors. In the next step the total value of the back EMF is projected via no-load characteristic to a line perpendicular to the back EMF with start in the origin of the coordinate system.

Similarly to cylindrical rotor synchronous machines the phasor of magnetomotive force F_a‘ is drawn from the ending point of previous construction (point F_1) and in parallel to the machine current. But, in this case it is necessary to respect the saliency of the machine and draw the armature reaction in form of components, F_{d1} a F_{q1}, which result from the magnetic field factors C_{d1} and C_{q1}, dissolution of the armature magnetomotive force to components *d* and *q* and inner power factor angle ψ, which is constrained by phasors F_q‘ and F_{d1} as

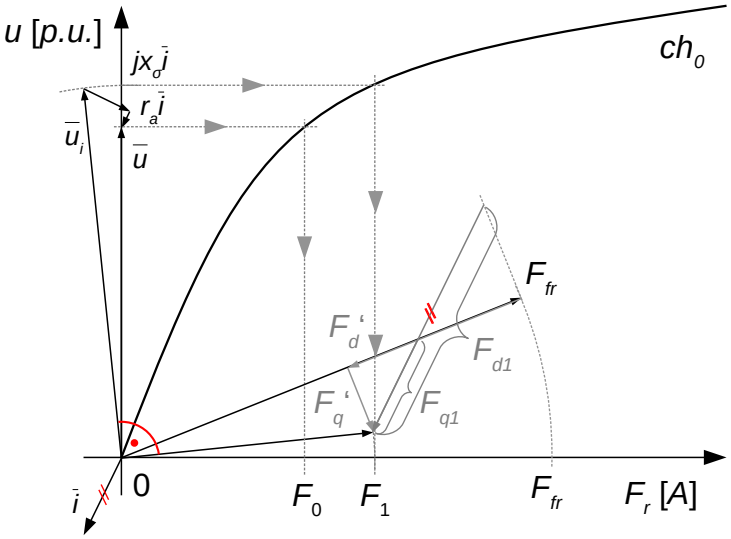


Fig. 10.7: The determination of rated excitation magnetomotive force of a salient pole machine

$$F_{d1}=\frac{F_d'}{\sin\psi}=\frac{C_{d1}F_a'\sin\psi}{\sin\psi}=C_{d1}F_a'$$
$$F_{q1}=\frac{F_q'}{\cos\psi}=\frac{C_{q1}F_a'\cos\psi}{\cos\psi}=C_{q1}F_a' \qquad (10.22)$$

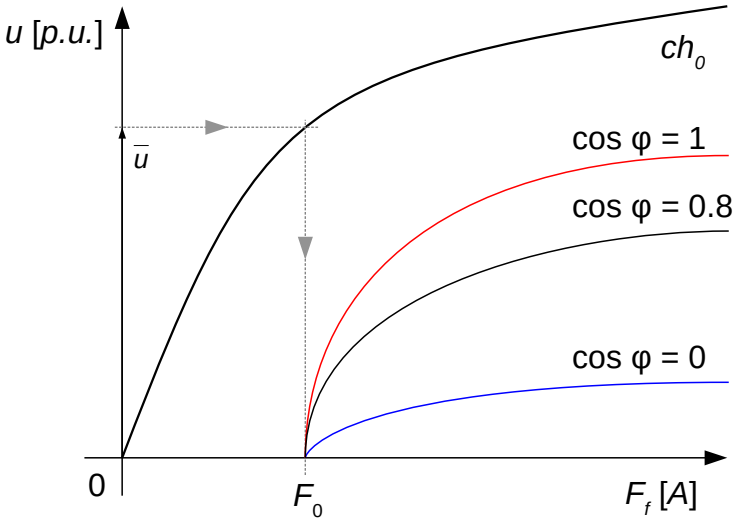


Fig. 10.8: Load characteristics of synchronous machines for a constant power factor

Through the endpoint of the phasor F_{q1} a half line is led, on which the endpoint of the rated excitation F_{fr} is located. In a similar way the construction may be performed using components F_d‘ and F_q‘, but in this case it is necessary to know the inner power factor angle of the machine, which is constrained by F_d‘ and F_{d1}. The above mentioned construction is then a base of Sumec’s construction of phasor diagram of a salient pole synchronous machine. Using above mentioned construction it is also possible to con-

struct the load characteristics of synchronous machines for a constant power factor, as shown in fig. 10.8.

The design of the excitation winding is then identical to the design of the excitation winding of externally excited direct current machines. The field winding wire cross-section is chosen according to

$$S_f = \frac{2\,p\,l_f\,F_{fr}}{0{,}9\,\gamma\,U_f} \quad , \tag{10.23}$$

where the field winding voltage U_f is chosen in standard row 65, 110, 220 and 440 *V*. The field winding current then results from chosen current density

$$I_f = J_f S_f \quad , \tag{10.24}$$

whereas this value is chosen in case of common generators between 2 and 4 A/mm^2. The number of field winding turns then results from necessary magnetomotive force

$$N_f = \frac{F_f}{I_f} \quad . \tag{10.25}$$

In case of permanent magnet synchronous machines it is necessary to proceed individually according to permanent magnet placement. Since there is a large variety in permanent magnet mounting options which differ by electromagnetic properties, they have to be considered during the whole design of the machine. According to location of the permanent magnets the electromotive force coefficient k_E varies from previously mentioned values (its value must be determined from the phasor diagram of the machine) and also the permanent magnet leakage flux coefficient k_σ rises, whereas its value starts from units of per cents for surface mounted permanent magnets and it may rise up to 25 per cent in case of buried permanent magnets. Since the magnetic flux of the permanent magnets cannot be controlled, the excitation is always designed for rated working point.

The permanent magnet excitation design of the synchronous machines is equivalent to the design of permanent magnet excitation of DC machines, thus it is necessary to calculate the total magnetic flux through permanent magnets as

$$\Phi_{PM} = (1 + k_\sigma)\,\Phi_\delta \quad , \tag{10.26}$$

from which the permanent magnet width b_{PM}, the permanent magnet magnetic flux density B_{PM} and magnetic field strength H_{PM} may be obtained. Then it is possible to determine the height of the permanent magnets from

$$h_{PM} = \frac{\Theta}{2\,(H_c - H_{PM})} \quad . \tag{10.27}$$

10.3 Damper Design

Although the damper of synchronous machines is basically a squirrel cage as known from induction machines, its design is significantly simplified, since most of the duty time it is not actively used. To avoid magnetic "gluing" of stator and rotor slots, it is necessary to choose different slot pitches on both sides. Commonly they are chosen according to

$$0.9\,t_{s1} < t_{s2} < t_{s1} \vee 1.1\,t_{s1} < t_{s2} < 1.2\,t_{s1} \quad . \tag{10.28}$$

The choice of damper cross-section is based purely on the cross-section of the damper bar, whereas for copper damper it is common to choose

$$Q_d S_d = (15 \div 30)\,\% \sum S_{Cu1} \quad , \tag{10.29}$$

where Q_d is the total number of damper bars,
S_d is the damper bar cross-section
and ΣS_{Cu1} is the total cross-section of the armature copper.

The cross-section of the shorting ring, which may be also manufactured as incomplete (the damper is then composed of squirrel-cage sections), the cross-section is

$$S_{sr} = (40 \div 50)\,\% \frac{Q_b S_b}{2\,p} \quad . \tag{10.30}$$

In case when a more robust performance of the damper is necessary, it is designed in the same way as the squirrel cage of the induction machines. This case is related especially to large hydro alternators, which may be started without use of an external induction machine.

11 Specific Parts of Design of Induction Machines

The induction machines are one of most robust type of electric machines. Due to simplicity of their construction and duty they are supposed to work in heavy industry with frequent run-ups without need of power converters. In connection with power converters they gained to be most used machines in electric traction, where they are nowadays being replaced (because of higher power density) by permanent magnet motors., which are significantly more expensive.

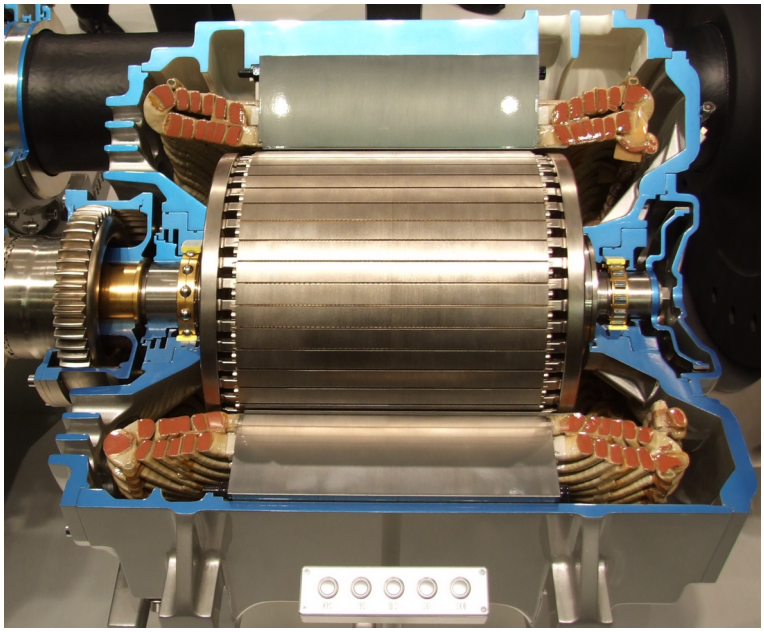


Fig. 11.1: Partial corr-section through traction IM

Even though the induction machines are able – by principle – to work as generators, in praxis they are almost never used that way. So, in contrast to synchronous machines which are most commonly used as generators, the induction machines are most commonly used as motors. This corresponds with their power range, where induction machines achieve maximal power if tens of megawatts.

The induction machines are made in two basic constructions – with wound rotor, which is equipped most commonly with three phase winding connected to slip rings, and with so-called squirrel cage. The squirrel cage rotor can be made with a simple “squirrel cage” winding, or it may be equipped with more sophisticated slot designs (eddy current cage) or it can be divided to two squirrel cages connected in shorting rings or fully separated. This concept is mechanically very robust, so the induction machines are able to work for a very long time without need of service maintenance.

The wound rotor induction machines were historically used in may applications, nevertheless due to the presence of a slip ring contact it is more advantageous to avoid this type of machine. The reason is, that the main advantage of this solutions – connection of an external circuit into the rotor winding to control the start of the machine – is now fully compensated by usage of power converters. Nowadays the experiments are made with wound rotor induction machines for wind turbines. In this case there is a converter connected to the rotor winding, which allows smooth reaction on different speed and pressure on blades of the turbine. In this case the term “doubly fed induction machine” is commonly used [21].

The fundamental requirements on the design of induction machines are similar as in case of other machine types. Since the induction machines are together with permanent magnet synchronous machines constructionally simplest machines, the design of the machine includes only design of stator and rotor winding and the design of magnetic circuit of both armatures[18].

18 A very specific type is from this point of view the shaded-pole induction machine, which must be designed using different approach.

The design of the induction machine must be derived from following parameters, which have to be given by the customer:

rated power of the machine	P_r [W]
rated voltage	U_r [V]
number of poles or synchronous speed	$2p$ [-], n_s [ot/min]
number of stator phases	m_1 [-]
machine type	motor/generator
rotor type	wound/squirrel cage
protection type	IP code
construction and mounting	IM code
cooling type	IC code

Among other parameters, which can be required, are for example machine dimensions, start-up current or machine overloadability. These parameters must be then fine-tuned using equivalent circuit parameters. A very common design of induction machines is with codes IM 1001 (IM B3) with IP 44 and IC 411 – so a machine with heels and cylindrical shaft on front side of the machine, terminal box on its side, resistant against squirting water and a fan of its shaft, which blows air on ribs in the chassis[19].

11.1 The Determination of Fundamental Dimensions of the Machine

Due to a large variety of usage of the induction machines even the designer's variable influencing Essons factor vary in a wide range. Although in case of small and medium sized machines it is preferred to use the above mentioned TEFC construction, large machines are often made as partially opened and their iron stack is supplemented by radial (industrial machines) or axial (traction machines) ventilation ducts. The used values of linear current density are commonly in range between 20 000 *A/m* in case of small machines up to 80 000 *A/m* in case of large and traction motors. In dependence on the air gap length also the air gap magnetic flux density is chosen in range from 0.6 *T* to approximately 1.15 *T*. It is necessary to note, that the air gap magnetic flux density projects in the total magnetomotive force drop on the magnetic circuit of the machine, which in case of induction machines means, that it affects also the

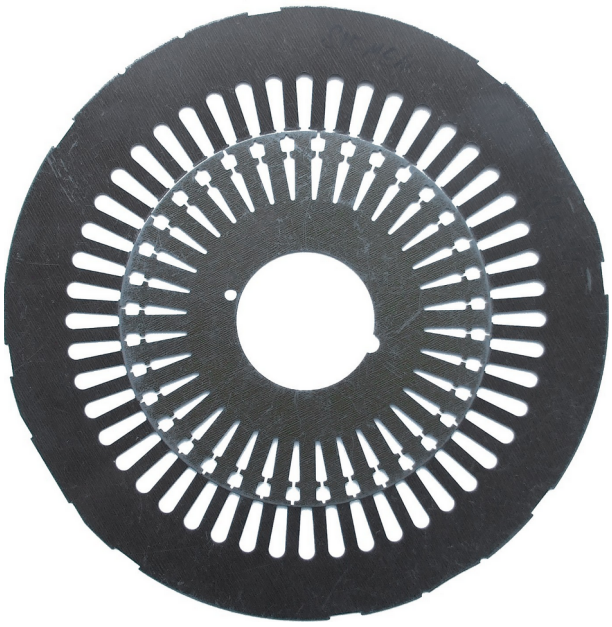


Fig. 11.2: Lamination of an induction machine with eddy current squirrel cage

19 This design is very common and it is marketed as TEFC motor – totally enclosed fan cooled motor.

power factor of the machine. Thus, excessively high values of the magnetic flux density as well as excessively large air gaps lead to lowering of the power factor of the machine.

Since the mechanical pole coverage factor has, in case of induction machines, no meaning, only its electromagnetic variant α_δ is being examined. In the first iteration of the design or when no excessive saturation is presumed, it is possible to choose the value of the electromagnetic pole coerace factor $\alpha_\delta = 2/\pi$ in combination with magnetic field shape factor $k_B = \pi/2\sqrt{2}$. Both factors are then further adjusted during the design in dependence on magnetic field saturation factor k_{sat}.

The winding of the induction machines is then oriented for possibly smoothest torque of the machine. This means, that an integral number of slots per pole and phase q is preferred, a fractional number is being chosen only in case of large machines supposed to work as generators. In case of small machines only single layer windings are used due to their simple manufacture, otherwise induction machines are equipped most commonly by two layered windings. Similarly to synchronous machines the windings of induction machines are designed to damp higher order harmonic components, so in case of three phase windings the winding pitch shortening factor is chosen approximately $\beta = 5/6$. The number of stator slots is the chosen according to available space and possible slot pitch, which is commonly between 10 and 35 *mm*.

The outer diameter of the machine D_e and the armature diameter D_1 are chosen according to customer's demands or in terms of possible shaft height. Commonly the armature diameter is being chosen in dependence on outer diameter of the machine using ratio

$$k_D = \frac{D_1}{D_e} \quad , \tag{11.1}$$

which is related to the number of machine poles. Commonly used values of the diameter coefficient k_D are shown in tab. 11.1. The length of the machine may be then determined from the power equation

$2p$ [-]	k_D [-]
2	0.52 ÷ 0.57
4	0.62 ÷ 0.68
6	0.7 ÷ 0.72
8	0.74 ÷ 0.77
≥10	0.75 ÷ 0.78

Tab. 11.1: The dependence of ratio k_D on the number of poles

$$l_i = \frac{S_i}{C D_1^2 n} \quad . \tag{11.2}$$

For the purpose of verification of optimality of resulting length a helping factor is commonly used in the literature, named as slimness ratio λ, which is often defined as a ratio

$$\lambda = \frac{l_o}{D_1} \tag{11.3}$$

according to [4] or

$$\lambda = \frac{l_i}{D_1} \tag{11.4}$$

according to [3]. The purpose of the slimness ratio is verification of suitability of dimensions of the machine to avoid excessive length of winding overhangs in comparison to the length of the machine, so there are not too high losses in the winding overhangs. Nevertheless this ratio is not a binding parameter, so it may not be respected in many applications.

The inner power of the machine S_i is determined as

$$S_i = k_E S \quad , \tag{11.5}$$

where the electromotive force factor k_E is chosen according to the machine type in range of 0.92 to 1 for motors, and 1 to 1.05 for generators. Based on its definition if may be calculated from the equivalent circuit parameters as

$$k_E = \frac{U_i}{U} \quad , \tag{11.6}$$

where the value of back EMF U_i results from the equivalent circuit of the machine as

$$\bar{U}_i = \bar{U} - R_1 \bar{I}_r - j X_{1\sigma} \bar{I}_r \quad . \tag{11.7}$$

The design of magnetic circuits of stator and rotor correspond to standard armature design, similarly to the case of synchronous machines. The limiting values of the magnetic flux densities are commonly chosen very similar for both stator and rotor, whereas for teeth the magnetic flux densities $B_{z1,2}$‘ are chosen between 1.8 to 2.2 *T* and for yokes their values are commonly between $B_{y1,2}$ = 1.2 to 1.5 *T*, whereas considering shorter magnetic flux lines in the rotor, the rotor values may be slightly higher.

Since the resulting properties of the machine are defined from a large part by its air gap, it is necessary to choose possibly shortest air gap length. From electromagnetic point of view another influencing parameter is the Carter’s factor, which is often minimized by usage of semiclosed or fully closed (in case of squirrel cage motors) slots. The minimal possible air gap length is approximately 0.2 *mm*, often it is chosen larger, at least 0.3 *mm*. For large machines it is possible to estimate the air gap length from

$$\delta \geq \frac{D_1}{1000} \quad [mm] \tag{11.8}$$

or for two pole machines

$$\delta = 0.1 + 0.225 \sqrt[3]{P_r} \quad [mm; kW] \tag{11.9}$$

or using

$$\delta = 0.1 + 0.145 \sqrt[3]{P_r} \quad [mm; kW] \tag{11.10}$$

for machines with four and more poles.

The suitability of chosen air gap length and magnetic circuit saturation may be verified using magnetic circuit saturation factor, whose limiting value is considered about k_{sat} = 1.35. Below this value the machine is relatively poorly saturated, above this value it it highly saturated. Even in this case this is a non-binding value, which is, especially in case of traction machines, almost always overcome and in case of atypical machines its predictive value is very limited. Then the machine must be evaluate only on base of resulting characteristics.

11.2 The Design of Induction Machine Rotor

The design of the magnetic circuit of the rotor is identical to the design of the armature, the main difference is formed by the design of the rotor winding. In case of wound rotor the limiting output power is approximately 100 *kW*, below this value the winding is designed according to desired rotor voltage, above this value the winding topology changes to construction made of bars (half-coils), which gives the resulting rotor voltage.

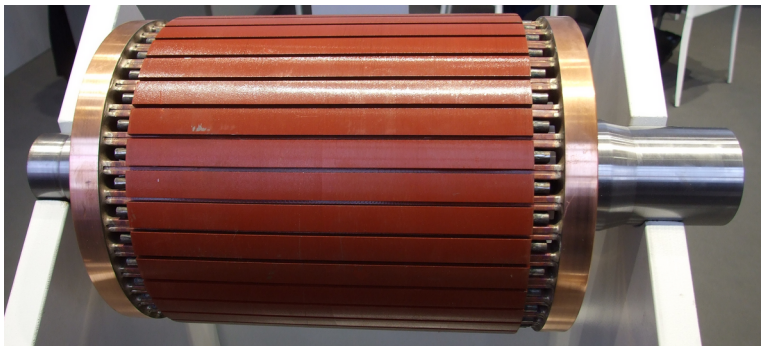


Fig. 11.3: Rotor of an induction machine equipped with soldered copper squirrel cage

In case of machines with output power below 100 *kW* the rated rotor voltage is chosen according to available starters, whereas the approximate voltage of the starter may be estimated according to

$$U_2 = 38 \sqrt{P_r [kW]} \pm 17\% \quad . \tag{11.11}$$

Above 100 *kW* of output power the rotor current is extremely high, thus two layered bar winding is chosen for these machines, whereas one winding layer corresponds to one conductor in a slot (V_s = 2). This solution leads to design of relatively high and thin bars, which are affected by skin-effect, which results to higher start-up resistance and lowering of start-up current. Based on chosen number of slots the number of rotor winding turns then results

$$N_{s2} = \frac{Q_2}{m_2} \quad , \tag{11.12}$$

where m_2 is the number of rotor phases, in this type of machine commonly m_2 = 3.

The rotor voltage is then calculated from the rotor magnetic flux and calculated number of winding turns in series. In case of wound rotor the number of rotor slots is chosen not to be equal to the number of stator slots:

$$Q_2 \neq Q_1 \tag{11.13}$$

together with

$$Q_2 \neq Q_1 \pm 2\,p \quad . \tag{11.14}$$

This may be avoided by choice of

$$q_2 = q_1 \pm 1 \tag{11.15}$$

while having identical number of stator and rotor phases, i.e. $m_1 = m_2$ [8].

The current through rotor phase then results from equality of magnetomotive forces, thus

$$F_1 = F_2 \tag{11.16}$$

$$\frac{m_1}{\pi}\frac{N_{s1}k_{w1}I_{m1}}{p} = \frac{m_2}{\pi}\frac{N_{s2}k_{w2}I_{m2}}{p} \quad , \tag{11.17}$$

which gives the current transformation factor

$$k_I = \frac{I_1}{I_2} = \frac{m_2 N_{s2} k_{w2}}{m_1 N_{s1} k_{w1}} \quad . \tag{11.18}$$

But this factor is further influenced by leakage magnetic fluxes, thus to be able to identify the correct value of the rotor current of an induction machine a coefficient κ_I, which depends on the power factor of the machine (see fig. 11.4). The real rotor current is then

$$I_2 = \frac{\kappa_I}{k_I} I_1 \quad . \tag{11.19}$$

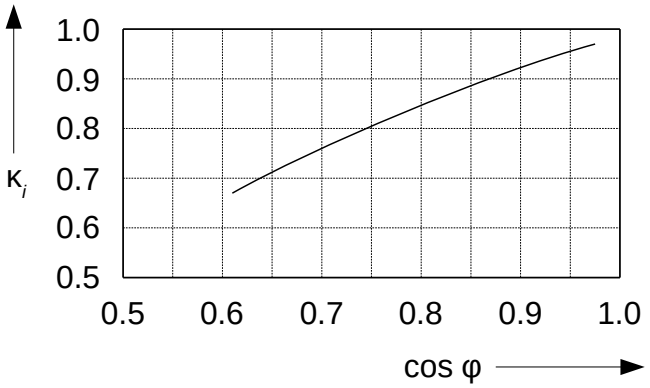


Fig. 11.4: The dependence of κ_i on power factor

The rotor winding factor k_{w2} is identified in the same way as in any other alternating winding type, i.e. even in this case it is necessary to calculate separately the winding pitch factor k_{y2} and the winding distribution factor k_{d2} and their multiplication gives the final winding factor k_{w2}. The current density is in case of wound rotor machines chosen as $J_2 = 1.2J_1$ because of better rotor cooling due to rotor movement. This gives rotor conductor cross-section

$$S_{Cu2} = \frac{I_2}{J_2} \quad . \tag{11.20}$$

The rotor slots are then chosen more likely semiclosed because of better mechanical support of the winding against centrifugal forces. In case of larger machines with longer air gap the slots are often fully opened (N-type slots) with wedges made of non-magnetic steel.

The squirrel cage winding is made of two rings (shorting rings) connected by bars placed in rotor slots. This whole concept is similar to a real squirrel cage, so this is where its name came from. From the winding design point of view the winding is formed by Q_2 slots, which project to P_2 phasors with angular pitch α_2. If the number of rotor slots has a common divider with the number of machine pole pairs, the it is possible to determine the number of projections of slot phasors to one direction

$$\kappa_2 = GCD(Q_2; p) \tag{11.21}$$

and the angular pitch between phasors is then

$$\alpha_2 = \frac{360\,°}{P_2} \quad , \tag{11.22}$$

whereas the number of phasors in star of slots is

$$P_2 = \frac{Q_2}{\kappa_2} \quad . \tag{11.23}$$

Each of these phasors has its own unique orientation in complex plane (= unique phase shift) and it is not connected to series with none of others, since the shorting rings form, in fact, winding nodes. Because of this reason each of resulting phasors can be considered a separate phase of the rotor winding, thus the number of squirrel cage rotor phases is

$$m_2 = P = \frac{Q_2}{\kappa_2} = \frac{Q_2}{GCD(Q_2, p)} \quad . \tag{11.24}$$

The greatest common divisor of the number of rotor slots and rotor pole-pairs shows the number of projections of each phasor to one direction, thus each of rotor bars corresponding with one phasor have the same phase and they can be considered as rotor winding parallel branches, thus

$$a_{\sim 2} = \kappa_2 = D(Q_2; p) \quad . \tag{11.25}$$

Since the bars of the rotor winding do not form enclosed coils, it is not possible to define any of winding factors for them, so they have a full interaction with all harmonic components from the air gap, thus their winding factor is $k_{w2v} = 1$ and since a par forms only one half of the coil turn, the number of winding turns in series is $N_{s2} = ½$. The negative after-effect of this topology is, that all harmonic components from the air gap magnetic flux are fully induced into rotor winding, spatial harmonic components as well as time harmonics. This leads (without compensation) to creation of

torque saddles and noisier motor duty. To suppress these effects, the rotor slots are commonly skewed by 0.5 to 1 slot pitch of the opposite side of the machine[20]. The electrical angle of the slot skewing is then

$$\varepsilon = \frac{t_{sk}}{t_p}\pi \quad , \tag{11.26}$$

where t_{sk} is the skewing pitch.

The resulting skew factor is the defined as

$$k_{sk} = \frac{2}{\varepsilon}\sin\frac{\varepsilon}{2} \quad .^{21} \tag{11.27}$$

The resistance of one phase must be derived from the resistance of one bar and adjacent part of the shorting ring. The rotor bar resistance is

$$R_b = \frac{1}{\gamma}\frac{l_b}{S_b} \quad , \tag{11.28}$$

where l_b is the bar length
and S_b is its cross-section.

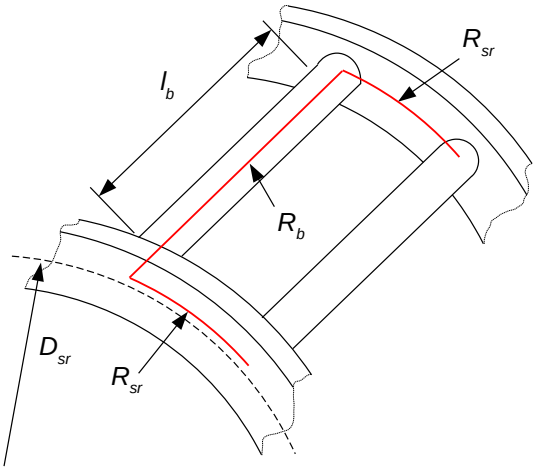


Fig. 11.5: Squirrel cage section corresponding to one rotor phase

Similarly the resistance of corresponding part of the shorting ring is

$$R_{sr} = \frac{1}{\gamma}\frac{l_{sr}}{S_{sr}} \quad , \tag{11.29}$$

where the length of corresponding part of the shorting ring is

$$l_{sr} = \frac{2\pi D_{sr}}{Q_2} \quad , \tag{11.30}$$

where D_{sr} is the medium diameter of the shorting ring.

The resulting phase resistance must be then determined from the comparison of losses in shorting ring and corresponding bar in a “substituting phase” of a rotor, i.e. for one parallel winding branch, we can write

$$R_{a2} I_a^2 = R_b I_a^2 + 2 R_{sr} I_{sra}^2 \quad , \tag{11.31}$$

20 This is also often used in case of permanent magnet synchronous machines.
21 For $\varepsilon \to 0$ the solution is $k_{sk} = 1$, which may be proven by L’Hopital rule.

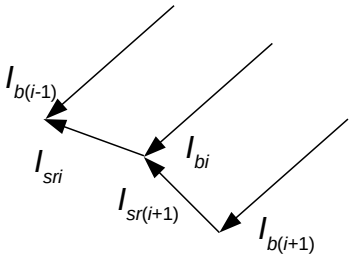


Fig. 11.6: Currents in the squirrel cage

thus the equivalent resistance of one rotor parallel branch is

$$R_{a2} = R_b + 2R_{sr}\left(\frac{I_{sra}}{I_a}\right)^2 \quad . \tag{11.32}$$

For currents from next two bars it is valid, that the amplitude of the current, which flows through them is identical ans the phase shift between them is equal to electrical angle between following slots, i.e. angle α_2. This phase shift then corresponds with phase difference in following two segments of the shorting ring, whereas bars form in the phasor diagram the difference between following phasors of the current through shorting rings. From construction shown in fig. 11.7 we can derive, that the amplitude of the current through a bar is

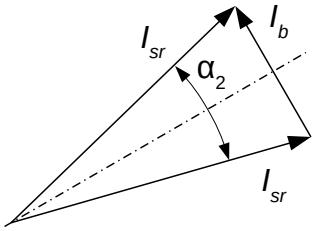


Fig. 11.7: Current through a bar as a difference between currents in shorting ring

$$I_b = 2I_{sr}\sin\frac{\alpha_2}{2} \quad , \tag{11.33}$$

whereas the mechanical angle between following bars is

$$\alpha_{mech} = \frac{2\pi}{Q_2} \tag{11.34}$$

and the electrical angle results

$$\alpha_2 = p\,\alpha_{mech} = \frac{2\pi}{Q_2}p \quad . \tag{11.35}$$

The ratio between these currents may be marked as

$$\Delta = \frac{I_b}{I_{sr}} = 2\sin\frac{\alpha_2}{2} \quad . \tag{11.36}$$

Thus the resistance of one parallel branch of the squirrel case results

$$R_{a2} = R_b + 2\frac{R_{sr}}{\Delta^2} \tag{11.37}$$

and the resistance of the whole squirrel cage phase is

$$R_2 = \frac{R_{a2}}{a_{\sim 2}} = \frac{R_{a2}}{\kappa_2} \quad . \tag{11.38}$$

Similarly for current through one bar we can write

$$I_b = I_{a2} = \frac{I_2}{a_{\sim 2}} \quad , \tag{11.39}$$

where the current through the rotor may be derived from (11.19). The cross-section of rotor bars is

$$S_b = \frac{I_b}{J_2} \quad , \tag{11.40}$$

where the current density is chosen according to the material approximately 6 to 8 A/mm^2 for copper squirrel cages, and 4 to 5 A/mm^2 for aluminium squirrel cages. The number of rotor slots is chosen according to the same rule as in case of wound rotors. From constructional point of view the design of the squirrel cage is very variable and in can include simple cages, eddy current cages but also doubled cages, which are often made of two different materials (start-up cage could be made of brass or bronze, running cage can be made of copper).

The leakage inductance of the rotor winding may be calculated equivalently to the rotor resistance as

$$L_{2\sigma} = L_{\sigma b} + 2\frac{L_{sr}}{\Delta^2} + L_{dif} \quad , \tag{11.41}$$

where $L_{\sigma b}$ is the bar leakage inductance,
L_{sr} is the leakage inductance of the shorting ring, which may be calculated in the same way as leakage inductance of winding overhangs or we can use simply winding overhang reluctance coefficient $\lambda_{sr} \approx 0.3$,
and L_{dif} is the differential leakage inductance of the squirrel cage, which is calculated from

$$L_{dif} = \tau_{dif} L_{2\mu} \quad , \tag{11.42}$$

where the magnetizing inductance is determined as magnetizing inductance from the point of view of the whole squirrel cage, i.e. considering squirrel cage properties (N_{s2} = ½, k_{v2} = 1) on base of (6.23) as

$$L_{2\mu} = \frac{1}{2}\frac{\mu_0 m_2}{\pi^2 p}\frac{t_p l_i}{\delta'} \quad . \tag{11.43}$$

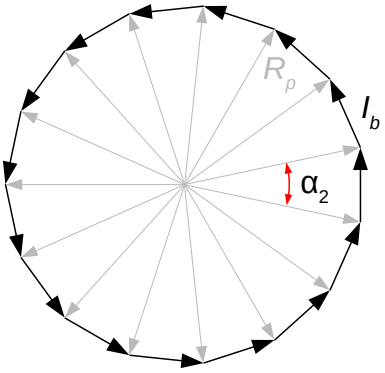


Fig. 11.8: Görges' pattern of a squirrel cage with m_2 = 15 phases and 2p = 2 poles

The differential leakage flux factor is then determined similarly to traditional winding, whereas in this case it is possible to express the radius of the Görges' circle explicitly from the magnetomotive force generated by the squirrel cage as

$$R_{1g} = F_m = \frac{m_2}{\pi} \frac{N_{s2} k_{w2}}{p} I_2 \quad , \tag{11.44}$$

where we can include the parameters of the squirrel cage (N_{s2} = ½, k_{w2} = 1, $I_2 = \kappa_2 I_t$), which gives

$$R_{1g} = \frac{\kappa_2 m_2}{\pi} \frac{I_t}{2p} \quad , \tag{11.45}$$

where the multiplication of κ_2 and m_2 corresponds with the number of the squirrel cage bars Q_2, thus

$$R_{1g} = \frac{Q_2}{2\pi p} I_t \quad . \tag{11.46}$$

The equivalent diameter of the Görges' pattern (see fig. 11.8) is then formed by phasors of unique length and from the bar current we obtain

$$R_g = R_p = \frac{I_t}{2\sin\frac{\alpha_2}{2}} = \frac{I_t}{2\sin\frac{\pi p}{Q_2}} \tag{11.47}$$

The general expression of differential leakage flux coefficient for squirrel cage windings is then

$$\tau_{dif} = \frac{R_g^2 - R_{1g}^2}{R_{1g}^2} = \frac{R_g^2}{R_{1g}^2} - 1 = \frac{\left(\frac{\pi p}{Q_2}\right)^2}{\sin^2\frac{\pi p}{Q_2}} - 1 = \frac{\left(\frac{\alpha_2}{2}\right)^2}{\sin^2\frac{\alpha_2}{2}} - 1 \quad . \tag{11.48}$$

11.3 Equivalent Circuit Parameters and Important Points of Machine Characteristics

The induction machine is in many aspects similar to the transformer, thus a very similar approach is applied to the mathematical description of the induction machine and its equivalent circuit. As an addition to current transformation ratio derived in (11.18) it is necessary to know the voltage transformation ration, which is, similarly to transformers, derived from the equality of the induced voltages in short-circuit state (with blocked rotor)

$$U_{i1} = U_{i2}' = k_U U_{i20} \quad . \tag{11.49}$$

Thus we can derive

$$k_U = \frac{U_{i1}}{U_{i20}} = \frac{4 k_B N_{s1} k_{w1} \Phi f_1}{4 k_B N_{s2} k_{w2} \Phi f_2} \quad , \tag{11.50}$$

whereas in short-circuit state the frequencies in the stator and in the rotor are equal. The voltage transformation ration is then

$$k_U = \frac{U_{i1}}{U_{i20}} = \frac{N_{s1} k_{w1}}{N_{s2} k_{w2}} \quad . \tag{11.51}$$

Together with current transformation ratio we can derive the impedance transformation ratio

$$k_Z = \frac{k_U}{k_I} = \frac{m_1}{m_2} \left(\frac{N_{s1} k_{w1}}{N_{s2} k_{w2}} \right)^2 \quad . \tag{11.52}$$

For transformation of variables it is valid, that

$$\begin{aligned} U_2 &\rightarrow U_2' = k_U U_2 \\ I_2 &\rightarrow I_2' = k_I I_2 \\ R_2 &\rightarrow R_2' = k_Z R_2 \\ X_{2\sigma} &\rightarrow X_{2\sigma}' = k_Z X_{2\sigma} \end{aligned} \quad .^{22} \tag{11.53}$$

Using determined parameters of the equivalent circuit it is possible to determine the parameters of the machine in extreme states, i.e. in no-load and in short-circuit. The no-load current may be derived from the iron core losses and from armature magnetomotive force in no-load. In no-load state the air gap magnetic flux density is equal to B_δ, which gives a certain magnetomotive force drop for the whole magnetic circuit Θ. To cover this magnetomotive force drop, it is necessary to generate

$$F_0 = \Theta \quad , \tag{11.54}$$

which corresponds with (6.15) reactive part of the current

$$I_{0r} = \frac{\pi \, p \, F_0}{m_1 N_{s1} k_{w1} \sqrt{2}} \quad . \tag{11.55}$$

Similarly we can derive the active part of the no-load current from the R_{Fe} resistance as

$$I_{0a} = \frac{U_{i1}}{R_{Fe}} \quad . \tag{11.56}$$

It is necessary to note, that in case of induction machines the iron core loss resistance R_{Fe} includes among iron core losses also mechanical losses. The total no-load current then results from both components as

$$I_0 = \sqrt{I_{0a}^2 + I_{0r}^2} \tag{11.57}$$

22 The transformed variable are sometimes referred as U_{21}, I_{21}, R_{21}, X_{21} instead of using apostrophe.

and the phase shift between the voltage and the current in no-load state is

$$\varphi_0 = \operatorname{atan} \frac{I_{0r}}{I_{0a}} \quad , \tag{11.58}$$

which leads to no-load power factor of the machine.

The no-load state may be on base of the equivalent circuit described as a serial connection of winding resistances and leakage reactances, thus the short-circuit current of the machine at rated load results

$$I_{sc} = \frac{U_r}{\sqrt{(R_1 + R_2')^2 + \omega_1^2 (L_{1\sigma} + L_{2\sigma}')^2}} \quad , \tag{11.59}$$

which is also a start-up current of the machine. The phase shift between voltage and current in short circuit is

$$\varphi_{sc} = \operatorname{atan} \omega_1 \frac{L_{1\sigma} + L_{2\sigma}'}{R_1 + R_2'} \quad . \tag{11.60}$$

The characteristics of the machine may be drawn using equivalent circuit of the machine, whereas the location of the rated working point may be determined from presumption, that the rated slip is equal to the rotor resistance in per units.

12 Notes to the Design of Special Types of Electric Machines

If we would use the traditional definition of electric machines as devices serving for transformation of electrical energy to electrical energy of different parameters or to mechanical energy, this term would include much wider group of electrical device than only traditional electric machines. The identical definition may be fulfilled by various actuators, loudspeakers, magnetic vents etc. For the purpose of further approach let us now limit to variations of traditional electric machines, which come into interest nowadays, either because of the evolution of the power electronic converters or because of possible increase of power density of drive systems.

12.1 Synchronous Reluctance Machines

The synchronous reluctance machines are a variation of traditional salient pole electrically exited synchronous machines. In contrast to electrically excited synchronous machines the torque of these machines is generated only due to the difference in inductances in direct and quadrature axes. The design of the machine, or more precisely its rotor is therefore focused on maximization of difference of inductances in both axes. For this purpose a variety of rotor topologies was proposed, whereas the most common are shown in fig. 12.1 [22].

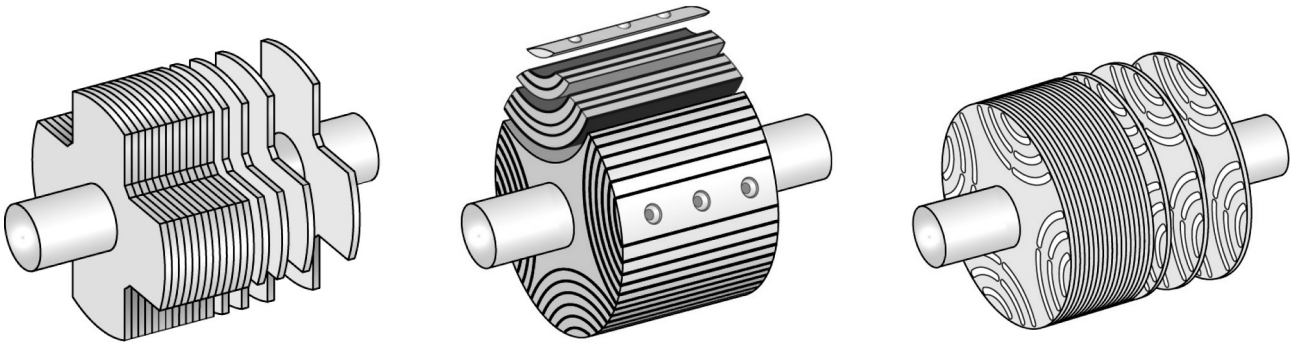


Fig. 12.1: Synchronous reluctance motor rotor topologies

From the figure 12.1 an inspiration by traditional salient pole synchronous machine is obvious (left), but this topology does not offer required difference in inductances in both axes. This is compensated by so-called axially laminated topology (middle) and radially laminated topology with flux barriers (right, practical performance in fig. 12.2 [23]). In these case it is possible to achieve significantly higher differences in inductances, even in this case the saliency ratio L_d/L_q is not greater than 4.



Fig. 12.2: The performance of synchronous reluctance motor rotor by Siemens

From designer's point of view the design of the machine is identical to the design of synchronous motors with electrical excitation, i.e. even in this case traditional distributed winding is used with integral number of slots per pole and phase q. The

tooth windings are also possible to be used, but due to their large differential leakage flux factor the leakage inductance of these machines rises and leads to lowering of the saliency ratio, which forms a disadvantage of this solution.

Since the rotor of synchronous reluctance machines is a purely passive part, it does not generate back EMF and the magnetic flux through the air gap must be derived from terminal voltage. Together with that the electromotive force factor cannot be defined for these machines, thus value of $k_E = 1$ is used.

In case of flux barriers rotor the design of the magnetic circuit avoids higher saturation of the rotor, which would again lead to lower saliency. Because of this both teeth and rotor magnetic bridges are designed for lower saturation – approximately 1.8 *T* in case of teeth and below 1.5 *T* in case of magnetic bridges. The flux barriers, especially their ends near to the air gap, act similarly to openings of slots of induction machines, thus the choice of the number of rotor flux barriers must be derived from conditions for choice of number of induction machine rotor slots. The number of rotor barriers N_b must therefore meet condition

$$N_b \neq \frac{Q_1}{2p} \pm 1 \quad . \tag{12.1}$$

From the losses point of view although the rotor is fully passive, the pulsation losses are still generated in magnetic bridges due to the stator slotting, so even in this case it is necessary to use electrical steel sheets for rotor construction.

A crucial factor in synchronous reluctance machine design is the choice of the air gap size. It influences the value of the direct axis inductance, which can result very high for small air gaps and the impedance of the machine may be so high so it is not possible to pull required current through the machine and it does not produce required torque. A suitable clue can be in this case the MTPA criterion for synchronous reluctance machines [24], which leads to phasor diagram including required parameters of the machine in relation to its output power and rated voltage [25].

For example by analysis of the phasor diagram with knowledge of the condition for optimal duty of the synchronous reluctance machine (MTPA; $i_d = i_q$) can be, presuming saliency ratio $L_d/L_q = 4$, derived remaining sizes of reactances, whose values should be $x_d = 1.37$ *p.u.* and $x_q = 0.34$ *p.u.* The power factor of such machine will be cos φ = 0.51.

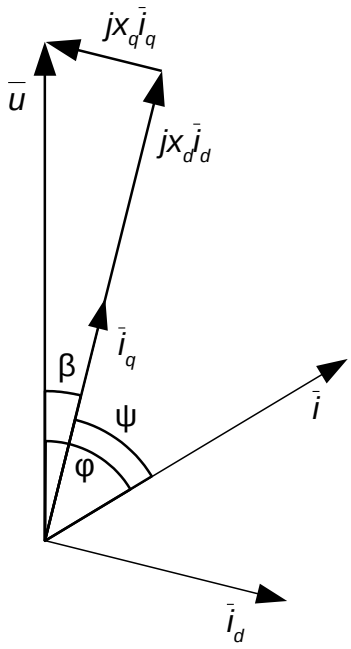


Fig. 12.3: Phasor diagram of an optimally controlled synchronous reluctance machine in per units

A considerable increase of the power factor may be achieved by addition of permanent magnet excitation, which can be placed in the flux barriers. This topology is often marked as permanent magnet assisted synchronous reluctance machine. He key difference between these machines and traditional permanent mag-

net synchronous machines is that the major part of the torque is not generated by permanent magnets but by the rotor saliency.

12.2 Switched Reluctance Machines

The switched reluctance machine are in a certain view extreme case of synchronous reluctance machines, whereas the stator winding is formed by tooth winding, which is directly switched to the direct current voltage. After connection of a coil to the DC voltage the current starts to flow through the coil, which excites the magnetic flux going through the rotor with extremely salient poles. This leads to its rotation into direction with lowest reluctance – in the direction of power supplied coils (see fig. 12.4 [26]). This procedure the repeats, so by separate connection of each coil to the power supply the rotor starts to rotate.

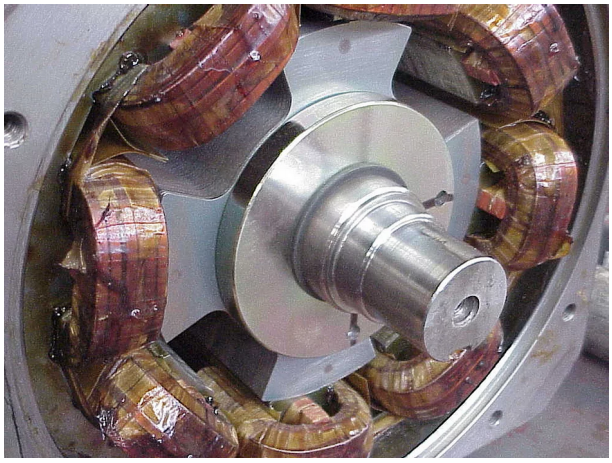


Fig. 12.4: Switched reluctance motor

It is obvious, that in comparison to previously mentioned types of electric machines the principle of this machine is significantly different – instead of presumption of sine wave power feeding, this machine is kept all the time in a transient state. This effects projects also into its torque, which includes significant torque ripples, and its current, which has a nature of a saw curve. Even through its properties the switched reluctance machines are often used because of simplicity and robustness of their construction, which allows their usage even for highest speeds. One of most renown application of switched reluctance motor is the electric turbocharger of Audi Q7 [27], a synchronous reluctance motor is also due to its robustness used in a mine truck by Komatsu [28].

For the purpose of the design of synchronous reluctance motors it is not possible to use traditional approach, when the initial dimensions of the machine are defined by power equation, which results from the presumption of harmonic power supply. The design of the synchronous reluctance machines is therefore not oriented on resulting dimensions with regard to the power equation, but on correct process of the transient phenomena, in which it should work. From the dimensions point of view it is crucial to design the machine so it is able to lead required magnetic flux linkage $\psi(t)$ without excessive saturation of the iron core. The time description of the magnetic flux is

$$\psi(t)=\int (u-Ri)\,dt \quad , \tag{12.2}$$

where u is the terminal voltage,
R is the phase resistance
and i is the time dependency of the current.

During its motion the rotor of the machine moves within elementary time step dt by angle $d\xi$, thus it is possible to write

$$\omega = \frac{d\xi}{dt} \tag{12.3}$$

and if we presume zero stator resistance R and constant motor terminal voltage U we can substitute to (12.2), which gives

$$\psi(\xi) = \frac{1}{\omega}\int U\, d\xi \quad . \tag{12.4}$$

The maximal change of the magnetic flux linkage appears when the rotor moves from the position between stator teeth to position aligned with stator teeth. Then we can write

$$\psi = \frac{1}{\omega}\int_{\xi_1}^{\xi_2} U\, d\xi = \frac{U}{\omega}(\xi_2 - \xi_1) = \frac{U}{\omega}\varepsilon \quad , \tag{12.5}$$

where ε is the switch angle, which results from the number of stator phases m_1 and the number of the rotor teeth N_r as

$$\varepsilon = \frac{2\pi}{m_1 N_r} \quad . \tag{12.6}$$

The magnetic flux through the machine may be determined as

$$\Phi = \frac{\psi}{K_1 N_c} = \frac{\varepsilon U}{\omega K_1 N_c} = \frac{2\pi U}{\omega m_1 K_1 N_c N_r} \quad , \tag{12.7}$$

where K_1 is the number of stator coils connected in series
and N_c is the number of the coil turns.

The relation to the motor torque may be approximately determined from analytical calculation

$$M = \frac{\partial W_m}{\partial \xi} = \frac{1}{2\varepsilon}(L_{max} - L_{min})\, i^2 \quad , \tag{12.8}$$

where L_{max}, L_{min} are the values of inductances in positions with aligned stator and rotor teeth and in position of the rotor teeth between stator teeth.

It is obvious that the design of the switched reluctance machine is an optimization task, whose target is finding suitable dimensions for achieving required inductances L_{max} and L_{min}, whereas the limiting factors are the stator current density and the saturation of the stator magnetic circuit.

Since most of used variable show analytically hardly describable properties, it is suitable to supplement the design using finite element method, whose output are the flux linkage maps of the designed machine (dependencies of flux linkage on rotor angle and motor current, see fig. 12.5 [29]), from which it is possible to derive the current and torque curves. These dependencies are then res-

ults of simulations, in which the current resulting from used terminal voltage and rotor position is the current is solved according to

$$\psi(\xi,i)=\frac{1}{\omega}\int (U-Ri)\,d\xi \qquad (12.9)$$

in connection to dependency of the inductance on current and rotor angle

$$\psi(\xi,i)=\int L(\xi,i)\,di \quad . \qquad (12.10)$$

The torque of the machine is then calculated as

$$M(\xi,i)=\frac{\partial}{\partial t}\left[\int_0^i \psi(\xi,i)\,di\right] \qquad (12.11)$$

with magnetic flux linkage factor

$$K(\xi,i)=\frac{\partial \psi(\xi,i)}{\partial t} \quad . \qquad (12.12)$$

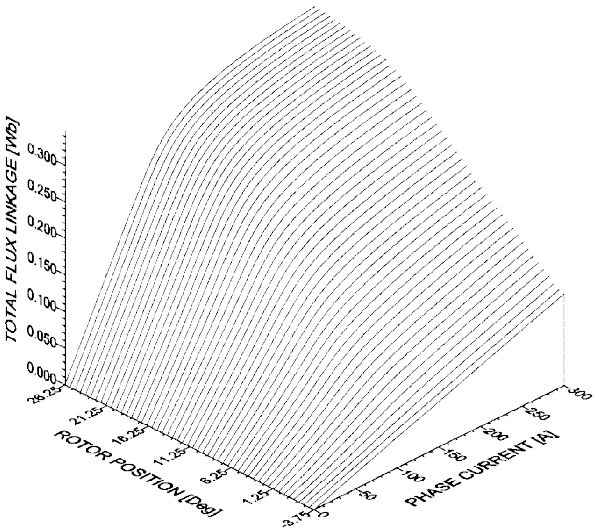


Fig. 12.5: Flux map of a synchronous reluctance machine derived from finite element method

12.3 Axial Machines

The axial form of electrical machines gains more and more attraction, especially in automotive industry. In general, any electric machine may be transformed to its axial variant – i.e. it is possible to build axial synchronous machine, induction machine (see Fig. 12.6 [30]), DC machine or one of switched machines. The reason of the popularity of these machines is both increase of machine power density (expressed as a ration of output power to the mass or volume of the machine) as well as relatively easy scaling of the output power – the result of the design is almost in all cases relatively thin motor and the obtained axial space may be used for serial connection of multiple machines. A similar connection may be achieved also in chassis of one machine by connection of multiple stators and rotors.

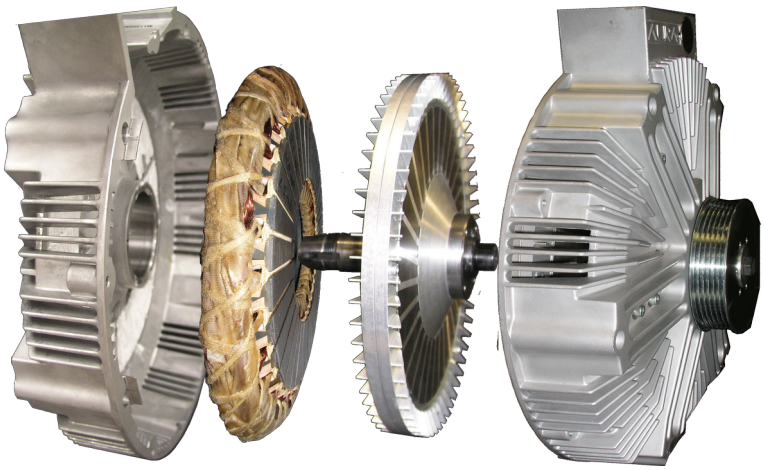


Fig. 12.6: Axial form of a squirrel cage induction machine

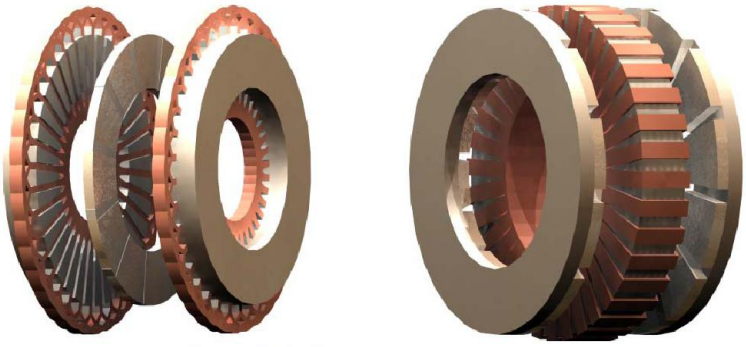


Fig. 12.7: Axial machine with distributed winding and two stators (left) and axial machine with a single stator and toroidal coils (right); taken from [31]

From the configuration point of view there are several topologies of stator and rotors, which, in general, differ by total usage of the material, but also in manufacturing technology. The easiest solution is the usage of armature in its traditional form, i.e. as a part with teeth and yoke, as shown in fig. 12.6. The rotor may be then also an axial variation of a traditional rotor, or simply an interpart between two stators. The advantage of this solution is a large cooling are of both stators, so these types of machines can be cooled using common cooling techniques, e.g. by air.

An alternative performance is the usage of two rotors and one stator. Even in this topology the initial constructions were variations on traditional armature (teeth connected by yoke; winding in traditional distributed form or in form of toroidal sections), but nowadays the yokeless variant is more often used. In case of these machines the winding is wound around one tooth and the magnetic flux goes directly from one rotor though the tooth to the opposite rotor. These machines are manufactured e.g. by English manufacturer YASA (see fig. 12.8 [31]) or Belgian Magnax. The disadvantage of this solution is a problematic mechanical connection of teeth with coils and the cooling of the machine. Because of this these machines are often liquid cooled (water, oil).

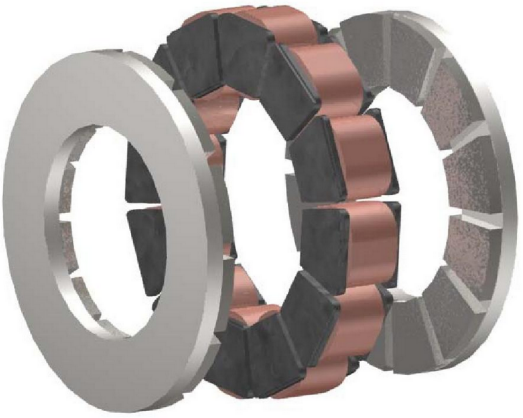


Fig. 12.8: YASA motor topology

The design of the axial machine may be performed “by intuition”, i.e. by simple transformation of the power equation to the conditions of the axial machines[23], nevertheless this approach appears to be unsuitable, since it does not lead to optimal usage of the material of the machine and it does not fully use all of the cooling area [32]. Consequently the linear current density may increase near to the inner diameter of the machine leading to excessive losses in the same place. Because of this reason it is suitable to introduce as a reference point of the design a ratio

23 In this case the armature diameter D_1 would be an arithmetic average between inner and outer diameter

$$D_1 = \frac{D_e + D_i}{2} \tag{12.13}$$

and the machine length is one half of the difference between both diameters

$$l = \frac{D_e - D_i}{2} \quad . \tag{12.14}$$

Then it is possible to use the power equation in its traditional form.

$$\lambda = \frac{D_i}{D_e} \quad , \tag{12.15}$$

and with respect to the losses in inner winding overhangs for the purpose of evaluation of Esson's factor the linear current density on inner diameter A_i will be used. The power equation form is then

$$S_i = \frac{1}{4} C D_e^3 (1 - \lambda^2) \lambda n \quad , \tag{12.16}$$

where the Esson's factor is

$$C = \frac{\pi^2}{60} \alpha_\delta B_\delta A_i k_{w1} k_B \quad . \tag{12.17}$$

As an optimal ratio between inner and outer diameter of the machine with respect to losses in the machine the value of

$$\lambda = \frac{1}{\sqrt{3}} \tag{12.18}$$

is used. It is necessary to note, that the above mentioned form of the power equation relates to one single armature of the machine. In case the machine has more armatures (stators), the resulting power is a sum of powers of each armature.

12.4 Linear Machines

Similarly to axial machines, even in case of linear machines any principle of electric machine may be transformed to its linear form. The linear electrical machines are commonly used in applications, where transmission of rotating movement of traditional machine to linear movement brings significant disadvantages. This includes various positioning devices or drive systems of magnetically levitated transport systems. In the industry an often used type is the linear variant of permanent magnet synchronous machine, for magnetically levitated transport systems also variants of electrically excited synchronous machines (the excitation coils on the moving part may also serve as electromagnets attracting the cabin to the railway; this solution uses e.g. German Transrapid [33], [34]) or linear induction machines are used.



Fig. 12.9: A section of Transrapid drivetrain [33]

An example of transformation of rotary electric machine to a linear machine is shown in fig. 12.10. It shows a procedure of transition from rotary induction machine to linear induction machine. By principle it is obvious, that the lengths of both parts (static and moving) have to be different, or no motion of the machine would be possible. Similarly as in case of rotary machines it is possible to switch the static and moving parts, so two main topologies are distinguished – machines with short armature and machines with long armature (as shown in fig. 12.10).

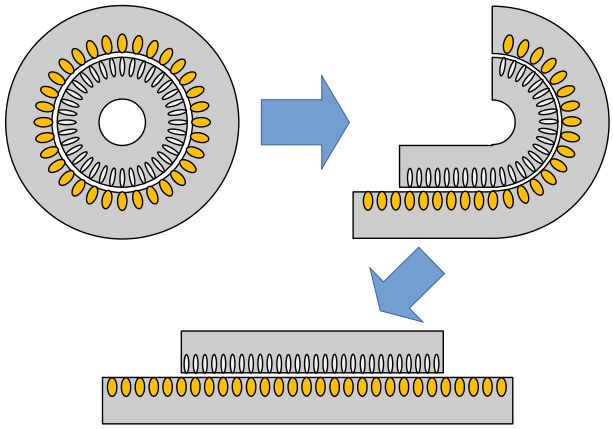


Fig. 12.10: Transition from rotary machine to linear machine

Mathematically the transition from rotary machine to a linear machine may be demonstrated using power equation in its full form, i.e. with substituted Esson's factor by all included variables

$$S_i = \frac{\pi^2}{60}\alpha_\delta A B_\delta k_{w1} k_B D_1^2 l n \quad . \tag{12.19}$$

From (12.19) we can select

$$\frac{\pi D_1 n}{60} = v \tag{12.20}$$

for the speed of the machine and

$$\pi D_1 = L \tag{12.21}$$

for its active length. Consequently it is suitable to change the designation of the length of the machine l to its width b. After these modifications the power equation is

$$S_i = \alpha_\delta A B_\delta k_{w1} k_B L b v \quad , \tag{12.22}$$

from which we can separate the linear form of the Esson's factor

$$C_l = \alpha_\delta A B_\delta k_{w1} k_B \tag{12.23}$$

and the final form of power equation for linear machines

$$S_i = C_l L b v \quad . \tag{12.24}$$

Using relation

$$P = F\,v \tag{12.25}$$

the electromagnetic force of the machine may be determined as

$$F_i = C_l\,L\,b \quad . \tag{12.26}$$

The length of the machine should correspond to a multiple of the wavelength of the progressive field of the machine (λ; $\lambda = 2t_p$), which determines the number of the machine poles

$$p = \frac{L}{\lambda} \quad . \tag{12.27}$$

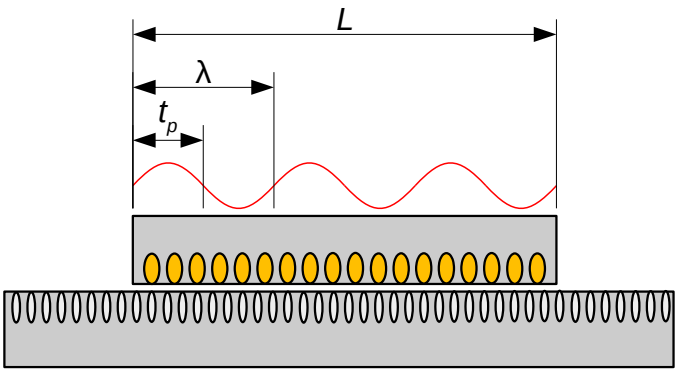


Fig. 12.11: Length of the machine and important parameters of linear machine with short armature

From the knowledge of the machine speed and the wavelength it is possible to determine the power supply frequency as

$$f = \frac{v}{\lambda} = \frac{p\,v}{L} \quad . \tag{12.28}$$

All above mentioned variables are shown in fig. 12.11 and their meaning is similar also in case of design with short moving part and long armature. In this case the active part is the short moving part, hence the power and traction force are again given by the length of the moving part.

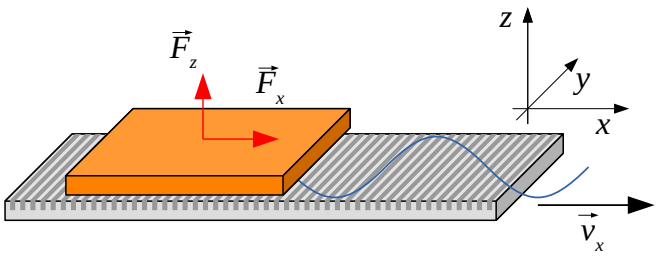
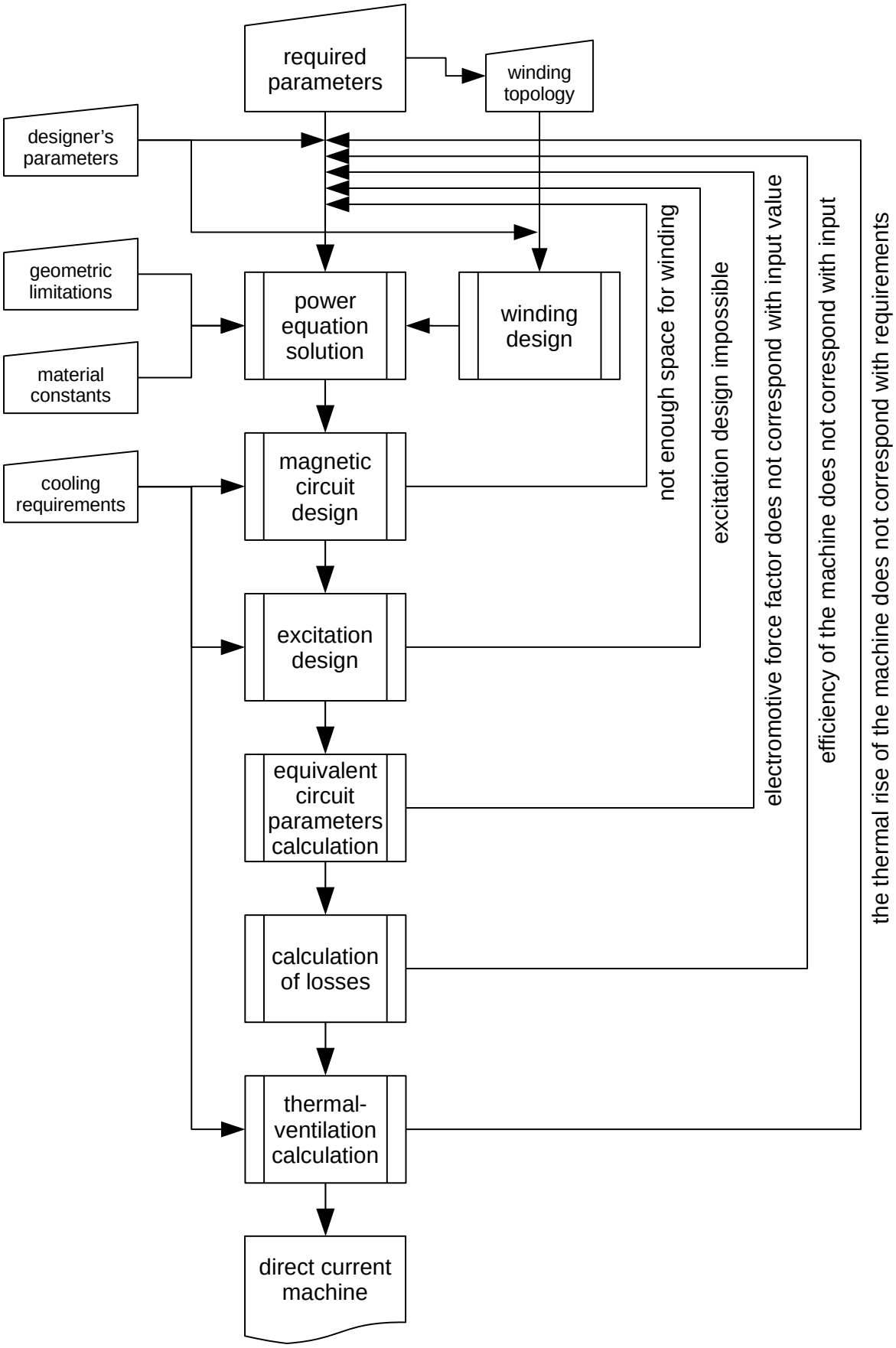


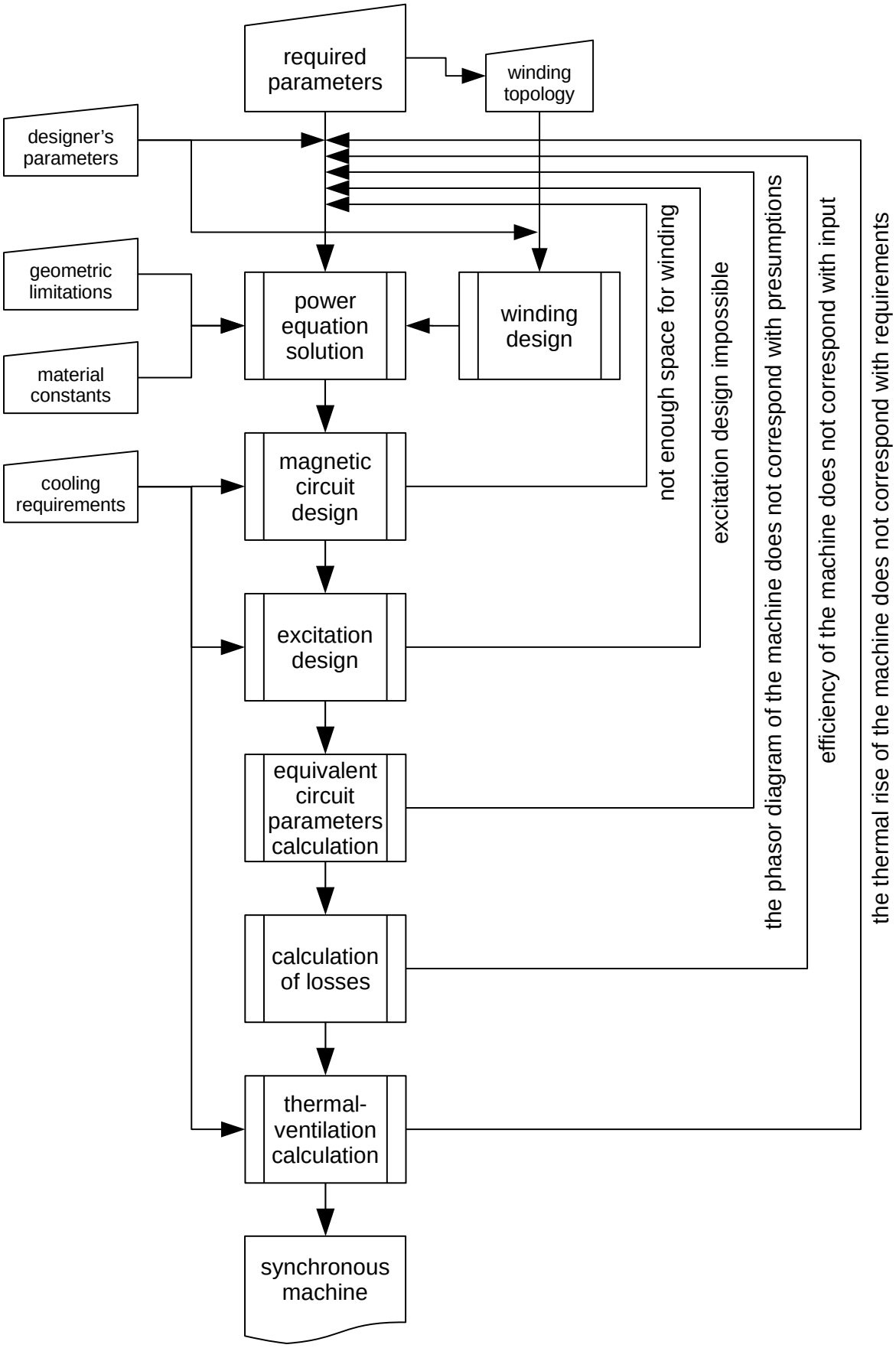
Fig. 12.12: Forces acting in linear induction machine with levitating effect

In comparison to traditional rotary machines, where the radial forces are in normal circumstances in equilibrium, in case of linear machines all these forces fully project in interaction between static and moving part. These forces are in most cases attracting and it is necessary to consider them during the design of moving parts of designed machine, especially during bearings proposal, where these forces add to the weight of the machine. In some cases the usage of these forces is wanted, e.g. in above mentioned Transrapid transport system. An opposite extreme is a case of linear induction machine, which can, in case the moving part is made of solid aluminium plate without steel yoke, generate a repellent force between the stator and the rotor and therefore it can be also used for levitation of driven transport system [35].

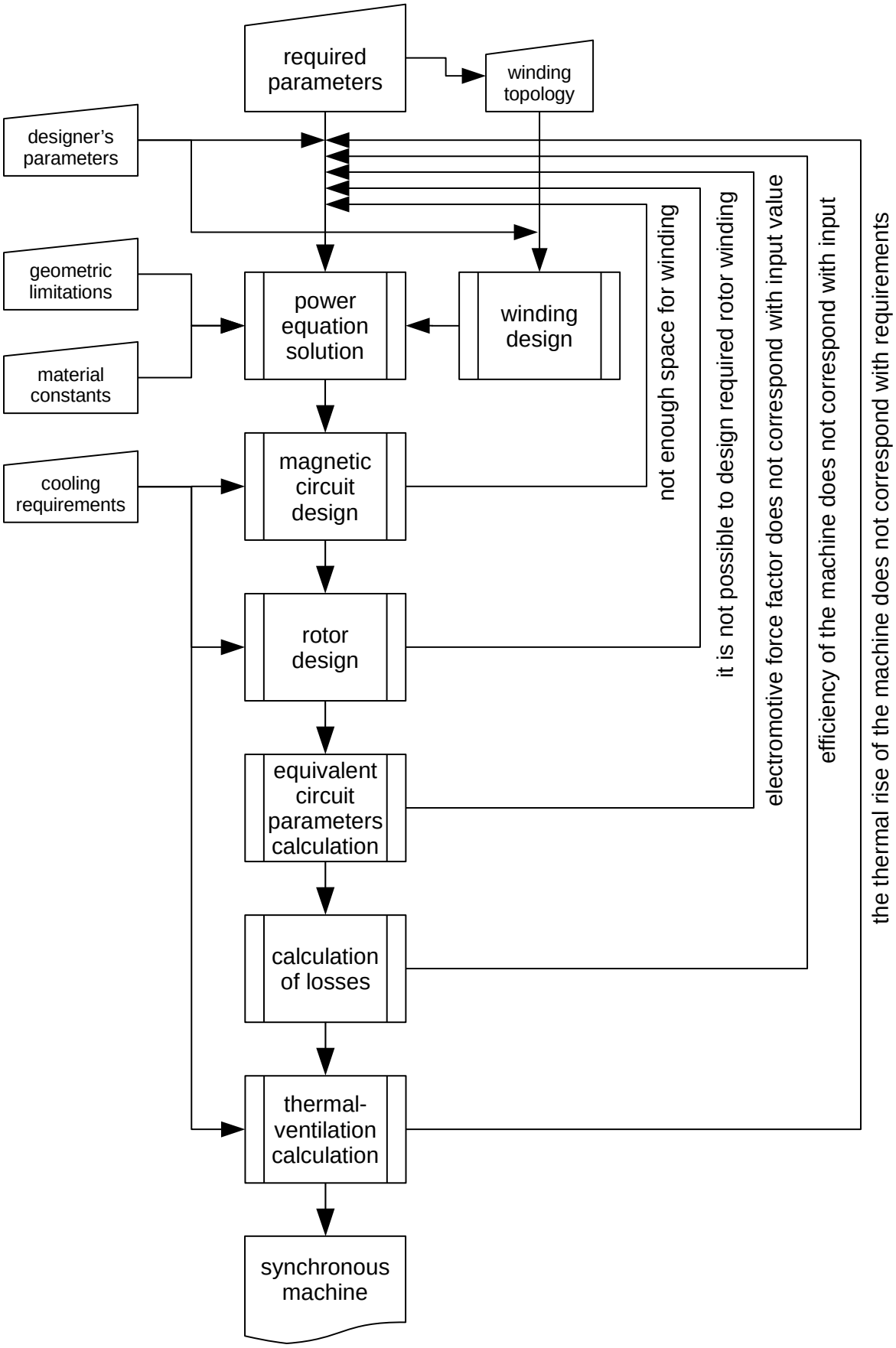
Appendix 1: Flowchart of the DC Machine Design



Appendix 2: Flowchart of the Synchronous Machine Design



Appendix 3: Flowchart of the Induction Machine Design



List of Figures

Fig. 2.1: DC Machine Air Gap Magnetic Flux Density....20
Fig. 2.2: AC Machine Air Gap Magnetic Flux Density....20
Fig. 2.3: The values of factors α_δ and k_B for different shapes of air gap magnetic flux density....22
Fig. 2.4: Fundamental machine dimensions....26
Fig. 3.1: The dependence of Esson's factor on linear dimension of the machine dimension x....31
Fig. 4.1: Field Winding of a Direct Current Machine....33
Fig. 4.2: Distributed drum winding (left) and a disk winding (right). The red line denotes the coil shape of the disk winding....33
Fig. 4.3: Parts of a winding coil....34
Fig. 4.4: Classification of windings according to coil shape....35
Fig. 4.5: Configuration of coils and winding overhangs....35
Fig. 4.6: Classification of winding according to manufacture technology....36
Fig. 4.7: Comparison of commutator connections for crossed and non-crossed windings....36
Fig. 4.8: A coil....37
Fig. 4.9: Numbering of elements in saw schema....38
Fig. 4.10: Slot layout with coil sides....39
Fig. 4.11: Parts of schematics for a lap winding and a wave winding....41
Fig. 4.12: Phasors of mathematical phases and their orientation in segment schema....43
Fig. 4.13: Possible winding connection for windings with $K_1 = 2,5$ and $S_c = 12$....43
Fig. 4.14: Segment schema of a winding with q = 3/8....45
Fig. 4.15: Turbo generator winding overhangs....45
Fig. 4.16: Shape of axial winding overhang....46
Fig. 4.17: Projection of axial winding overhangs and determination of minimal possible angle between winding overhangs and stator stack....46
Fig. 4.18: Involute winding overhangs: axially deflected (left), partially radial (middle) and radial (right)....47
Fig. 4.19: Shapes of involute winding overhangs for two, four and six pole machine....47
Fig. 4.20: The projection of an involute to cone plane....48
Fig. 5.1: Magnetic field of an induction machine....49
Fig. 5.2: A sketch of double side insulated electrical steel sheets....49
Fig. 5.3: Hysteresis loop of soft magnetic steel....50
Fig. 5.4: Eddy currents in electrical steel sheets....51
Fig. 5.5: Magnetic load of a tooth of distributed winding....53
Fig. 5.6: Magnetic flux through non-saturated tooth....54
Fig. 5.7: Desaturation of a tooth due to leakage of magnetic flux to a slot....54
Fig. 5.8: Determination of real tooth magnetic flux density....55
Fig. 5.9: Geometrical dimensions of a tooth....55
Fig. 5.10: Intersectional diagram....56
Fig. 5.11: One pole pitch of a yoke with related flux lines and dimensions....56
Fig. 5.12: Magnetic field strength curve in centre of a yoke....57
Fig. 5.13: The construction of magnetic field strength curve in the yoke as depending on position. 57

Fig. 5.14: Diagram for reading of the magnetomotive force correction factor k_y (translation from [3])....58
Fig. 5.15: Magnetic field of DC machine excitation poles....59
Fig. 5.16: Magnetic flux lines of leakage magnetic field of excitation poles....60
Fig. 5.17: Magnetic flux lines connecting pole shoes and magnetic flux element dx....60
Fig. 5.18: A comparison of ideal layout of the air gap magnetic flux density with FEM results....62
Fig. 5.19: Air gap magnetic flux lines between two smooth surfaces, smooth and slotted surface and between segmented stator and massive rotor....62
Fig. 5.20: Magnetic flux density pulsations resulting from slotting....62
Fig. 5.21: Border effects at the end of the air gap....64
Fig. 5.22: The determination of the saturation factor from the no-load characteristic....65
Fig. 6.1: Shape of a lap winding coil....68
Fig. 6.2: Magnetic field of a single coil turn....70
Fig. 6.3: Leakage magnetic field in a slot....72
Fig. 6.4: Leakage magnetic field around winding overhangs....73
Fig. 7.1: Magnetic flux lines between stator and rotor teeth....77
Fig. 7.2: Eddy currents in massive rotor surface....78
Fig. 7.3: Eddy currents induced into permanent magnet volume....79
Fig. 7.4: Eddy currents in a permanent magnet (finite element analysis)....80
Fig. 8.1: Winding wires....83
Fig. 8.2: Winding while embedding to slots....83
Fig. 8.3: Commutator cross-section....84
Fig. 9.1: Stator of a DC machine with interpoles and compensation winding....85
Fig. 9.2: DC machine armature with well visible fixation of the winding overhangs....87
Fig. 9.3: Shunt (left) and serial (right) connection of field winding....92
Fig. 9.4: Deformation of no-load characteristic due to demagnetization effects....92
Fig. 9.5: Magnetomotive force curves for each machine winding....93
Fig. 9.6: The relation between armature and commutator diameters....97
Fig. 9.7: Width of commutator lamellae and of insulation....97
Fig. 9.8: Commutator dimensions and brushes overlap....98
Fig. 10.1: The rotor of a synchronous machine equipped with salient poles and exciter (in front)…99
Fig. 10.2: Magnetic circuit of a turbo generator during manufacture....103
Fig. 10.3: Rotor of a turbo generator with well visible Lafoon’s slots....105
Fig. 10.4: The determination of deformed shape of the magnetic flux density....106
Fig. 10.5: The determination of excitation magnetomotive force for a machine with cylindrical rotor 106
Fig. 10.6: Dissolution of the armature reaction magnetomotive force to d and q components....107
Fig. 10.7: The determination of rated excitation magnetomotive force of a salient pole machine. .108
Fig. 10.8: Load characteristics of synchronous machines for a constant power factor....108
Fig. 11.1: Partial corr-section through traction IM....111
Fig. 11.2: Lamination of an induction machine with eddy current squirrel cage....112
Fig. 11.3: Rotor of an induction machine equipped with soldered copper squirrel cage....115
Fig. 11.4: The dependence of κ_i on power factor....116
Fig. 11.5: Squirrel cage section corresponding to one rotor phase....118

Fig. 11.6: Currents in the squirrel cage.....119
Fig. 11.7: Current through a bar as a difference between currents in shorting ring.....119
Fig. 11.8: Görges' pattern of a squirrel cage with m_2 = 15 phases and 2p = 2 poles.....120
Fig. 12.1: Synchronous reluctance motor rotor topologies.....124
Fig. 12.2: The performance of synchronous reluctance motor rotor by Siemens.....124
Fig. 12.3: Phasor diagram of an optimally controlled synchronous reluctance machine in per units 125
Fig. 12.4: Switched reluctance motor.....126
Fig. 12.5: Flux map of a synchronous reluctance machine derived from finite element method….128
Fig. 12.6: Axial form of a squirrel cage induction machine.....128
Fig. 12.7: Axial machine with distributed winding and two stators (left) and axial machine with a single stator and toroidal coils (right); taken from [31].....129
Fig. 12.8: YASA motor topology.....129
Fig. 12.9: A section of Transrapid drivetrain [33].....130
Fig. 12.10: Transition from rotary machine to linear machine.....131
Fig. 12.11: Length of the machine and important parameters of linear machine with short armature 132
Fig. 12.12: Forces acting in linear induction machine with levitating effect.....132

List of Tables

Tab. 3.1: Comparison of properties of machine sets designed by different approaches.....31
Tab. 4.1: Nomenclature of variables independent on winding type.....38
Tab. 4.2: Tingley’s schema of a winding with q = 3/8.....45
Tab. 7.1: Values of surface losses factors according to used materials (translation from [3]).....79
Tab. 7.2: The values of mechanical losses factors for different cooling types (translation from [3]) 81
Tab. 10.1: Reference values of d-axis reactances of generators.....104
Tab. 11.1: The dependence of ratio k_D on the number of poles.....113

References

[1] J. Červený: *Přehled konstrukce elektrických strojů točivých*. ZČU, Plzeň, 2016. ISBN (není)

[2] J. Červený: *Stavba elektrických strojů*. ZČU, Plzeň, 2016. ISBN (není)

[3] Müller, G., Vogt, K., Ponick, B.: *Berechnung elektrischer Maschinen*. Wiley-Vch, Weinheim, Germany, 2007. ISBN 978-3527405251

[4] Kopylov, I.P. a kol.: *Stavba elektrických strojů*. SNTL, Praha, 1988. ISBN 04-531-88

[5] Kučera, J., Hapl, J.: *Vinutí elektrických strojů točivých*. ČSAV, Prague, Czechoslovak Republic, 1959. ISBN není

[6] Bašta, J.: *Teorie elektrických strojů*. Nakladatelství ČSAV, Praha, 1957. ISBN neuvedeno

[7] F. W. Carter: *The Magnetic Field of the Dynamo-Electric Machine*. In Journal of the Institution of Electrical Engineers, pp. 1115 – 1138. IET, New York, 1926. ISBN/ISSN 0099-2887

[8] Heller, B.; Hamata, V.: *Přídavná pole, síly a ztráty v asynchronním stroji*. Nakladatelství ČSAV, Praha, 1961. ISBN není

[9] Evropský parlament a Rada: *Směrnice Evropského parlamentu a Rady 2009/125/ES*. 2009 [online] <https://eur-lex.europa.eu/legal-content/CS/TXT/PDF/?uri=CELEX:32009L0125&from=DE> [cit. 4. 3. 2021]

[10] J. Lammeraner, M. Štafl: *Vířivé proudy*. SNTL, Praha, 1964. ISBN není

[11] Isovolta: *Magnoval ® 2067*. 2020 [online] <http://agaus.com.au/wp-content/uploads/2014/01/Magnoval-2067-TDS.pdf> [cit. 4. 3. 2021]

[12] Arnold Magnetic Technologies: *Laminated Magnets*. 2021 [online] <https://www.arnoldmagnetics.co.uk/products/l-type-laminated-magnets/> [cit. 6. 3. 2021]

[13] R. Deeb: *Calculation of Eddy Current Losses in Permanent Magnets of Servo Motor*. In Electroscope, pp. N/A. ZČU, Plzeň, 2011. ISBN/ISSN 1802-4564

[14] ČSN CLC/TS 60034-25: *Točivé elektrické stroje - Část 25: Návod pro navrhování a vlastnosti střídavých motorů navržených speciálně pro napájení z měničů*. Úřad pro technickou normalizaci, metrologii a státní zkušebnictví, Praha, 2009.

[15] Arnold Magnetic Technologies: *N40UH*. 2015 [online] <https://www.arnoldmagnetics.com/wp-content/uploads/2017/11/N40UH-151021.pdf> [cit. 8. 3. 2021]

[16] Siemens AG: *DC Motors*. 2004 [online] <http://opis.cz/siemens/pdf/cat_da12_2004_en.pdf> [cit. 8. 3. 2021]

[17] K. Sedlazeck, C. Richter, S. Strack, S. Lindholm, J. Pipkin, F. Fu, B. Humphries, L. Montgomery: *Type Testing a 2000 MW Turbogenerator*. In IEEE International Electric

Machines and Drives Conference, pp. 465-470. IEEE, New York, 2009. ISBN/ISSN 978-1-4244-4251-5

[18] Ch. Morris: *Improved motor and controller gives Renault Zoe a range of 149 miles*. 10. 3. 2015 [online] <https://chargedevs.com/newswire/improved-motor-and-controller-gives-renault-zoe-greater-range/> [cit. 11. 3. 2021]

[19] Cigánek, L.: *Elektrické stroje*. Technicko-vědecké vydavatelství, Praha, 1951. ISBN není

[20] C. M. Laffoon, A. C. Hagg, C. H. Janthey, P. R. Heller: *Modern Practice in the Balancing of Large Turbine-Generator Rotors*. In Transactions of the American Institute of Electrical Engineers, pp. 593 - 598. IEEE, New York, 1951. ISBN/ISSN 0096-3860

[21] S. Muller; M. Deicke; R. W. De Doncker: *Doubly Fed Induction Generator Systems for Wind Turbines*. In IEEE Industry Applications Magazine, pp. 26 - 33. IEEE, New York, 2002. ISBN/ISSN 1077-2618

[22] T. Fukami, M. Momiyama, K. Shima, R. Hanaoka, S. Takata: *Steady-State Analysis of a Dual-Winding Reluctance Generator With a Multiple-Barrier Rotor*. In IEEE Transactions on Energy Conversion, pp. 492 - 498. IEEE, New York, 2008. ISBN/ISSN 0885-8969

[23] Siemens AG: *Synchronous-reluctance drive system*. 2021 [online] <https://new.siemens.com/global/en/products/drives/topic-areas/reluctance-drive-system.html> [cit. 20. 3. 2021]

[24] K. Malekian, M. R. Sharif, J. Milimonfared: *An optimal current vector control for synchronous reluctance motors incorporating field weakening*. In IEEE International Workshop on Advanced Motion Control, pp. 393 - 398. IEEE, New York, 2008. ISBN/ISSN 978-1-4244-1702-5

[25] Boldea, I.: *Reluctance synchronous machines and drives*. Clarendon Press, Oxford, 1996. ISBN 0-19-859391-0

[26] Illinois Electric Works Inc.: *Switched reluctance motor repair*. 2016 [online] <https://www.illinoiselectric.com/switched-reluctance-motor-repair> [cit. 21. 3. 2021]

[27] M. Panait: *Electric Superchargers - the Next Big Thing for the Automotive Industry*. 2014 [online] <https://www.autoevolution.com/news/electric-superchargers-the-next-big-thing-for-the-automotive-industry-88356.html> [cit. 21. 3. 2021]

[28] Komatsu Mining Corp.: *SR (Switched Reluctance) hybrid drive*. 2019 [online] <https://mining.komatsu/technology/controls-and-drives/sr-hybrid-drive> [cit. 21. 3. 2021]

[29] A. M. Omekanda, C. Broche, M. Renglet: *Calculation of the electromagnetic parameters of a switched reluctance motor using an improved FEM-BIEM-application to different models for the torque calculation*. In IEEE Transactions on Industry Applications, pp. 914 - 918. IEEE, New York, 1997. ISBN/ISSN 0093-9994

[30] Aura Systems, Inc.: *Aura - AuraGen*. 2021 [online] <https://www.aurasystems.com/auragen.html> [cit. 21. 3. 2021]

[31] T. J. Woolmer, M. D. McCulloch: *Analysis of the Yokeless And Segmented Armature Machine*. In IEEE International Electric Machines & Drives Conference, pp. 704 - 708. IEEE, New York, 2007. ISBN/ISSN 1-4244-0742-7

[32] F. Caricchi, F. Crescimbini, E. Fedeli, G. Noioa: *Design and construction of a wheel-directly-coupled axial-flux PM motor prototype for EVs*. In Proceedings of IEEE Industry Applications Society Annual Meeting, pp. 254 - 261. IEEE, New York, 1994. ISBN/ISSN 0-7803-1993-1

[33] M. Schweiß: *Datei:Transrapid-Versuchsanlage Emsland Stator 01.jpg*. 2004 [online] <https://de.wikipedia.org/wiki/Datei:Transrapid-Versuchsanlage_Emsland_Stator_01.jpg> [cit. 22. 3. 2021]

[34] Transrapid International: *High-Tech for "Flying on the Ground"*. 2011 [online] <https://www.ncl.ac.uk/media/wwwnclacuk/pressoffice/files/pressreleaseslegacy/TRI_Flug_Hoehe_e_5_021.pdf> [cit. 22. 3. 2021]

[35] E. Bachelet: *Levitating transmitting apparatus*. 1911 [online] <https://patents.google.com/patent/US1020942A/en> [cit. 22. 3. 2021]

© 2021 Karel Hruska
University of West Bohemia
Faculty of Electrical Engineering
Department of Power Electronics and Machines